Republic of Iraq
Ministry of Higher Education and Scientific Research
University of Babylon / College of Engineering
Civil Engineering Department

Quality and Hydraulic Assessment of Groundwater for Drinking and Irrigation Purpose in Al-Mahaweel District -Iraq

A Thesis
Submitted to the Department of Civil Engineering, College of Engineering, University of Babylon in Partial Fulfilment of the Requirements for the Master Degree in Engineering /Civil Engineering /Water Resources

By:

Teeba Mohammed Yehia Ibrahim

(B.Sc. in Civil Engineering 2017)

Supervised by:

Asst. Prof. Dr. Imad Habeeb Obead ***Asst. Prof. Dr. Yahya Kadhim Hussien***

February, 2022 **1443, شباط**

بسم الله الرحمن الرحيم

"وَإِذِ اسْتَسْقَىٰ مُوسَىٰ لِقَوْمِهِ فَقُلْنَا اضْرِب بِّعَصَاكَ الْحَجَرَ ۖ
فَانفَجَرَتْ مِنْهُ اثْنَتَا عَشْرَةَ عَيْنًا ۖ قَدْ عَلِمَ كُلُّ أُنَاسٍ مَّشْرَبَهُمْ ۖ كُلُوا
وَاشْرَبُوا مِن رِّزْقِ اللَّهِ وَلَا تَعْثَوْا فِي الْأَرْضِ مُفْسِدِينَ"

صدق الله العلي العظيم

سورة البقرة {الأية: 60}

Supervisors' Certificate

We certify that this thesis entitled (***Quality and Hydraulic Assessment of Groundwater for Drinking and Irrigation Purpose in Al-Mahaweel District -Iraq***) was Prepared by **(Teeba Mohammed Yehia)** under our supervision at the Department of Civil Engineering/ College of Engineering/ University of Babylon in partial fulfilment of the requirements for the degree of Master of Science in Civil Engineering/ Water Resources Engineering.

Signature: imad h. obead

Asst. Prof. Dr. Imad Habeeb Obead

Date: / / 2022

Signature:

Asst. Prof. Dr. Yahya Kadhim Hussein

Date: / / 2022

EXAMINATION COMMITTEE CERTIFICATE

We certify that we have read this thesis entitled (***Quality and Hydraulic Assessment of Groundwater for Drinking and Irrigation Purpose in Al-Mahaweel District -Iraq***) presented by **(Teeba Mohammed Yehia)** and as an examining committee, we examined the student in its content and in what is connected with it, and that in our opinion it meets standard of a thesis for the degree of Master of Science in Civil Engineering / Water Resources Engineering.

Signature: imad H. Obead

Name: **Asst. Prof. Dr. Imad H. Obead**

(Supervisor and Member)

Date: / / 2022

Signature: yahya

Name: **Asst. Prof. Dr. Yahya K. Hussein**

(Supervisor and Member)

Date: / / 2022

Signature: M. O. K

Name: **Prof. Dr. Mahdi O. Karkush**

(Member)

Date: / / 2022

Signature: N. Al-Mansori

Name: **Prof. Dr. Nisren J. Hussien**

(Member)

Date: / / 2022

Signature: R. H. Irz

Name: **Prof. Dr. Raad H. Irzooki**

(Chairman)

Date: / / 2022

Approved by the Head of the Civil Engineering Department

Signature:

Name: **Prof. Dr. Thair J.Mizhir Alfatlawi**

Date: / /

Approved by the Dean of college of Engineering

Signature:

Name: **Prof. Dr. Hatem Hadi Obeid**

Date: / /

Deduction

"To Al-Mahdi Al-Montadar (may Allah hasten his reappearance)"

"To my gorgeous family"

"To all those, who helped me to move the rocks on my way to stand here, those who believed in me."

With love and respect

Teeba Mohammed

Acknowledgements

In the name of Allah, the Most Gracious, the Most Merciful. Praise be to Allah for the blessing he has bestowed upon me, and prayers and peace be upon the one who was sent with mercy, and upon his family, and upon his honourable companions and after.

"Who does not thank people does not thank God". And when I am putting the final touches on my humble effort, which would not have seen the light without the strenuous efforts and meticulous follow-up of those loyal and in the forefront of them ***"Asst. prof. Dr Imad Habeeb Obead"*** *and* ***"Asst. Prof. Dr Yahya Kadhim Hussein"*** *my supervisors those who spared no effort in helping me, may Allah reward them with the best reward and I have all the appreciation and respect. Also, I cannot forget the efforts made by all of my teachers since I took my first steps in my primary school until today, especially my department, the head of the department and all the people of the hidden effort in there.*

As I stand here, I can't express enough thanks to my dearest persons ever ***my mother and father*** *who provide me with all the financial and moral support so that I can reach what I have reached with their prayers.*

Finally, many thanks to all my family members, my best friends and everyone who helped me in the departments and companies and everyone who contributed to showing this effort for existence.

Teeba Mohammed

ABSTRACT

During the drought season which is extend from May to September, groundwater becomes a vital water resource for main irrigation and for drinking in some regions of Al-Mahaweel district. The main objective of this study is to provide a report on present groundwater quantity using groundwater modelling system (GMS) software, quality for drinking and irrigation purposes, and finally produce thematic maps representing their distribution by using Geographic Information systems (GIS) software. To achieve this aim thirteen ground water samples were taken from different locations throughout the study area and analyzed for, concentration of hydrogen ion (pH), electrical conductivity (EC), temperature (T), total hardness (TH), total dissolved solids (TDS), cations (K^+, Na^+, Mg^{+2}, Ca^{+2}), anions (Cl^- ,SO_4^{-2}, HCO_3^-, NO_3) and five heavy metals (Fe, Zn,Cd, Pb, Ni). The result of these concentrations was compared with World Health Organization (WHO) and Iraqi standards for drinking water. Three indices were used to evaluate and compare groundwater quality for drinking purposes, these are, water quality index (WQI), heavy metal pollution index (HPI) and heavy metal evaluation index (HEI). In addition, the water quality for irrigation uses was evaluated by irrigation suitability classification measures, which are the electrical conductivity (EC), sodium adsorption ratio (SAR), residual sodium bicarbonate (RSCB), soluble sodium percentage (SSP), magnesium hazard ratio (MH), permeability index (PI), and Kelly's ratio (KR).

The results of the hydraulic modelling for the steady-state groundwater were calibrated, for hydraulic conductivity and recharge rates and one scenario was used to simulate a drought condition with zero recharge and five operating wells with 48 m^3/day pumping rate, this scenario showed a major decline in the water table in the entire area. According to WHO and Iraqi standards, the computed water quality index revealed that, for the study period, no well was found to be suitable for drinking purposes. also the qualitative assessment of groundwater via two-water quality pollution indices reveled that, except of three wells fall out the range of low pollution and was categorized as medium-heavy metals pollution when HPI limited

to Iraqi standards during summer season, the findings indicate a low pollution rate in all winter and other summer groundwater samples, so the risk potential for drinking water in groundwater was declared as low-level pollution. Assessment of groundwater quality for irrigation purposes based on different irrigation quality indices indicated that for the measured values of electrical conductivity, only 38.46% and 30.77% of wells were "permissible" during the winter and the summer seasons, respectively. Moreover, about 38.5% were classified as "unsuitable" during the study period, while the rest were categorized as "doubtful". Almost, all the calculated indices involved that more than 80% of the groundwater samples were considered as excellent to good categories, and less than 20% of samples were considered as unsafe. Therefore, it was concluded, that the groundwater throughout the study area was in general suitable for irrigation. The spatial distribution of groundwater quality parameters results showed a large variations and generally increased toward the southeastern parts of the study area. For heavy metals, it was showing a randomly distributed behavior throughout the study area.

Finally, the overall review of obtained results indicates that all concentrations that measured for cations and anions were increased in the dry season rather than for the wet season, which attributed to the evaporation and intensive withdrawal of groundwater from wells in summer. On the other hand, the concentrations that measured for the heavy metals indicate lower values in the dry season than in the wet season; such findings reveal that there is no certain source for these metals within the subsurface layers, and on the ground surface throughout the study region. However, the presence of concentrations of heavy metals was attributed to agricultural activity such as intensive use of fertilizers and agricultural pesticides, where the leachate of contaminations will be infiltrated and percolated deeply in soil strata vertically downward toward the water table by irrigation water and rainfall in the wet season.

LIST OF CONTENTS

LIST OF CONTENTS. CONT.

LIST OF FIGURES

LIST OF FIGURES.CONT.

LIST OF FIGURES.CONT.

LIST OF FIGURES.CONT.

LIST OF TABLES

LIST OF TABLES.CONT.

LIST OF SYMBOLS

Symbol	Definition	Dimension
A	Area	L^2
HK	Hydraulic conductivity	L/T
C	Conductance	L^2/T
k_x, k_y, k_z	Hydraulic conductivity of soil in x, y, z Cartesian directions	L/T
h	Groundwater head level	L
$h^i_{Obs.}$, $h^i_{Comp.}$	The observed and computed heads	L
S_y	Specific yield for the aquifer medium	
W	Flux per unit volume	L/T
R^2	Correlation coefficient	---
RCH	Recharge rate	L^3/T
t	Time	T
T	Temperature	C°
Δx, Δy, Δz	Finite difference grid intervals	L

LIST OF ABBREVIATION

Abbreviation	Description
APE	Absolute Percentage Error
EC	Electrical Conductivity
FD	Finite Difference
GIS	Geographic Information System
GMS	Groundwater Modeling System software
GPS	Global Positioning System
HEI	Heavy metal Evaluation Index
HPI	Heavy metal Pollution Index
IDW	Inverse Distance Weighted interpolation method
IQS	Iraqi Standards
KR	Kelley's Ratio
m.a.s.l	Meter above sea level
MAE	Mean Absolute Error
MAPE	Mean Absolute Percentage Error
MH	Magnesium hazard
MODFLOW	Modular finite-difference flow model
PEST	Parameter Estimation Tool
PI	Permeability Index
RMSE	Root Mean Square Error
RSBC	Residual Sodium Bicarbonate
SAR	Sodium Adsorption Rate
SSP	Soluble Sodium Percentage
TDS	Total Dissolved Solids
TH	Total Hardness
WHO	World Health Organization
WQI	Water Quality Index

CHAPTER ONE

INTRODUCTION

CHAPTER ONE

INTRODUCTION

1.1 Introduction

Water is the most important constituent of life. There are two types of fresh water on earth, surface water such as rivers and lakes or groundwater. So that, groundwater is considered the second main source of fresh water around the world. it's a most essential resource for millions of people for drinking and irrigation uses (Ghalib, 2017; Kaur et al., 2017). In recent years, the rapid urbanization, industrialization uses, and population growth, caused a burden on water resources has increased, which their conservation and sustainability are one of humanity's major challenges (Abbasnia et al., 2018).

Natural and anthropogenic activities have a significant effect on groundwater quality, making it unsafe for domestic and irrigated agriculture (Mallick et al., 2018). As well as toxic elements are added to the groundwater by natural and anthropogenic souses including rainfall quality and quantity, geological structure, aquifer mineralogy, and selectivity accumulated heavy metals by plants reaching the groundwater-surface (Abbasnia et al., 2018; Shankar, 2019). Other sources of pollution come from anthropogenic activates such as pesticides, fertilizers and sewer leakage to groundwater (Seyedmohammadi et al., 2016). Heavy metals are considered hazardous contaminants in the environment because of their characteristics of stability, toxicity, and bioaccumulation (Mirzabeygi et al., 2017).

The rapidly increasing water demand in the past years has resulted in water scarcity in many parts of the world since Iraq is an arid country, in particular, the middle and southern parts, further, the improper management of water resources, water policies of the riparian countries (i.e., Turkey, Syria, and Iran) and the occurrence of drought conditions due to severe climate changes, all are created a probable water crisis (Ghalib,

2017). Of the above, it is very important nowadays to explore other water sources and have a full version of the groundwater quality and quantity because the quality of the groundwater is as critical as its quantity (Aghazadeh and Mogaddam, 2010).

1.2 Problem Statement

Al-Mahaweel district suffers from decreasing the inflow in the Euphrates River and its branches that does not cover the water demand purposes for drinking and irrigation. The abrupt growth in population and the subsequent increase in water consumption, the exceeding the water quota by neighbored governorates such as Al-Qadisyia, illegal overexpansion of fish farming projects, and many other reasons, which can summarize the main reasons for the severe water shortage problem in the middle Euphrates region (DWRB, 2017).

For a long time, attention has turned to depend on groundwater sources to fill this shortage in surface water resources. A hydraulic and quality evaluation of the groundwater in Al-Mahaweel district is a necessary aspect for purposes of safe and reliable drinking and irrigation, which represents the reason for conducting the present research.

1.3 Study Area

Al-Mahaweel district is located in Babil Governorate, Iraq. It is about 80 km from Baghdad. The district extended from longitudes from 44 20'50" to 45 6'40" East, and latitudes from 32 25'20" to 32 49'20" North, with an estimated area to be 1667 km^2, therefore, it contributes 33% of Babylon governorate's total area, as shown in Figure (1.1) which it was drawn using Arc-Map software.

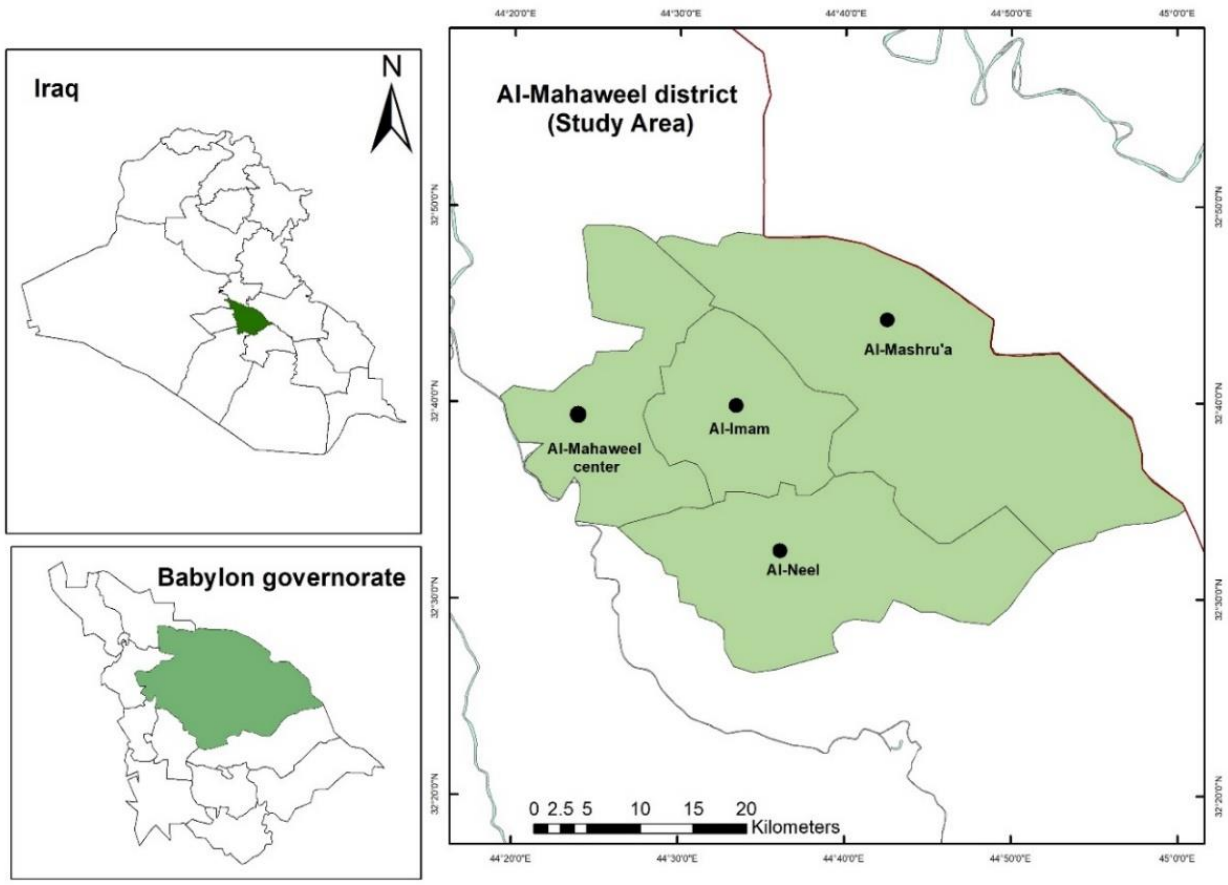

Figure (1.1): Layout of the study area location.

The study area is located in the Middle East center in Babylon governorate, that is gave it a great role in economic and political aspects (Al-Hessnawi et al., 2018). The rural population was 181770 person, while the urban population was 95043 person as per the 2018 statistic (Al-Saffar and Al-Shemmari, 2019). The study area is administratively divided into four sub-districts, namely; Al-Imam, Al-Neel, and Al-Mashrou'a as well as the center of Al-Mahaweel district.

The major parts of the district are agricultural areas; hence, the agriculture activities represent the keystone of the economics of the region and a valuable national resource in this field (Makki et al., 2021). Thus, the district depends mainly on surface water for irrigation and drinking.

1.3.1 Climate Conditions of the Study Area

Iraq is considered among the countries in the Middle East and North Africa that undergo from the implications of drought due to climate changes (Al-Ansari, 2013). The large difference in temperature between summer and winter, day and night are a distinctive climatic characteristics of Iraq, in the central regions (particularly the middle Euphrates region, where the study area is located).

The temperature variances were reported by the historical records of the Iraqi meteorological organization and seismology (IMOS, 2019), the monthly averages maximum and minimum temperatures, for January of 2019 was 18 °C and 5°C, respectively. For August, of 2019 was 45°C and 28°C, respectively.

The annual rainfall was 141.7 mm for 2019 at rain season that was started from October to May. The maximum average value of 62.6mm was recorded at January and a minimum average value of 0.5mm that was recorded at May for the same year (IMOS, 2019). The study area is characterized by abundant solar radiation, where the annual average of radiance hours 8.4 hr/day, with an annual average wind speed of 1.8m/s and annual relative humidity of 49.3% (Al-Hessnawi et al., 2018).

Makki (2021) reported that the climate change investigation is critical in shallow groundwater studies, rainfall and humidity rate, which affect the water content in the soil, are influenced by a variety of climate factors, as temperature rises, low rainfall, and dust storm, for it all have a direct impact on groundwater quality because of climate change.

1.3.2 Water Resources of the Study Area

The study area located within the Mesopotamia plain in Iraq, which is considered one of the most recent composition of the Iraqi surface, the region south of Baghdad that is bounded by the Tigris and Euphrates rivers and the Arabian Gulf.

In this region the groundwater is generally found in recent alluvial deposits, and groundwater level is very near to the surface, this location gave the area the characteristics of the flat surface and the small earth's gradient, it is covered with two types of deposits; these are the fluvial and wind deposits, the first type include flood plain deposits consisting of clay, silt, sand layers with chemical sediments (gypsum, carbon and dissolved salts), and depressions sediments consisting of silty clay, sand, silt and salt shells. The second type is spreading in the east parts of the study area, consist mainly from silt and rock that can be seen as sandy dunes and sandy waves and that layers made the soil of the area inserted to the transported soil type (Al-Ansari et al., 2014; Al-Hessnawi et al., 2018).

Al-Mahweel district is depending on the Euphrates River and its branches for water requirements; that is flows outside the administrative borders of Al-Mahaweel city on the west side, it is characterized by higher flow head, in addition to the lower levels of the surrounding agricultural lands toward it east side. Many channels have been passed from Mashrou'a Al-Mussayab Al-Kabeer, and south of AL-Mussayab city at Al-Hindya barrage that was branched to Shat Al-Hillah and Shat AL-Hindya.

In recent years, the study area faced a higher decline in the water inflow of the Euphrates River, which obviously affected the amount of surface water in the study area. Therefore, the dependence on the groundwater source has increased significantly, particularly throughout the summer season. Figure (1.2) shows a map for the distribution of water resources in the study area which it was mad using GMS.

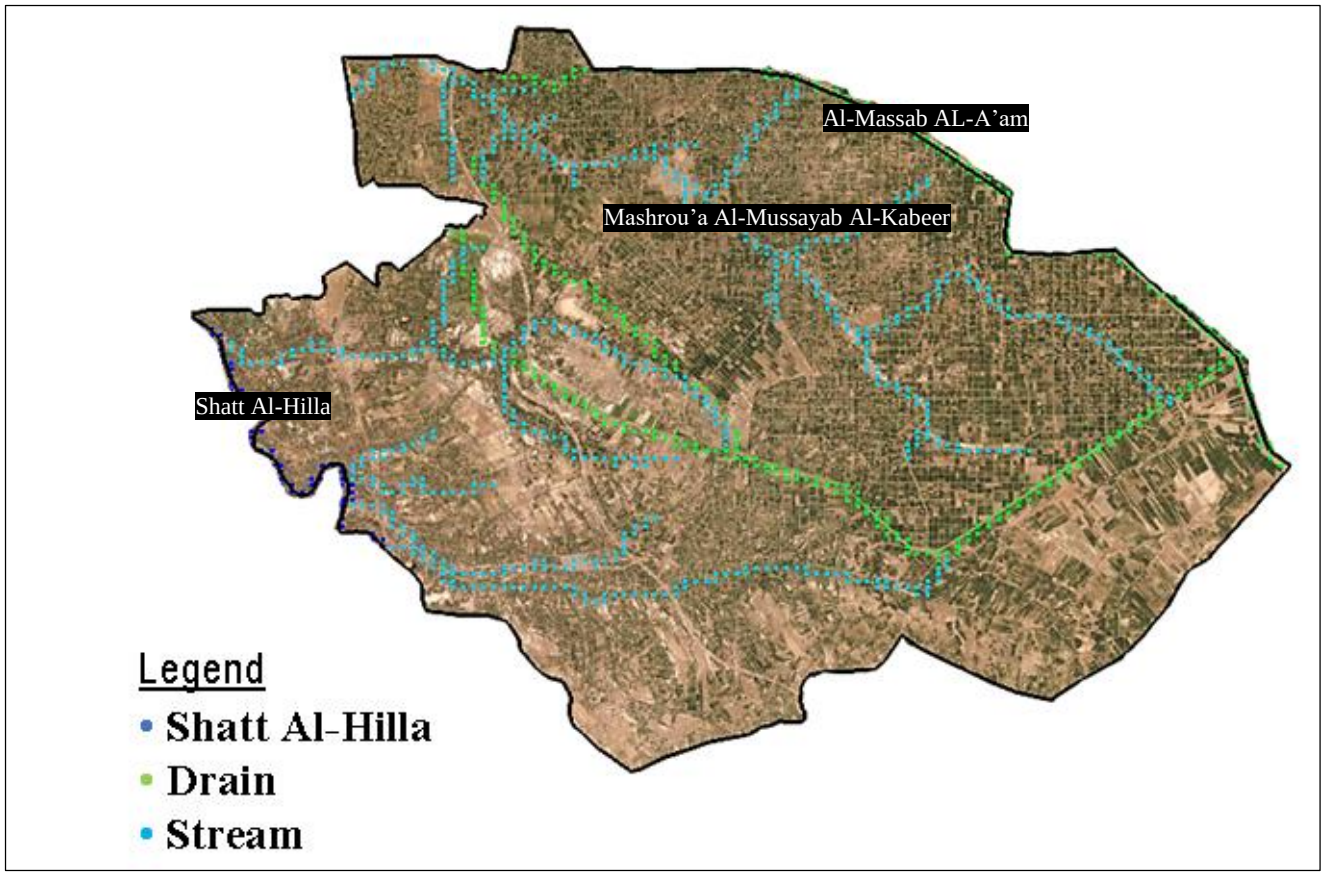

Figure (1.2) A map for the distribution of water resources in the study area.

1.4 Aim and Objectives of the Study

The overall goal of the present research is to carry out a comprehensive hydraulic and qualitative assessment of groundwater in the district of the Al-Mahaweel City, Babil, Iraq. Consequently, the main objectives are:

1. Develop a groundwater conceptual model in the study area via Groundwater Modeling System (GMS) software to simulate the hydraulic characteristics of groundwater movement, and heads distribution for the study area during the study period.

2. Assess the groundwater quality and suitability for drinking purposes based on Iraqi standards (IQS) and world health organization standards (WHO), as well as, the quality of groundwater for irrigation purposes.

3. The assessment processes will be achieved by measuring the concentrations of heavy metals, chemical elements, major cations, and anions in the extracted samples from wells extended in the study area. This is carried out by calculating pollution indices of heavy metal and water quality indices for both dry and wet seasons.

1.5 Thesis Structure

The outlines of this research and results are introduced in five chapters as summarized below:

Chapter one present an introduction of the study subject , description, location, and characteristics of the study area such as climate, hydrology, geology, topography, type of soil and underlying soil layers, the slope of the ground, land use as well as the aim and objectives of the present study.

Chapter Two present a review of literature that is most relevant to the present research such as the evaluation of the water quality for drinking and irrigation purposes, evaluation of heavy metal pollution in the groundwater throughout the study area.

Chapter Three deals with the methodology used in the present research and, steps of the creation of the conceptual model.

Chapter Four presents the obtained results based on laboratory tests for the groundwater samples extracted from wells in the study area with detailed discussion. In addition, thematic GIS maps are prepared to show the spatial distribution for the heavy metals and chemical elements entirely in the study area. As well, the results of hydraulic simulation performed by GMS software were presented.

Chapter Five summarizes the main conclusions drawn from this research and recommendations for future works.

CHAPTER TWO

LITERATURE REVIEW

CHAPTER TWO

LITERATURE REVIEW

2.1 Introduction

Groundwater quality assessment has a vital role in recent years due to the increase of water demand upon all scales of life, also, because of the fact of uneven distribution of surface water resources over the world. Many researchers have contributed to this sector of knowledge to provide an entire qualitative and quantitative understanding of many aspects of groundwater.

An intensive, but brief in detail for relevant local and global previous studies that cover groundwater assessment will be introduced in this chapter.

2.2 Review of Previous Studies

Al-Mussawy and Khalaf (2013) developed a three-dimensional conceptual model using Groundwater Modeling System (GMS), to simulate the flow of Dammam confined aquifer in the remote Karbala area to develop decision-making tools for identifying groundwater efficiency to meet future needs. According to the calibrated model, hydraulic characteristics of the aquifer had identified, the hydraulic conductivity in the study area was ranging between (0.65-50.3) m/day and recharge rate varied from 0.001 to 0.031 m/year. A good match was obtained between observed and computed heads with a correlation factor (R^2= 0.9747) for steady-state conditions.

Hosseinifard and Aminiyan (2015) tested the parameters that control the quality of groundwater in the Rafsanjan plain. To achieve their aim, 1040 groundwater samples were collected randomly from different areas of Rafsanjan, Iran, each sample was analyzed for concentration of hydrogen ions, total dissolved solids,

electrical conductivity, total hardness, major cations and anions. Based on standard methods, groundwater quality was unfit for drinking use, and its state of agricultural practices was unsuitable these places due to magnesium hazard.

Ghalib (2017) evaluated groundwater quality of shallow groundwater in the northeastern Wasit Governorate, Iraq. The physicochemical parameters were used to evaluate the appropriateness of groundwater resources for human consumption by comparison with both the WHO and Iraqi requirements. For this purpose, 98 samples were taken from shallow wells in the study field and analyzed for total dissolved solids (TDS) and other parameters. Sodium adsorption ratio (SAR), residual sodium bicarbonate (RSBC), permeability index (PI) and magnesium ratio (MR) were used for irrigation suitability assessment. Analysis showed that its geographical distribution for TDS, EC values, and main ions in all these samples collected considerably were varying from one region to the other largely due to geological characteristics of the field of study. The analyzed underground water species were observed most groundwater were unsuitable for drinking purposes. On the other hand, most groundwater was unsuitable for irrigation purposes based on sodium and salinity hazards. However, soil type, as well as proper selection of plants, should be taken into consideration.

Elumalai et al. (2017) analyzed heavy metals in surface and groundwater, and define their origins, for two towns in South Africa. Using multivariate statistical methods as well as the risk of human exposure through the use of the drinking water pathway was also assessed. Except for 6 places of 35, electrical conductivity values showed that groundwater was desirable to permissible for drinking. In all locations, the concentrations of aluminum, lead, and nickel was higher than the recommended limit for drinking. At a few sites, levels of boron, cadmium, iron, and manganese exceeded the limit. Boron, nickel, and zinc posed no danger, cadmium and lithium posed a moderate risk, and silver, copper, manganese, and lead posed a high risk.

Hazard quotients for humans of all ages were high in all sampling sites, suggesting that groundwater was unfit for drinking. Polluted areas were found on the coast, near manufacturing activity, and at a landfill site, all of which were caused by human activity.

Kaur et al. (2017) highlighted the quality of groundwater and compared its suitability in the Malwa region, a southwestern part of Punjab, India, for drinking and irrigation purposes. Twenty four groundwater samples were obtained and analyzed for almost all major cations, anions and other physicochemical parameters. According to the results of physicochemical analysis, most samples were found to be above the acceptable limits of Indian specifications, the groundwater was varying hard and the relative abundance of major cations and anions was Na^{+}> Ca^{2+}> Mg^{2+}> K^{+} and HCO_3^{-}> SO_4^{2-}> Cl^{-}. The parameters like sodium adsorption ratio (SAR) and sodium percentage (Na%) revealed a good quality of groundwater for irrigation purposes, whereas magnesium ratio (MR) showed that water was not suitable for agriculture use. This work thus concluded that groundwater in the study area was chemically unsuitable for domestic and agricultural uses. It was recommended to carry out a continuous water quality monitoring program and development of effective management practices for the utilization of water resources.

Abbasnia et al. (2018) tested groundwater suitability for drinking and irrigation uses, groundwater physiochemical characteristics in Sistan and Baluchistan province, Iran. Six hundred and fifty four groundwater samples were taken from open dug wells, then the chemical analysis was carried out and the water quality index was then calculated, many other indices were considered to assess the suitability of groundwater for industrial purposes. Results of the analysis of the parameters were then represented spatially using the environment of Geographic Information System (GIS), and that clearly showed 1.2 percent of groundwater samples were excellent, 52.1 percent were good, 39 percent were poor, 6 percent

were very poor and finally 1.7 percent were unsuitable for drinking purpose classes according to the drinking water quality index (WQI) results. And it was illustrated that 19.9 percent were excellent and 80.1 were good classes according to the irrigation water quality index.

Issa and Alshatteri (2018) evaluated the risk of heavy metal contamination in drinking water in the three districts of Garmian Region, East Iraq. Sixteen water samples were collected from different locations and analyzed for 23 heavy metals and 6 chemical pollutants. At certain sites in the studied area, high levels of Aluminum, Selenium, Strontium and Iron have been found. The heavy metals pollution index (HPI) and heavy metals evaluation index (HEI) were used according to the newest release of the WHO drinking water guidelines. According to HEI the most reliable contamination evaluation index for drinking water, 44 percent of the water samples were critically contaminated. Natural geological sources were most likely to cause the pollution and a few sites in the study area showed signs of anthropogenic effects.

El-Rawy et al. (2019) assessed groundwater quality in Qena Governorate, Egypt, using geographic information system (GIS) and hydrochemistry. 73 groundwater samples were taken and then analyzed for many Physico-chemical parameters, major cations and anions then represented spatially in the environment of GIS. Results of the calculated water quality index showed that 62 percent of the well's water were safe for drinking according to WHO and Egyptian standards. The suitability of groundwater for irrigation was determined according to, sodium adsorption ratio (SAR), sodium percentage (Na%), residual sodium carbonate (RSC), Kelly ratio (KR) and magnesium hazard (MH). The results showed that 50 percent of the wells water were suitable for irrigation when considering sodium percentage, residual sodium carbonate and Kelly ratio while 99 percent were suitable if electrical conductivity and sodium adsorption ratio were only considered.

Shankar (2019) assessed heavy metal concentrations in groundwater of Bangalore's Peenya Industrial Area, India. Six eco-toxic metals, including chromium, copper, cadmium, iron, nickel and lead, were analyzed for thirty groundwater sampling stations using an atomic absorption spectrometer. Cr> Fe >Pb>Cu> Ni> Cd was the order of heavy metal concentration. The results of the analysis were used to calculate two pollution indices in groundwater: the heavy metal pollution index (HPI) and the metal index (MI). The HPI values of 63.33 percent of the groundwater samples were well above the critical value. The mean metal index concentration was 10.36, and 46.67 percent of the groundwater samples were classified as severely contaminated. The research results not only showed that the groundwater in this study was unfit for drinking, but also showed the impact of urban, industrial, and agricultural activities on the groundwater in this region.

Al-Areedhi and Khayyun (2019) presented a conceptual model for a large area from the upper zone of Iraqi aquifers by using (GMS). It was evaluated the groundwater movement and flow directions to compute the water budget for the studied aquifer system by considering the hydrologic features for a study date and future conditions, respectively, which were affected by climate changes.

It was found that based on the parameters calibration process, a strong correlation (i.e., R^2=0.9993) between observed and predicted groundwater heads, the variation in hydraulic conductivities was ranged between (0.559 to 31.44 m/day), also, the estimated rates of groundwater recharge were ranged between (zero to 0.000488 m/day). It was concluded that the model was sensitive to both recharge and hydraulic conductivity, which was highly sensitive to increasing and decreasing the recharge, while it was strongly sensitive to the decrease than the increase in hydraulic conductivity.

Ismael et al. (2019) tested water quality and hydrochemical indicators and seasonal variations of surface water in terms of heavy metals in Al-Tarmiyah region,

Baghdad, Iraq. Ten water samples were collected, four was surface water and six was groundwater samples in two seasons. All samples were analyzed for physic-chemical parameters and trace elements. The suitability of water for drinking purposes was evaluated depending on the criteria or standards of acceptable quality for that use (WHO and Iraqi Standard). All surface and groundwater samples from the studied area were not suitable for drinking purposes and within "excellent type" for livestock and poultry use. Additionally, almost all surface water samples were within the Good class based on the suggested limits of EC value for irrigation while most of the groundwater samples were within the unsuitable class. All surface water and groundwater samples ranged within the low hazard class of the irrigation water based on SAR values.

Megahed (2020) aimed to evaluate the quality of groundwater and its suitability for drinking purposes based on Egyptian and WHO standards and, finally, to evaluate groundwater for irrigation purposes based on international irrigation guidelines in the outlet and central sections of Wadi El-Assiuti, Egypt. One hundred and fifty nine groundwater samples were collected to accomplish this objective, to be analyzed for major ions, trace elements and heavy metals. The research showed that the TDS values differed between 1972 and 6217 ppm, while the trace element concentration (Fe^{++}, Mn^{++} and Ni^{+}) varied between 0.05 and 0.46, 0.11 and 0.221 and 0.01 and 0.6 ppm, respectively. These results indicated that, due to the high content of total dissolved solids, trace elements and heavy metals, all groundwater samples were inappropriate and inadequate for human drinking according to WHO and Egyptian standards for drinking water quality. Then the spatial analysis of TDS values in the geographic information system (GIS) software, demonstrates that salinity was higher in the northeast and decreases steadily southwards. Sodium adsorption ratio, classification of the US salinity laboratory (1954), residual sodium

carbonate (RSC), soluble percentage of sodium (SSP) and permeability index (PI) indicated that most samples of groundwater were acceptable for irrigation purposes.

Egbueri (2020) investigated the level of heavy metal pollutants, the sources of pollution, and the human health risks of groundwater from the shallow Aquifer in Onitsha, Nigeria. All of the groundwater samples had low levels of nitrate contamination. The majority of heavy metals, however, exceeded their maximum permissible limits. According to the heavy metal pollution index (HPI), 45.83 percent of the total samples are unfit for human use, respectively. The water quality index showed that 91.67 percent of the samples are unfit for human consumption. According to the ecological risk index, 58.33 percent of the samples was extremely hazardous to the environment. The release of these heavy metals into the groundwater system was largely influenced by anthropogenic inputs rather than natural processes.

Hadi and Alwan (2020) constructed a conceptual model in GMS software to compute the interaction between different feeding sources. With the application of the observed heads in the field, hydraulic conductivity and recharging were measured using PEST. The model's results showed a hydraulic conductivity of (0.958 - 24.932) m/day and a recharge rate of (5.392810^{-5}) m/day. The observed groundwater levels and the model-calculated levels showed a good match. According to the results, Shatt Al-Diwaniya currently draws approximately (3466.37) m^3/day from groundwater, with a recharge feed of approximately (2576.20) m^3/day. Except for a small amount of feeding for the city's northern areas, it was acting as a drain, drawing groundwater in different amounts of recharge.

Jalut (2021) simulated Khanaqin's southwest part in Iraq, using GMS mathematical model, to know how the increasing aquifer withdrawal rates affect groundwater quality. However apart from the impact of decreasing recharge rate on the groundwater in the studied area. The steady-state calibration process revealed

good agreement between the model and observed groundwater head levels. For the unsteady state, five different scenarios were used. The maximum drawdown value was reported on the left side of the modelled region in the study area, whereas the minimum value was recorded near Al-Wand River.

Hussain et al. (2021) modulated groundwater in the central part of Iraq within Karbala Governorate, using GMS software. The model was initially performed in a steady-state, and the results of this case were used as inputs to run the model in the unsteady state after obtaining a good match between the model results and the initial values of groundwater levels. Approximately 22 wells are spreading within the studied area, with discharge rates ranging from 7 to 100 l/s and rates up to 36 l/s. For three years award from the sight of these wells, the model was operated and the results show a declination in groundwater levels ranging from 2 to 21 meters, spread uniformly throughout the studied area.

Makki et al. (2021) investigated the quality of groundwater in a total of 5119-square-kilometre areas of central Iraq around Babylon. The data for this analysis came from the relevant government departments including maps, well locations, and water quality data and since 2015. Following data collection, a base map of the focused area was developed. Using the geographical information system (GIS) environment, the analyzed water quality parameters were used as an attribute database to construct thematic maps. The water quality index and irrigation water quality index were determined for various groundwater samples using various parameters such as electrical conductivity, major cations and anions. In addition, indices such as Kelly's ratio (KR), sodium absorption ratio (SAR), residual sodium carbonate (RSC), soluble sodium percentage (SSP), and permeability index (PI) were used to determine the suitability of groundwater for irrigation, The GIS environment was used to create water quality index maps. The results showed that the groundwater in the studied area need special consideration before it can be used.

2.3 Concluding Remarks

From the introduced review of literature, the conceptual hydraulic modelling of groundwater, the assessment of the groundwater quality for drinking and irrigation purposes, and the assessment of groundwater pollution by heavy metals, and chemical elements were highlighted. Several remarks were diagnosed with their inferences as:

1) A conclusion that many studies carried out individually the quality assessment, water quantity or groundwater pollution by heavy metals. The present study gives a wide-ranging investigation upon all groundwater concern sectors.
2) Similar studies in or near the study area is limited.

Therefore, the present study investigates and assesses groundwater quality in Al-Mahaweel district, Babylon governorate, Iraq, using Water Quality Index (WQI), Heavy metals Pollution Index (HPI), and Heavy metal Evaluation Index (HEI) for drinking assessment. Seven different criteria were used to classify irrigation water statue, namely; Electrical Conductivity (EC), Sodium Adsorption Ratio (SAR), Residual Sodium Bicarbonate (RSBC), Sodium Percentage (SP) Magnesium Hazard ratio (MH), Permeability Index (PI) and Kelly's ratio (KR). All indices interpreted statistically by a group of groundwater quality parameters into a single value reflecting the environmental system's health. As well as, groundwater hydraulic simulation were conducted by GMS software and finally a graphical representation will be carried out for the distribution of the results via ArcGIS.

CHAPTER THREE

MATERIALS AND METHODOLOGY

CHAPTER THREE

MATERIALS AND METHODOLOGY

3.1 Introduction

In this chapter, the methodology that was used in this research is described in detail.

3.2 Sampling Methods

A field reconnaissance throughout the study area is necessary to conduct the fieldwork. First, the fieldwork was divided into two stages, one started during January 2021 for sampling during the wet season (winter), and the other started during May 2021 for sampling during the dry season (summer).

The groundwater wells were selected randomly (based on the spatial distribution regarding to spread throughout the study area, and being in duty during the study period) from private farms. All wells depths are not less than 10 m. The geographic coordinates per each well have been positioned via Global Positioning System (GPS) device, and the well's depth are measured in situ. All the geometric characteristics are given in Table (3.1) and Figure (3.1) which was made using Arc-Map software.

Table (3.1): Geometric characteristics of the studied wells.

Well No.	Sample code	Coordinate (East)	Coordinate (North)	Elevation a.s.l. (m)	Drilling depth (m)
1	w1	454987.598	3615142.039	29.0	22
2	w2	459807.136	3613318.212	28.0	15
3	w3	453880.9	3614934.7	32.0	11
4	w4	452868.4	3612307.2	30.0	11.5
5	w5	458465.9	3607273.6	28.0	11
6	w6	461986	3602591.9	28.0	12
7	w7	477958.6	3601105.7	27.0	10.5

Table (3.1): Continue.

Well No.	Sample code	Coordinate (East)	Coordinate (North)	Elevation a.s.l. (m)	Drilling depth (m)
8	w8	461932.1	3600890.2	30.0	10
9	w9	447317.263	3613219.861	34.0	12
10	w10	446192.4	3623714.6	30.0	12
11	w11	443779.4	3625102.7	34.0	14
12	w12	443304.3	3612083.1	35.0	12
13	w13	443311.2	3611037.5	32.0	12

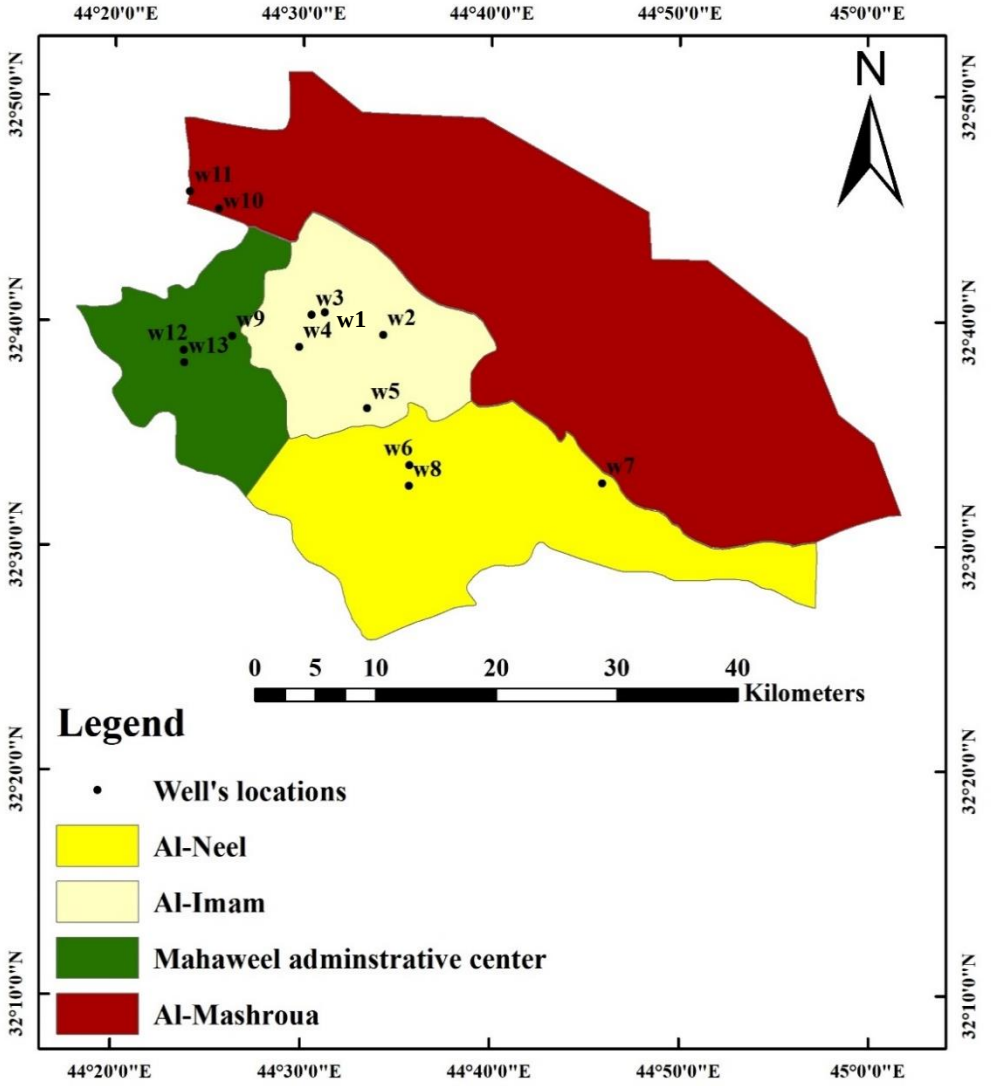

Figure (3.1): Layout map for wells distribution in the the study area.

3.2.1 Groundwater Sampling

The study area includes thirteen wells (from private farms), the groundwater samples were extracted and collected after pumping water for 15 minutes of steady withdrawals, the samples were stored in new clean and dry polyethylene bottles of 1.5 liters in capacity. The sampling bottles were rinsed three times with the groundwater, after that, the bottles were completely filled up and labeled by a specified code as shown in Figure (3.2).

Figure (3.2): Groundwater sampling process.

The groundwater samples were physically and chemically analyzed to obtain the temperature (T in °C), pH, electric conductivity (EC µs/cm) and total dissolved salts (TDS in ppm) in which measured in field. Four portable devices were used to measure these parameters, a thermometer, an electrical conductivity meter WTW (multi 350i), Germany, the total dissolved-solids tester (TDS) and pH meter that are manufactured by Hanna instruments Company, Romania, as shown in Figure (3.3).

Figure (3.3): Field measurements for pH, T in (°C), TDS in (ppm) and EC in (µs/cm) for groundwater samples.

Directly after that, the samples were reserve in an ice- box and transported to the laboratory subordinate to the consulting bureau of the collage of sciences in university of Babylon. The second set of samples were taken in May 2021 (represent the dry season during summer) by following the same steps and methods described above. The field work can be summarized in the flowchart illustrated in Figure (3.4).

3.2.2 Physio-Chemical Parameters for Groundwater Quality

Many chemical and physical parameters were measured to assess the quality of groundwater. Analytical methods that used in this research are as listed in Table (3.2).

Table (3.2): Methods of analysis implemented in the present research for quality of groundwater.

Parameter	**Description**	**Analytical Method**	**Work Method**
T (°C)	Temperature	Portable thermometer ± 0.1°C accuracy.	Field
pH	Concentration of hydrogen ion	pH test meter (portable).	
EC (µs/cm)	Electrical conductivity	EC test meter (portable).	
TDS (mg/l)	Total dissolved solid	TDS test meter (portable).	
TH, K^+, Na^+ (mg/l)	Hardness and Cations	Flame Photometer Model AFP 100 (AFP-100).	Laboratory
Mg^{+2}, Ca^{+2} (mg/l)	Cations	Titration with EDTA (EthyleneDiamineTetra Acidic Acid) ASTM, 1989.	
Cl^- (mg/l)	Anions	Titration with $AgNO_3$	
SO_4^{-2} (mg/l)	Anions	Gravimetric method with ignition of residue.	
HCO_3^- (mg/l)	Anions	Titration with HCl + methyl red indicator.	
NO_3^- (mg/l)	Anions	UV-visble spectrophotometer.	
Zn, Pb, Cd, Ni, Fe (ppm)	Heavy metals	Atomic-absorption spectrometer (APHA 3030A).	

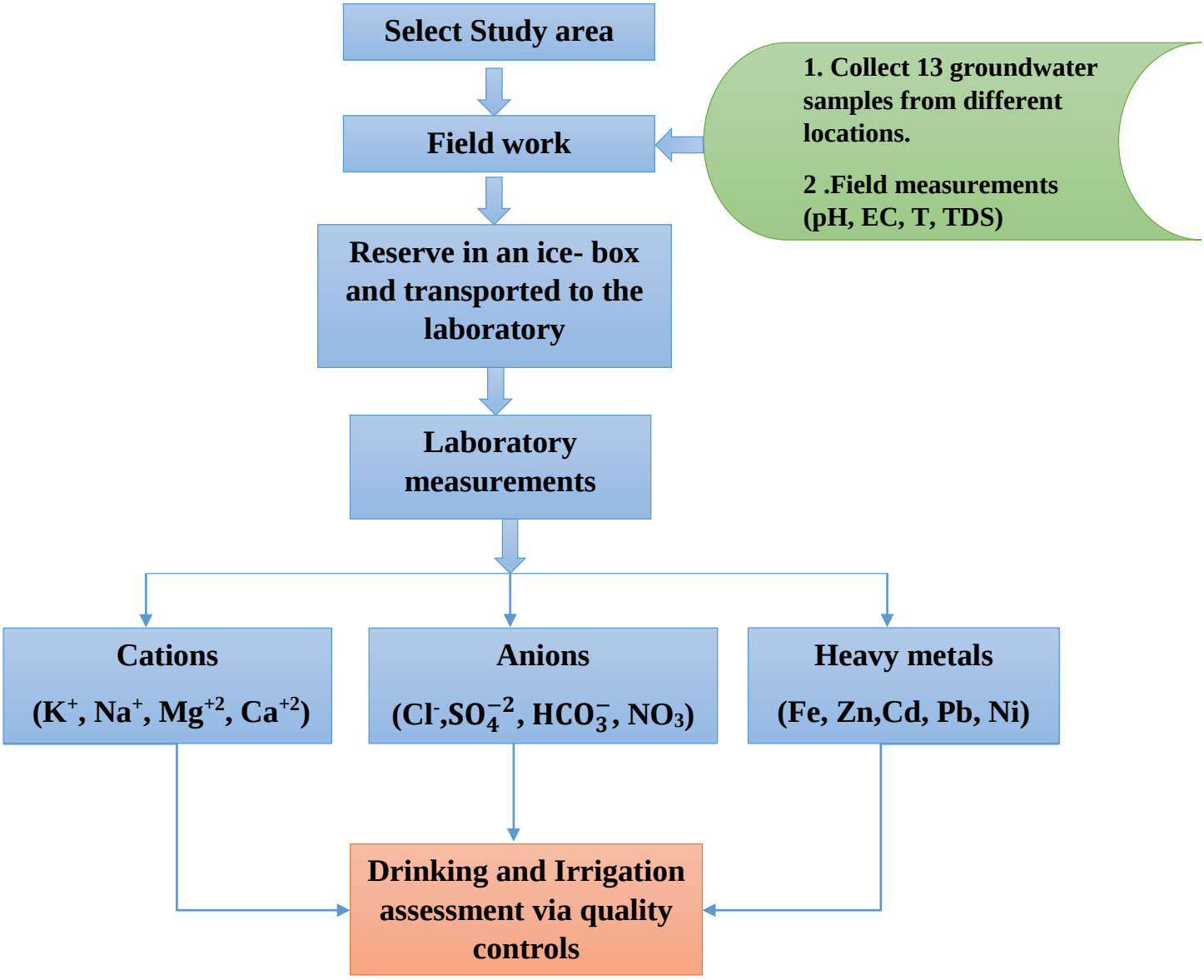

Figure (3.4): Methodology for field work in the present study.

3.3 Modeling Methodology

3.3.1 Hydraulic Modeling of Groundwater

The groundwater models are the result of three stages: system analysis, conceptual model creation, and then specifying the type of numerical solution, such as finite difference or finite elements (Al-Muqdadi, 2012). In order to solve the mathematical form of the groundwater model (i.e., the governing partial differential equation). Many codes have been written to solve the governing equations for various geological, spatial, and hydrogeological conditions, such as the MODFLOW code.

Laplace's equation development enables the possibility to explain the flow in a steady state, in which the storage term equals zero and the difference between the two states is unchanged or become constant with time (Al-Areedhi and Khayyun, 2019). In this research, the steady state groundwater model is used and solved by finite difference method.

Groundwater Modeling System (GMS) is a software developed by Aquaveo limited liability Company in Provo, Utah, in 1990. GMS a groundwater modeling and simulation software characterized generally, with a graphical user interface, the ability of working with variety of programs such as GIS, EXCEL and AutoCAD, and including various numerical models like (MODFLOW, MODPATH, PEST,…etc.), that, simplifying the entry and dealing with the large data required. The United States Geological Survey USGS developed MODFLOW, a three-dimensional numerical model of cell-centered finite difference; MODFLOW package supported by GMS can be used for both steady state and transient simulations. Estimation of groundwater levels and movement directions as well as prediction of groundwater levels changes in relation with climate conditions over long future periods ….etc. this program offers great facilities to represent and reflect the realty of field with high accurate results. It also handles with all groundwater problems, regardless of their difficulty in terms of

geological structure and tectonic conditions hydrogeological, which make it easy to understand by decision-makers.

GMS introduce two different approaches in order to construct MODFLOW numerical model that are the grid and conceptual approach. The grid approach works directly with the 3D grid and applies sources/sinks, and other model parameters on a cell-by-cell basis while the conceptual model approach uses the GIS tools in the map module to develop a conceptual model of the site being modeled. The location of sources/sinks, layer parameters (such as hydraulic conductivity), and all other data necessary for the simulation can be defined at the conceptual model level and once the conceptual model is complete, the grid is generated, the conceptual model is converted to the grid model, and all of the cell-by-cell assignments are performed automatically (GMS user manual, 2018). In this research, the conceptual model approach will be used for the construction of simulation model.

3.3.2 Analysis of Groundwater Flow in Porous Media

By Combining of both continuity equation and Darcy's law yielded the governing equation of flow of groundwater through porous media. Based on the law of conservation of mass, and for three dimensional flow, the mathematical simulation of three-dimensional flow for both steady and unsteady flow conditions in GMS is governed by (Abed and Hussain, 2020).

$$\frac{\partial}{\partial x} k_x h \frac{\partial h}{\partial x} + \frac{\partial}{\partial y} k_y h \frac{\partial h}{\partial y} + \frac{\partial}{\partial z} k_z h \frac{\partial h}{\partial z} \mp W = S_y \frac{\partial h}{\partial t} \qquad (3.1)$$

In which; k_x, k_y, k_z are the hydraulic conductivity of soil in x, y, z Cartesian directions, respectively in (L/T), h is the groundwater head level (L), W is the flux per unit volume (T^{-1}) that is Subtracted if it's a withdrawal value and added if it's an added flow to groundwater, t is the time (T), and S_y is the specific yield for the aquifer medium. For the steady state of flow, Equation (3.1) will be reduced to the following:

$$\frac{\partial}{\partial x}k_x h\frac{\partial h}{\partial x}+\frac{\partial}{\partial y}k_y h\frac{\partial h}{\partial y}+\frac{\partial}{\partial z}k_z h\frac{\partial h}{\partial z}\mp W=0 \quad (3.2)$$

3.2.3 Preparing of the Conceptual Model

The conceptualization of the flow system for the study area is the next step into a simple numerical data can be inputted to the program. The conceptual model requires a large field data to describe the really groundwater flow and then to be running with high efficiency and accuracy. The input data for this study were obtained from Ministry of health and environment, directorate of environment in Babylon (DEB, 2019), Ministry of water resources, directorate of water resources in Babylon (DWRB, 2019), Iraqi meteorological organization and seismology in Baghdad (IMOS, 2019), general commission of groundwater in Baghdad (GCGW, 2019), Al- Mawal company for soil investigations (Al-Mawal, 2019) and Babylon construction laboratory (BCL, 2019). The following steps are present a detail explanation for the methodology for creating of conceptual model.

3.3.3.1 Exporting base imagery map

Initially, select the display projection and units system. The differences in input parameter projections result in non-correspondence of input parameters within coverage, and an error within the tolerance of the operating model (Al-Areedhi and Khayyun, 2019). The selected projection display for the current modeled area is UTM (Universal Transverse Mercator) Projection; Zone 38 (42°E - 48°E Northern Hemisphere); Meters Planar Units, and units type is (meter) for length and (day) for time.

The base map for the modeled study area was obtained from directorate of water resources in Babylon as shown in Figure (3.5), this base map was georeferenced using Arc-Map 10.3 software. Then, the base map imported to GMS software and prepared to define boundary conditions.

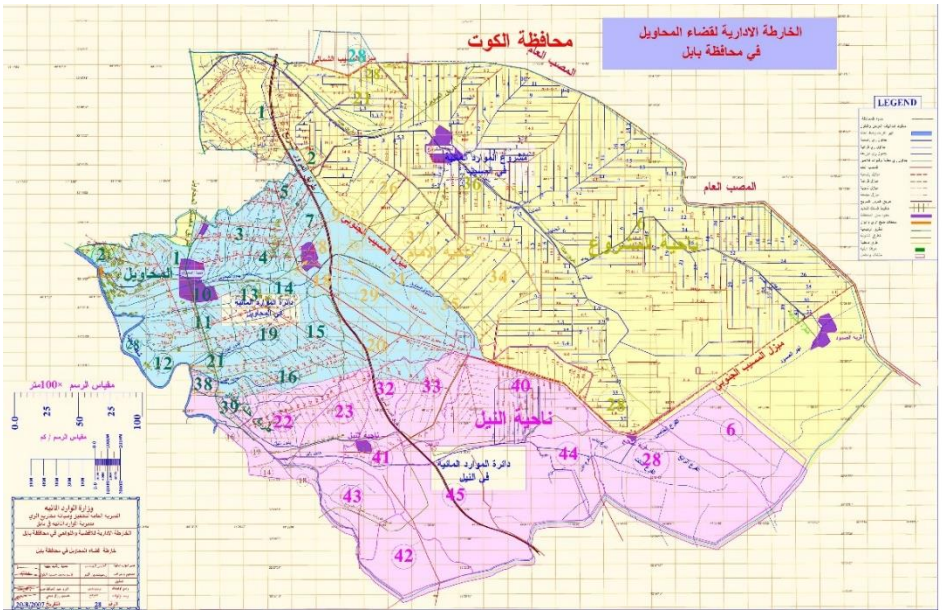

Figure (3.5): Base map for the study area (DWRB, 2019).

3.2.3.2 Preparing of 3D grid

From create arc tool, the boundaries of the area are drawn and modeled, by pressing right click in the project explorer, and from new select 3D grid, the finite difference grid dialog will opened. A cell centered cells is defined with $\Delta x=\Delta y=$ 120 and single layer in Z direction. The limits of X, Y, and Z directions were (70510, 48702.5, and 10) m, respectively. Since this study focuses on shallow groundwater, the thickness of cells is considered as the reservoir's height, in which to be 10 m (Hadi and Alwan, 2020). The total cells number is 14400 with 7162 active cells and 7238 inert cells as shown in Figure (3.6). 2D maps were adopted only for display purpose.

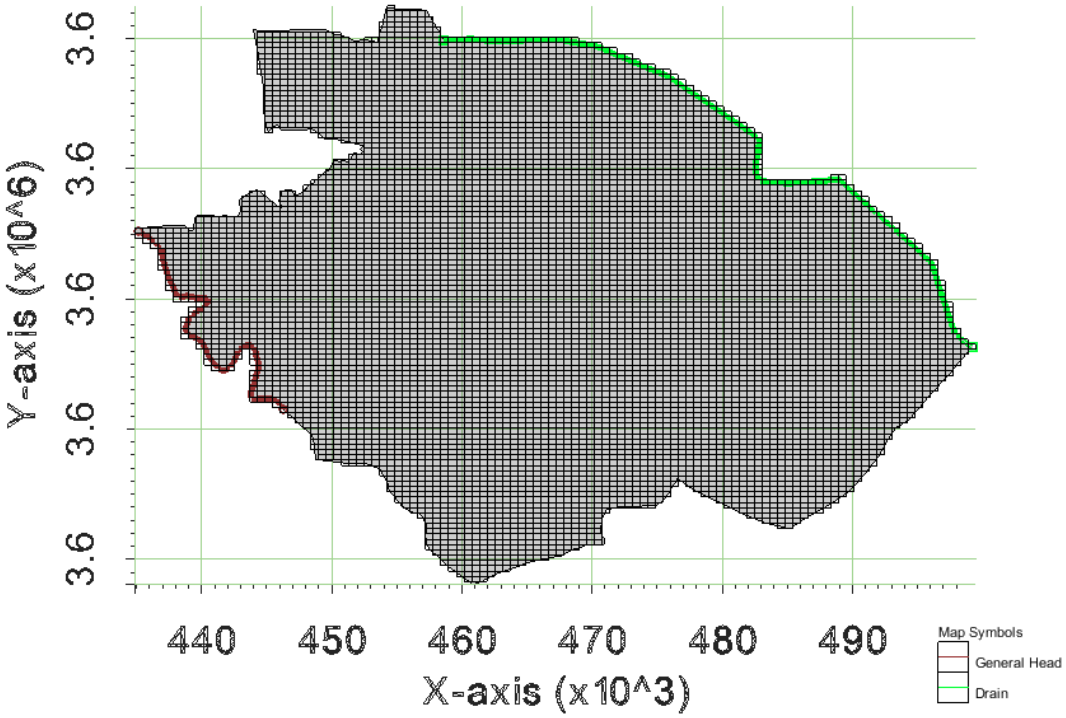

Figure (3.6): Grid of the modeled study area.

3.3.3.3 Boundary conditions

The boundary conditions that are applied for the steady- state of water flow in porous media are either a dependent variable (head) or the derivative of the dependent variable (flux) on the model boundaries. The boundaries can be physical or hydraulic. For example, impermeable rock, lakes or waterways are common types of physical, on other hand, water divides or flow lines are common examples of hydraulic boundaries (Anderson and Woessner, 1992). In MODFLOW, the constant-head, inactive or variable head cells are frequently used.

To estimate head at specific locations, numerical models use an approximate form of the governing equation. The finite-difference (FD) and finite-element (FE) methods are the most often used numerical methods in groundwater modeling. In the present research FD will be applied at steady state flow. In FD method, nodes are designated by i, j, k indices, which here represent the column, row, and layer, respectively, of a node

in 3D space. The spacing of nodes along rows is designated by Δx and the spacing along columns by Δy, while the spacing between layers is Δz. The node is situated within an FD cell or block. Heads are defined only at nodes and the head at a node represents the average head in FD cell. An approximate form of the governing equation is written by replacing the partial derivatives in Equation (3.1) by differences. For example, for a representative node, i, j, k, in a grid with uniform nodal spacing in the x-direction (Δx = constant), the approximation to the first derivative of h with respect to x is:

$$\frac{\partial h}{\partial x} = \frac{h_{i+1,j,k} - h_{i-1,j,k}}{2\Delta x} \tag{3.3}$$

Where $2\Delta x$ is the distance between the nodes $h_{i+1,j,k}$ and $h_{i-1,j,k}$. The finite difference approximation for equation (3.1) can be expressed by (Anderson and Woessner, 1992):

$$\begin{aligned}
&\frac{1}{(\Delta x)_{i,j,k}}\left[k_{x_{i+\frac{1}{2},j,k}}\frac{h_{i+1,j,k}^{n+1} - h_{i,j,k}^{n+1}}{\Delta x_{i+\frac{1}{2},j,k}} - k_{x_{i-\frac{1}{2},j,k}}\frac{h_{i,j,k}^{n+1} - h_{i-1,j,k}^{n+1}}{\Delta x_{i-\frac{1}{2},j,k}}\right] \\
&+\frac{1}{(\Delta y)_{i,j,k}}\left[k_{y_{i,j+1/2,k}}\frac{h_{i,j+1,k}^{n+1} - h_{i,j,k}^{n+1}}{\Delta y_{i,j+1/2,k}} - k_{y_{i,j-1/2,k}}\frac{h_{i,j,k}^{n+1} - h_{i,j-1,k}^{n+1}}{\Delta y_{i,j-1/2,k}}\right] \\
&+\frac{1}{(\Delta z)_{i,j,k}}\left[k_{z_{i,j,k+1/2}}\frac{h_{i,j,k+1}^{n+1} - h_{i,j,k}^{n+1}}{\Delta z_{i,j,k+1/2}} - k_{z_{i,j,k-1/2}}\frac{h_{i,j,k}^{n+1} - h_{i,j,k-1}^{n+1}}{\Delta z_{i,j,k-1/2}}\right]
\end{aligned} \tag{3.4}$$

There are four types of boundary conditions that represent the most common specified head and specified flux conditions as following (Al-Mussawy and Kalaf, 2013; Anderson and Woessner, 1992).

1. Specified head boundaries (Dirichlet Condition) in which, the hydraulic head was specified. Since total head, h, is known, an equation for head is not needed along the boundary.

2. Specified flow boundaries (Neumann Condition) where the flow across the boundary is prescribed. Known flux or specific discharge (mass per unit volume per unit time).
3. Head dependent boundaries HDB (Cauchy Condition) where the flow across the boundary is calculated from a given value of the head. Mathematically, volumetric flow rate, Q (L^3/T), across an HDB is computed using equation (3.5):

$$Q = C\Delta h \qquad (3.5)$$

Where Δh is the difference between user-specified boundary head and the model-calculated head near the boundary, C is conductance (L^2/T), which is computed using hydraulic conductivity (K) times area (A), divided by the distance (L) between the locations of user-specified boundary head and the model-calculated head.

4. Impermeable boundary in which the prescribed flux boundary is referred to as no-flow, or zero flux. It is modeled by setting grid blocks as inactive (i.e. hydraulic conductivity = 0).

Groundwater flows parallel to a streamline so that, by definition, no water crosses a streamline. Thus, streamlines can serve as groundwater divides that form hydraulic no-flow boundaries, one way to determine if a hydraulic streamline boundary is affecting modeling results is to replace the no-flow boundary with specified heads and re-run the model. If flow to or from the specified boundary nodes is insignificant, the assignment of a hydraulic no-flow boundary at that location is appropriate (Anderson and Woessner, 1992).

The number of flow boundaries were specified based on the general slope for land surface of the study area, and previous studies. Accordingly, Shatt Al-Hilla was specified as general head and Al-Massab AL-A'am as a drain as shown in Figure (3.7).

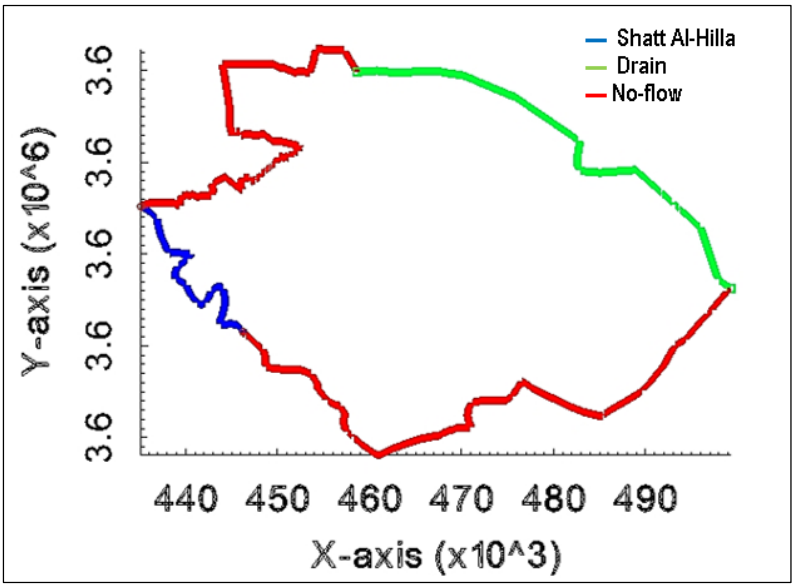

Figure (3.7): Boundary conditions of the modeled study area.

3.3.3.4 Conceptual model coverage

The completion and run of the conceptual model required to add other layers to define the rest of model coverage such as sources/sinks, areal properties and observation points. Al-Mahaweel conceptual model consists of six coverages as shown in Figure (3.8).

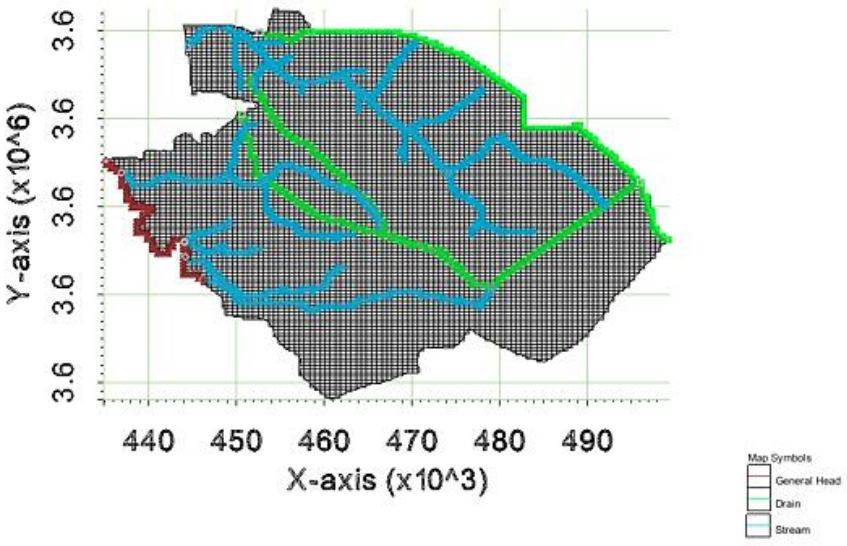

Figure (3.8): Coverages of the conceptual model for the study area.

This was followed by running MODFLOW program, from display options the grid could be displayed as contour lines representing the groundwater head levels after calibration process. Next, input all coverages in MODFLOW list to check simulation as shown in Figure (3.9).

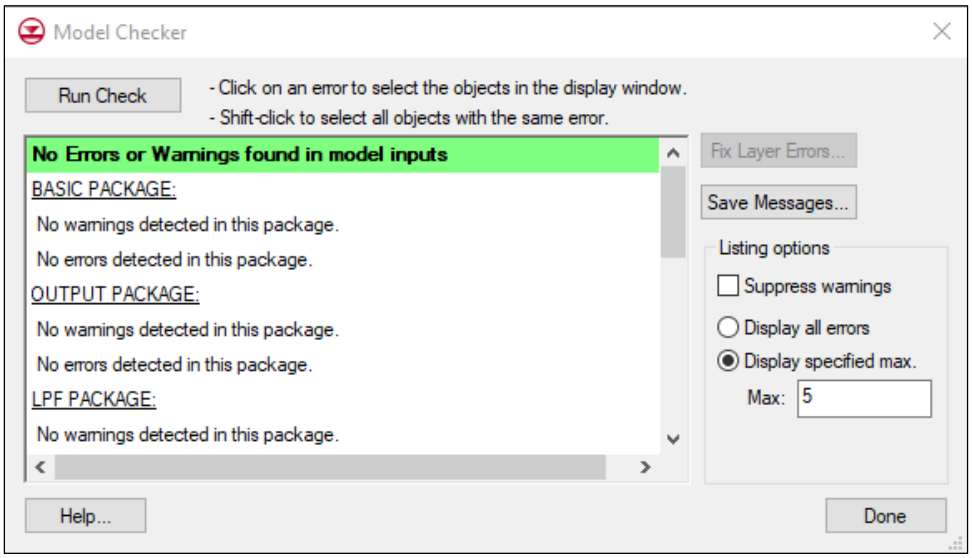

Figure (3.9): Simulation of model error check.

3.2.3.5 Estimation of hydraulic parameters

Estimation of hydraulic parameters such as hydraulic conductivity and recharge rate can be implemented by PEST tools under GMS software. The estimation process is carried out after input initial values of parameters and specify a range of maximum and minimum expected values. The modeled area will be divided into four administrative units. Initial guess values were adopted from (Al-Mawal, 2019) and (BCL, 2019) as shown in Figure (3.10) the value column.

As reported by (Al-Areedhi and Khayyun 2019), because Iraq is located in arid and semi-arid regions, the accurate estimation of recharge is essential since such regions mostly depend on rainfall. The initial guess of recharge is calculated according to metrological records for the year 2019 (after IMOS, 2019), in which, the annual average of rainfall amount was 141.7mm, consequently, the calculated recharge rate was

0.000019 m/day, for only 5% of daily average rainfall is counted to be a groundwater recharge (GMS user manual, 2018). Figure (3.11) presents the flow chart for the methodology of the hydraulic modeling used in this study.

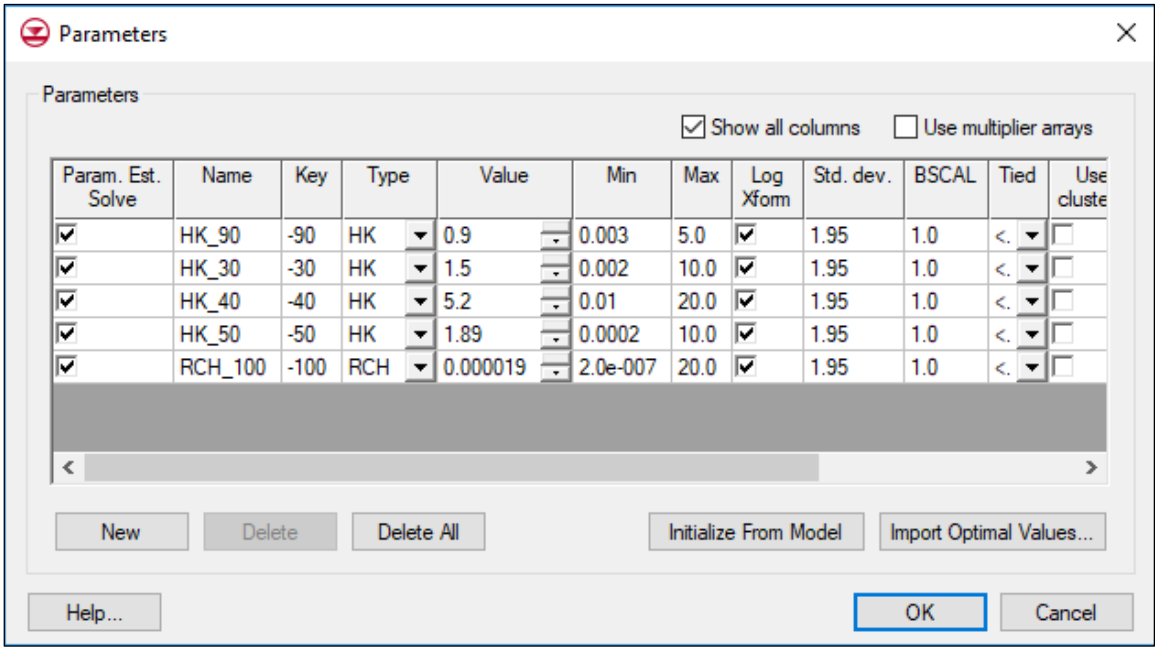

Figure (3.10): Parameters estimation via PEST tools for study area.

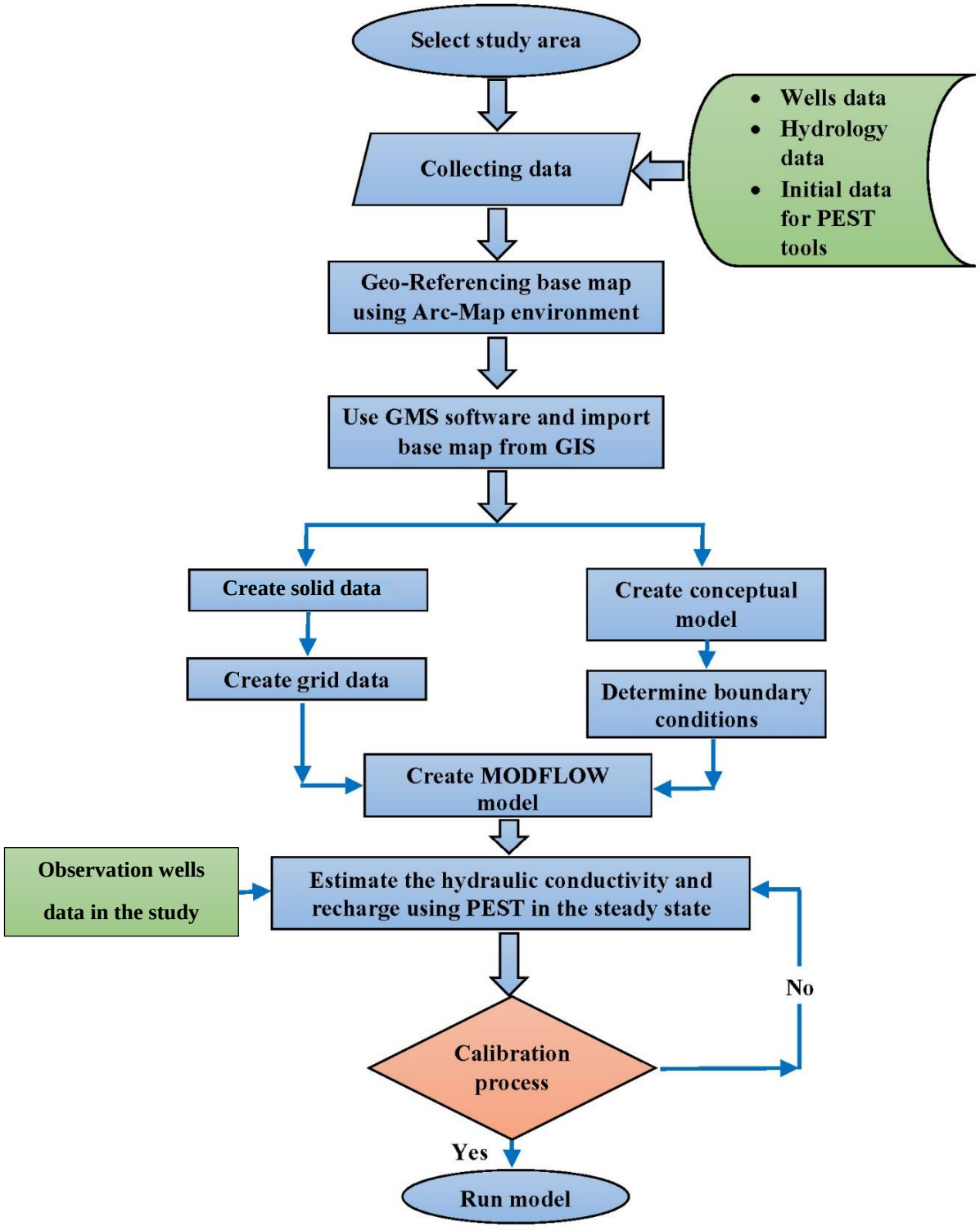

Figure (3.11): Methodology for hydraulic modeling in the present research.

3.3.4 Spatial Distribution Representation

For the purpose of full-scale representation of the studied hydraulic variables, a spatial distribution techniques will be used in this section, a well exploration of obtained results is targeted therefrom.

The Inverse Distance Weighted (IDW) spatial interpolation technique was used in this research to obtain thematic maps of all the parameters included in the hydraulic modeling of groundwater in the study area. It is also used to forecast unknown values based on known values (Burrough et al., 2015)

The IDW method is the most commonly used point data interpolation approaches, based on the concept that the interpolating area surface should be influenced more by adjacent points and less by points for distant, and weight assigned to each point on an interpolated area surface decreases as the distance to the interpolation place increases, resulting in a weighted average of the point data (Al-Areedhi and Khayyun, 2019). The IDW model can be expressed by Equation (3.6) (Aquaveo, 2019):

$$F(x,y) = \sum_{i=1}^{n} w_i \, C_i \qquad (3.6)$$

Where n represents the number of points were used to interpolate, C_i represents the data set values (parameter's measured concentrations) and w_i represents the weight functions given to each point.

3.4 Qualitative Criteria of Groundwater

In this research, a comprehensive assessment will be achieved for the drinking and irrigation purposes. Three indices where used to evaluate and compare the groundwater quality for drinking purpose, that is, Water Quality Index (WQI), Heavy metal Pollution Index (HPI) and Heavy metal Evaluation Index (HEI) this indices will be calculated according to the limitation of (WHO, 2011) and (IQS, 2001) which are listed in Appendix (A) . In addition, the water quality for irrigation uses was evaluated by irrigation suitability classification measures, which are the Electrical Conductivity

(EC), Sodium Adsorption ratio (SAR), Residual Sodium Bicarbonate (RSBC), Soluble Sodium Percentage (SSP), Magnesium Hazard ratio (MH), Permeability Index (PI) and Kelly's Ratio (KR).

The evaluation process involved in this research included groundwater samples during the study period that extracted from wells extended on the study area. Table (3.3) summarized the evaluation indices.

Table (3.3): Groundwater quality indices used in this research.

Index	**Formula**	**Definition**	**Interpretation of evaluations criteria**	**Reference**
WQI	$WQI = \sum_{i=1}^{n} \frac{W_i \times Q_i}{W_i}$ $W_i = \frac{K}{S_i}$ $K = \frac{1}{\sum 1/S_i}$ $Q_i = \left[\frac{(V_i - V_o)}{(S_i - V_o)}\right] \times 100$	In which; W_i: relative weight of the ith parameter, Q_i: quality rating scale for each contributed parameter in WQI calculations; K: proportionality constant V_i: concentration of ith parameter, V_o: recommended ideal value of ith parameter, S_i: standard concentration in mg/l and n: is the total number of parameters.	If WQI< 25: excellent (26- 50): good (51- 75): poor (76- 100): very poor > 100 unsuitable for drinking purpose.	(Brown et al., 1972)
HPI	$HPI = \frac{\sum_{i=1}^{n} W_i \times q_i}{\sum_{i=1}^{n} W_i}$	In which; q_i: sub- index of each parameter, W_i: weight of ith parameter, inversely proportional to S_i value, M_i; concentration value of ith parameter,	If HPI <19 low pollution, (19-38) medium > 38 high.	(Mohan et al., 1996) Cited by (Prasad and Bose, 2001)

Index	Formula	Definition	Interpretation of evaluations criteria	Reference
	$q_i = \sum_{i=1}^{n} \frac{\lvert M_i - I_i \rvert}{S_i - I_i} \times 100$	n: is the total number of parameters, S_i: standard concentration value and; I_i : ideal concentration value of ith parameter.		(Kumar et al., 2012)
HEI	$HEI = \sum_{i=1}^{n} \frac{H_c}{H_{MAC}}$	In which; H_c is the concentration of ith parameter, H_{MAC}: The ith parameter maximum concentration, n: is the total number of parameters.	If HEI < 400 low (400-800) medium > 800 high; contamination	(Edet and Offiong, 2002)
EC	---	In which; EC is measured in µS/cm.	If EC < 250: Excellent (250- 750): Good (750- 2250): Permissible (2250- 5000): Doubtful > 5000 Unsuitable	(Wilcox, 1954)
SAR	$SAR = \frac{Na^{+}}{\sqrt{(Ca^{+2} + Mg^{+2}}}$	In which; Na, Ca, and Mg are measured in meq./l.	If SAR < 10: Excellent (10-18) :Good (18-26) :Doubtful > 26 Unsuitable	(Richards, 1954)
RSBC	$RSBC = HCO_3^{-} - Ca^{+2}$	In which RSBC, HCO_3 and Ca in meq/l	If RSBC < 5 : satisfactory (5-10) : marginal > 10 unsatisfactory	(Gupta and Gupta, 1983) cited by (Ghalib, 2017; Rahman et al., 2017)

Index	Formula	Definition	Interpretation of evaluations criteria	Reference
SSP%	SSP% $= \frac{(Na^{+} +}{(Ca^{+2} + Mg^{+2} +}$	In which; Na, K, Ca, and Mg are measured in meq./l.	If SSP < 20: Excellent (20-40) :Good (40- 60): Permissible (60- 80): Doubtful > 80 Unsuitable	(Todd, 1980)
MH	MH $= \frac{Mg^{+2}}{(Ca^{+2} + Mg^{+2})} \times 100$	In which; Ca, and Mg are measured in meq./l.	Suitable <50 Unsuitable >50	(Raghunath , 1987)
PI	PI $= \frac{(Na^{+} + \sqrt{HC}}{(Ca^{+2} + Mg^{+2} +} * 100$	In which; HCO_3, Na, Ca, and Mg are measured in meq./l.	Class I >75 Excellent Class II 25-75 Good Class III < 25 Unsuitable	(Doneen, 1964)
KR	KR $= \frac{Na^{+}}{(Ca^{+2} + Mg^{+2})}$	In which; KR, Na, Ca and Mg are measured in meq./l.	Safe <1 Unsafe >1	(Kelley, 1963)

CHAPTER FOUR

RESULTS AND DISCUSSION

CHAPTER FOUR

RESULTS AND DISCUSSION

4.1 Introduction

In this chapter, the model calibration, running MODFLOW, model results as well as water quality parameters statistical results, spatial distribution and calculated indices results for the study period.

4.2 Modeling of Groundwater Flow in the Study Area

The GMS models simulate flow in two spatial dimensions were carried out to predict the hydraulic head distributions, and groundwater flow directions in the study area for both seasons, dry and wet.

The next key step is to calibrate the model. The calibration processes are an important part of any groundwater modeling, it is a process where certain parameters of the model such as recharge and hydraulic conductivity were changed in a systematic fashion and the model is repeatedly run until the computed solution matches field-observed values within an acceptable level of accuracy (Hussain et al., 2021). In order to calibrate the model, it is essential to add an observation coverage, which includes field observation data such as the groundwater level for selected well points. Based on previous studied (Abed and Hussien, 2020; Hadi and Alwan, 2020) an observed head confidence of 95% and observation interval of 0.25m were assigned. Extra data for fourteen wells were used in calibration process, in which collected from different reference (DEB, 2019; GCGW, 2019; Al-Mawal, 2019) and for the same time period.

Table (4.1) shows the geometric characteristics of the wells that used for calibrating the model.

Table (4.1): Geometric data of model calibration wells and calibration details.

Well No.	X-coordinate (East)	Y-coordinate (North)	Elevation a.s.l. (m)	Observed Head (m, a.s.l)
1	456435.9771	3611073.3803	28.0	27.0
2	441560.9551	3611580.6367	33.0	31.4
3	450151.5984	3610086.6344	30.0	29.2
4	451824.0995	3605674.9008	31.0	29.3
5	472332.6274	3602733.2721	26.0	24.6
6	472501.6215	3597805.9884	29.0	27.3
7	465112.963	3603772.0363	28.0	26.6
8	459806.1553	3613307.1489	26.0	24.3
9	453028.0	3618595.0	28.0	26.4
10	453440.0	3627540.0	32.0	30.3
11	462030.0	3624050.0	29.0	27.6
12	468100.0	3615510.0	28.0	26.2
13	477241.0	3616254.0	30.0	28.6
14	479286.0	3607903.0	29.0	27.5

The MODFLOW/ PEST module has been run to estimate the parameters hydraulic conductivity and recharge rates as given in Table (4.2).

Table (4.2): PEST module outputs.

Parameter / Value	HK_90	HK_30	HK_40	HK_50	RCH_100
Initial	0.9	1.5	5.2	1.89	0.000019
Computed	0.591668	3.84497	17.6699	3.80917	0.000012

The calibrated parameters were forward to the GMS software for the steady-state flow, accordingly, the simulation was ready to carry out hydraulic simulation for the groundwater flow in the steady area.

Finally, the sensitivity analysis for the model was performed. The basic principle of carrying out sensitivity analysis is to consider the effect exerted by the variance of the model parameters, and hydrogeological pressures on the aquifer environment, it helps to assess the importance of parameters in determining which data should be provided with high accuracy, and which data should provide with low accuracy (Hadi and Alwan, 2020). Figure (4.1) shows the sensitivity analysis obtained via plot wizard in GMS.

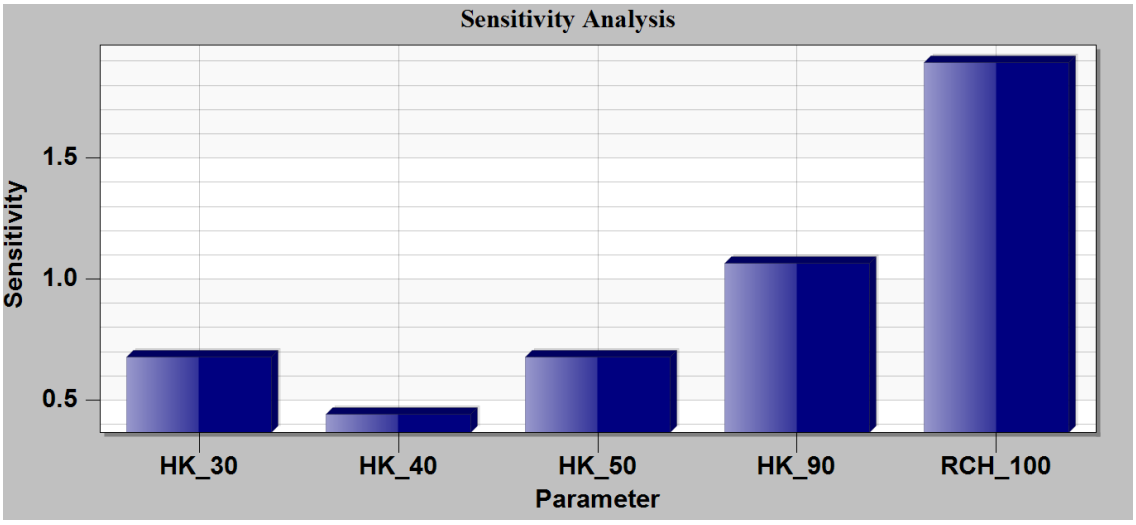

Figure (4.1): Sensitivity analysis for the parameters.

It obvious from Figure (4.1) that the recharge rate is more sensitive than hydraulic conductivity, therefore, it was essential to specified recharge rates precisely to prevent the divergence of result during calibration process. Calibration target Figure (4.2) have three degree of color (green, yellow and red) each one of them gives indication about the calibration result accuracy (Christensen and Cooley, 2003). If the error is within allowable limits, the column of the note will appear in green. If the error is slightly

above allowed limits, the column of note will appear in yellow. If the error is high, the column of the note will show up in red (Aquaveo, 2017).

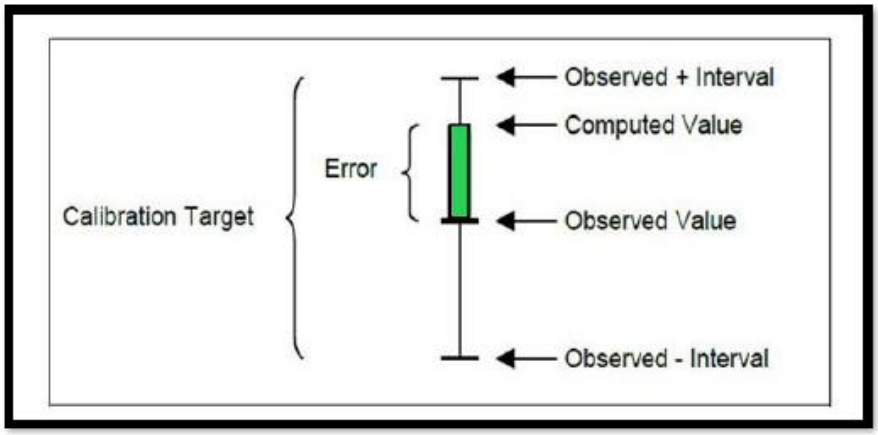

Figure (4.2): Calibration target.

In the present study a good match was obtained between observed and computed groundwater levels as shown in Figure (4.3).

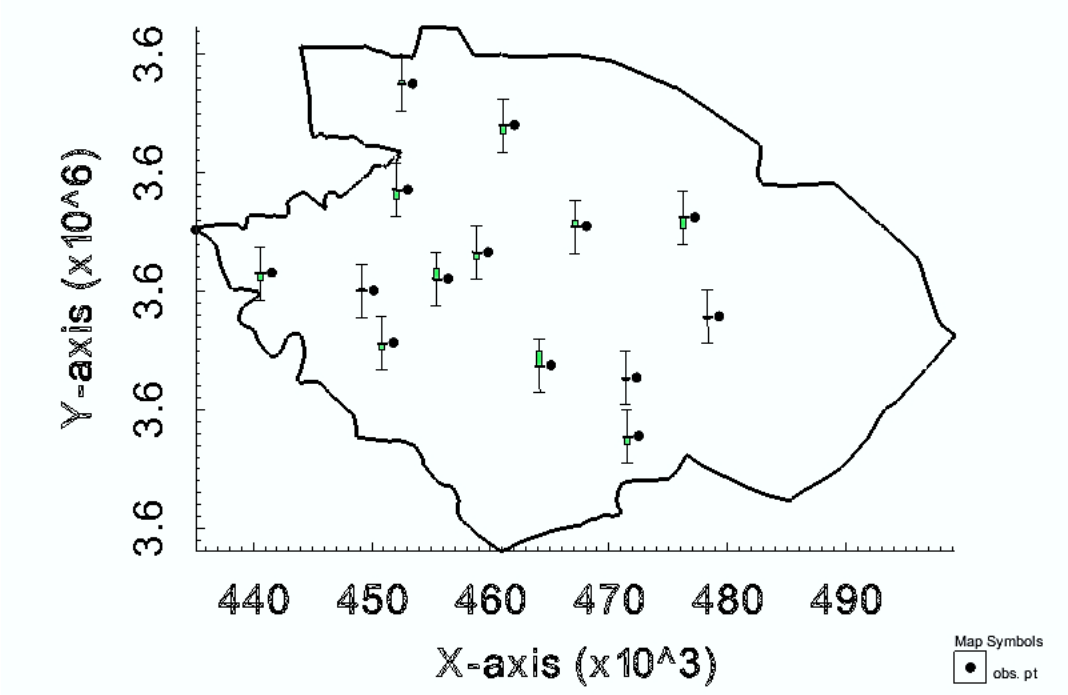

Figure (4.3): Present model calibration target.

The mean absolute percentage error (MAPE %) was used to measure the accuracy of the model prediction. The formula of MAPE is:

$$\text{MAPE} = \frac{1}{n}\sum_{i=1}^{n}\left|\frac{h^{i}_{\text{Obs.}} - h^{i}_{\text{Comp..}}}{h^{i}_{\text{Obs.}}}\right| * 100 \qquad (4.1)$$

In which;$h^{i}_{\text{Obs.}}$ and $h^{i}_{\text{Comp.}}$are the observed and computed heads in (m), respectively, and *n* is the total number of wells. Table (4.3) shows the comparison between observed and those computed by the model.

Table (4.3): Observed and computed groundwater levels.

well No.	**Observed Head (m, a.s.l)**	**Computed Head (m, a.s.l)**	**Residual Head, (m)**	**APE%**
1	27.0	27.19551	-0.19551	0.72
2	31.4	31.26669	0.13331	0.42
3	29.21	29.25957	-0.05957	0.20
4	29.3	29.17951	0.12049	0.41
5	24.6	24.56439	0.03561	0.14
6	27.3	27.16758	0.13242	0.49
7	26.7	26.88701	-0.18701	0.70
8	24.3	24.17515	0.12485	0.51
9	26.4	26.25154	0.14846	0.56
10	30.3	30.39706	-0.09706	0.32
11	27.6	27.46466	0.13534	0.49
12	26.3	26.42974	-0.12974	0.49
13	28.6	28.41013	0.18987	0.66
14	27.5	27.45525	0.04475	0.16

The MAPE value is about (0.45%) which indicates an acceptable mean deviation of model predictions that leads to conclude that the findings of the model are accurate.

Figure (4.4) shows the comparison between the observed and computed groundwater levels for the studied wells in the study area. It is obvious that the computed groundwater levels are strongly corresponding to those observed. This interpretation is supported by a high coefficient of determination (R^2) with a value of (0.97).

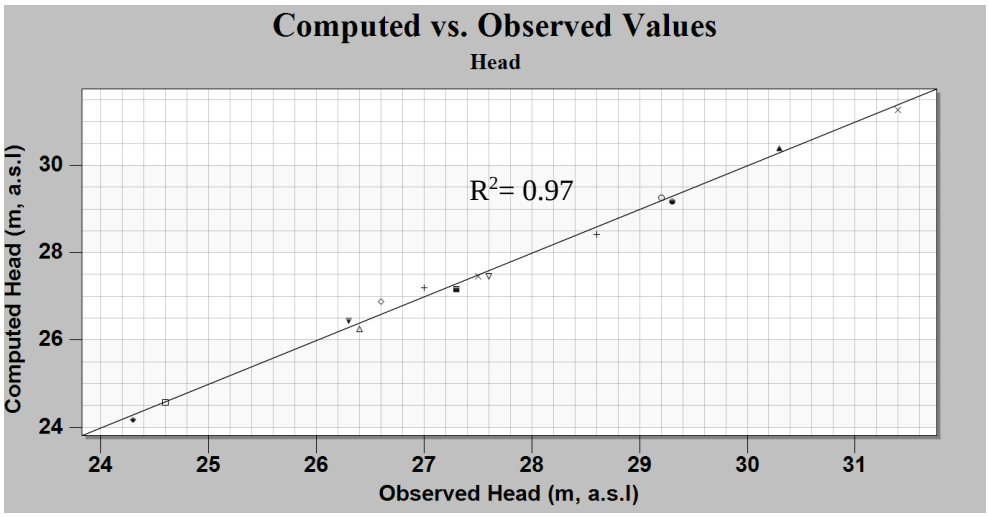

Figure (4.4): Comparison between computed and observed groundwater level for wells in the study area.

The mean absolute error (MAE) was used to measure the error accurate is the prediction model. The formula of MAE is:

$$\mathrm{MAE} = \frac{\sum_{i=1}^{n} \left| \mathrm{h}^{\mathrm{i}}_{\mathrm{Comp.}} - \mathrm{h}^{\mathrm{i}}_{\mathrm{Obs.}} \right|}{n} \qquad (4.2)$$

The root mean square error (RMSE) was used to measure the difference between the computed values by the model and those observed. The formula of RMSE is:

$$\mathrm{RMSE} = \sqrt{\frac{\sum_{i=1}^{n} \left(\mathrm{h}^{\mathrm{i}}_{\mathrm{Comp.}} - \mathrm{h}^{\mathrm{i}}_{\mathrm{Obs.}} \right)^2}{n}} \qquad (4.3)$$

The results of calibration error analysis is shown in Figure (4.5).

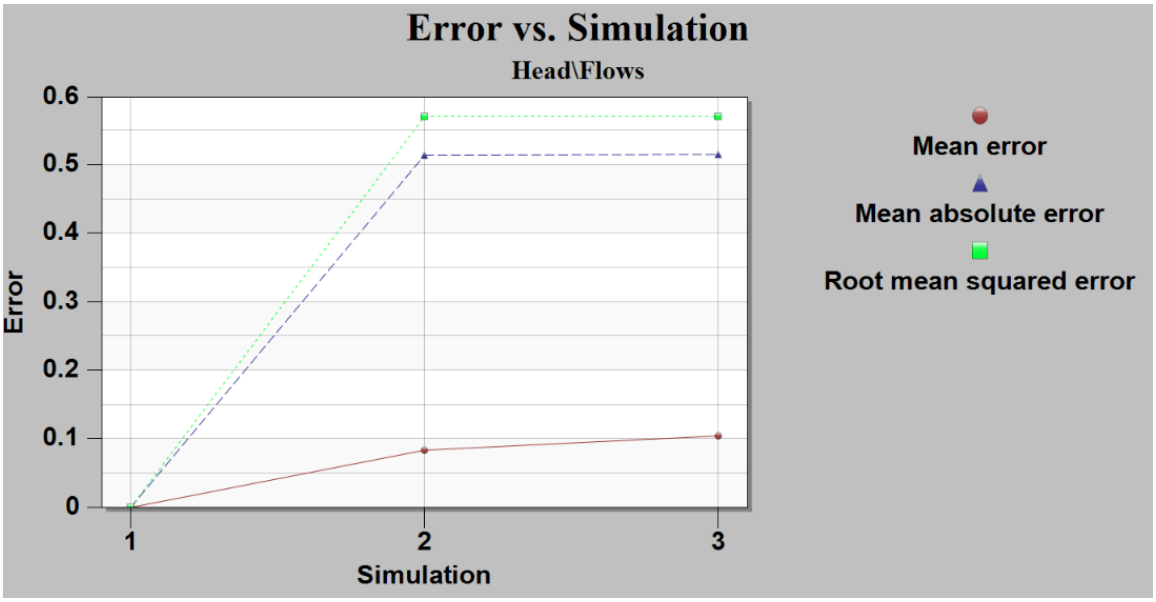

Figure (4.5): the model calibration errors.

From the results of Figure (4.5), the values of mean absolute error (MAE) and the root mean squared error (RMSE) were (0.45 and 0.55) m, respectively. Such results reveals that the conceptual model, boundary condition and final hydrological parameters used in the model are reliable.

The run of MODFLOW module was carried out by using the calibrated hydraulic parameter under steady state conditions for wet season as shown in Figure (4.6).

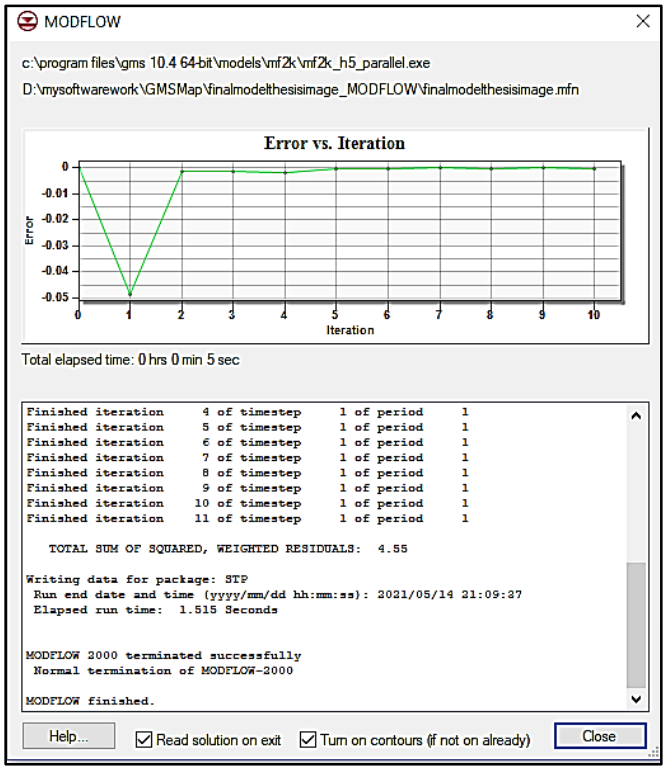

Figure (4.6): Screen shot for MODFLOW module running process.

The results for modeling of groundwater flow are shown in Figures (4.7), (4.8), and (4.9).

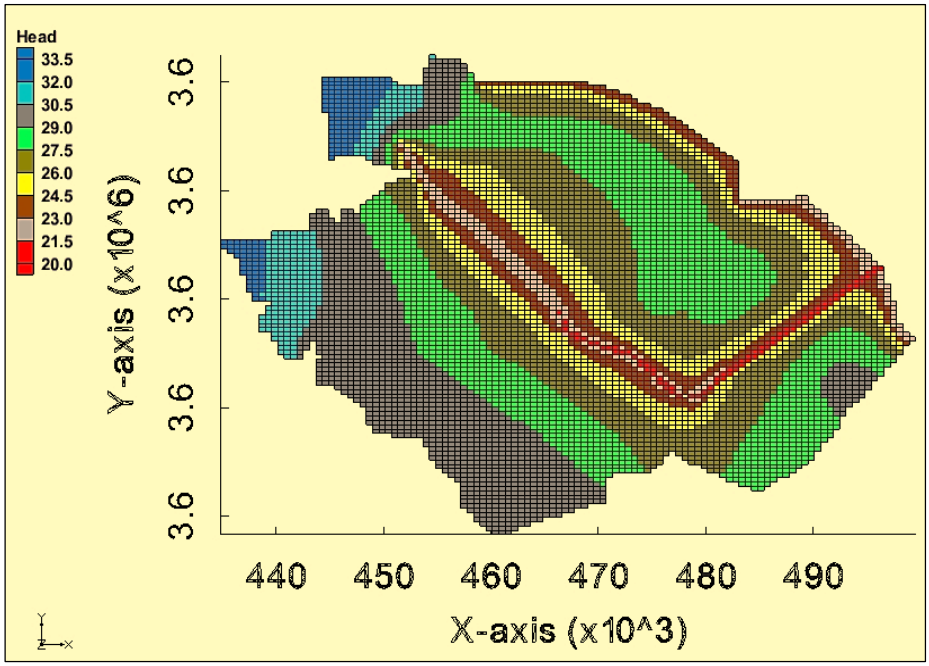

Figure (4.7): Map for groundwater heads distribution in study area at wet season.

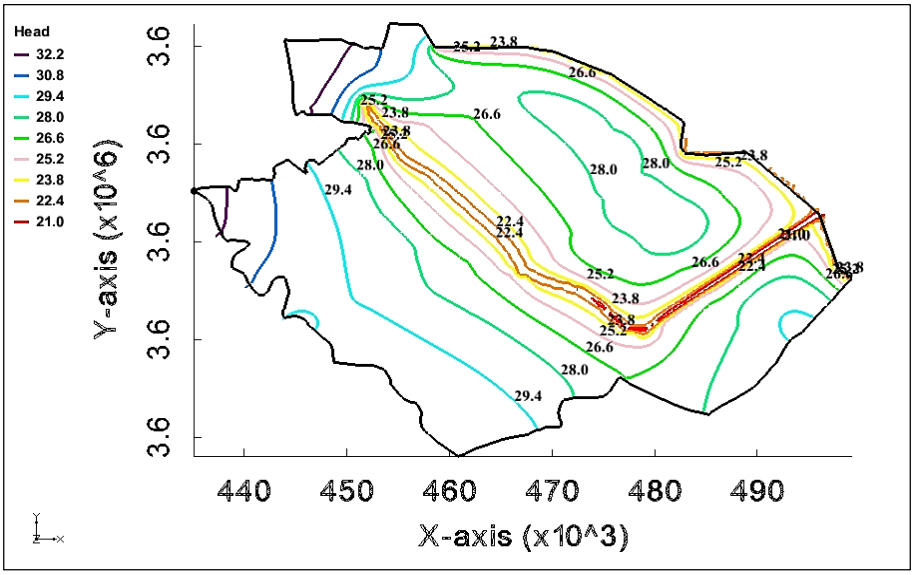

Figure (4.8): Contour map for groundwater levels in study area at wet season.

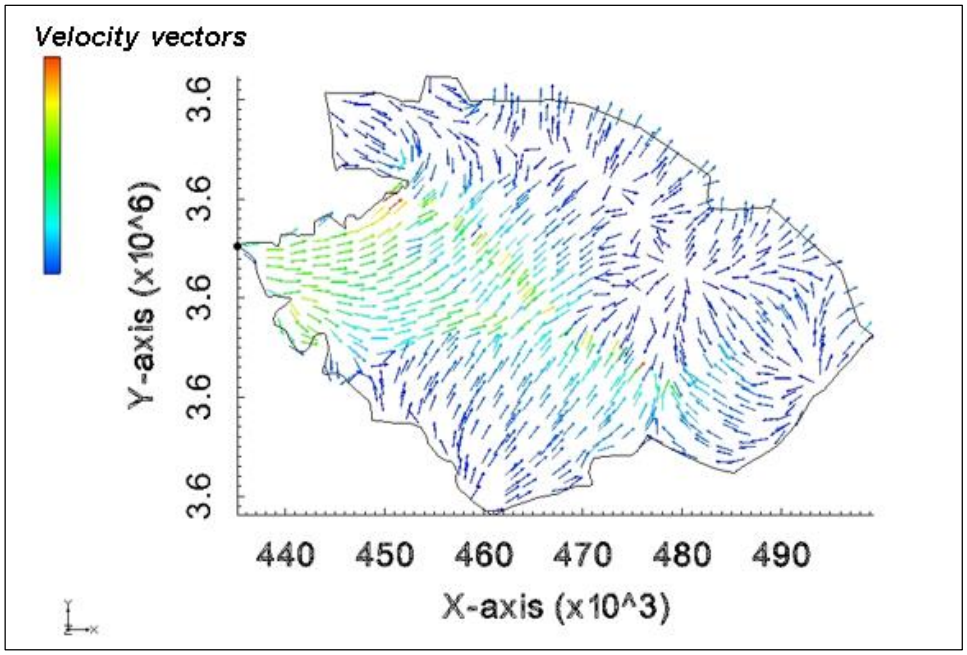

Figure (4.9): Groundwater movement directions map.

Figures (4.7) and (4.8) represent the modeled area with groundwater levels (heads) legend fixed on the left side, it is clear that the maximum groundwater levels was located in both Al-Mahaweel administrative center and Al- Mashroua district, with a range of 33.5 to 29 m above sea level, and it continue to drop toward northeast and south east respectively, until reaching its lowest value in Al-Musayyib Al-Janobi main drain, in the other hand Al-Neel and Al- Imam district shared the same range of water

levels of 20 to 30.5 m above sea level. Velocity vectors referring to the movement direction of groundwater overall study area is illustrated in Figure (4.9), with a minimum velocity value of 0.00001 m/day and maximum value of 0.05 m/day. It is clear that, the general direction of flow is from west and southwest to the north and northeast (i.e. towards main drains of study area) with a local deviation in directions due to the presence of streams and their branches. Finally, the flow budget of Al-Mahaweel district computed by MODFLOW under steady state is shown in Table (4.4). Negative sign indicates groundwater losses.

Table (4.4): Computed flow budget by MODFLOW.

Sources and Sinks	**In-flow (m^3/day)**	**Out-flow (m^3/day)**
Surface water bodies	1154.9851	955.7069
Drains	0	-2246.9542
Recharge (Rainful)	2049.5335	0
Total flow	3204.5186	-3202.6607
Summary	In flow -Out flow =1.858	Difference %= 0.058

According to the computed groundwater budget, as given in Table (4.4), the percentage of loosed water from the holding layers of groundwater to the three main drains (Al-Massab AL-A'am, Al-Mussayab Al-Janobi and Eskandaria-Mahaweel drain) in Al-Mahaweel district was about 2246.9542 m^3/day. While the total amount of recharge that supplied by rainfall were about 2049.5335 m^3/day, and that seeped by the surface water bodies to the groundwater was about 1154.9851 m^3/.

The second part of the modeling of groundwater flow is regarding the dry season (in summer). Due to the lack of enough information about the wells used during the dry season, the following scenario is adopted as nearly realistic for operating conditions in the summer season. In this scenario, only five production wells were used. Under such

circumstances, the productivity ranged from 2 to 5 Liters/sec on average operation time of 2 hours per day. The abstraction rate per each well and for summer season only (144 days of the year), can be calculated as:

$$= \left[3.4 \times 2 \times \frac{3600}{1000} \times 144\right] \times \left(\frac{5}{365}\right) = 48.3 \ \frac{m^3}{day}$$

The recharge rate (due to rainfall) is consider zero. The results for modeling of groundwater flow of dry season scenario are shown in Figures (4.10), (4.11), and (4.12).

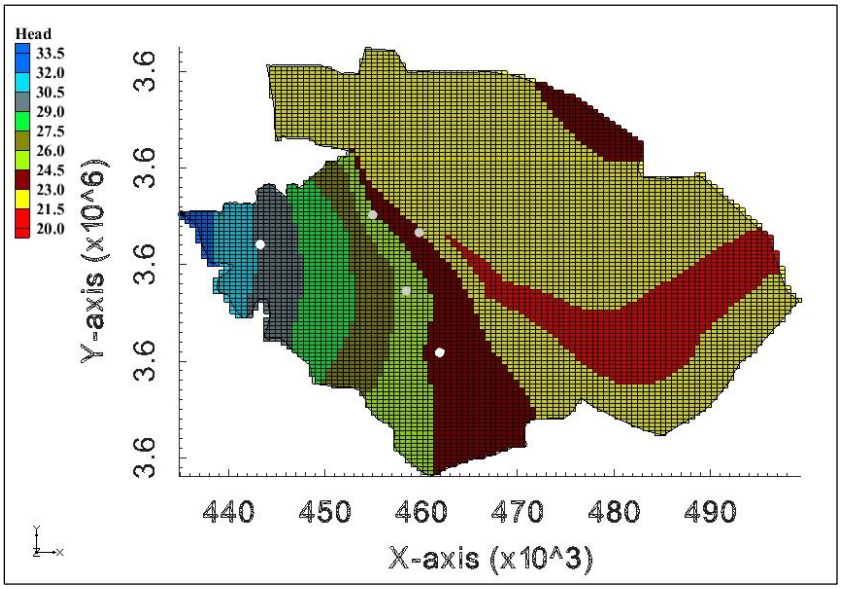

Figure (4.10): Map for groundwater heads distribution in study area at dry season.

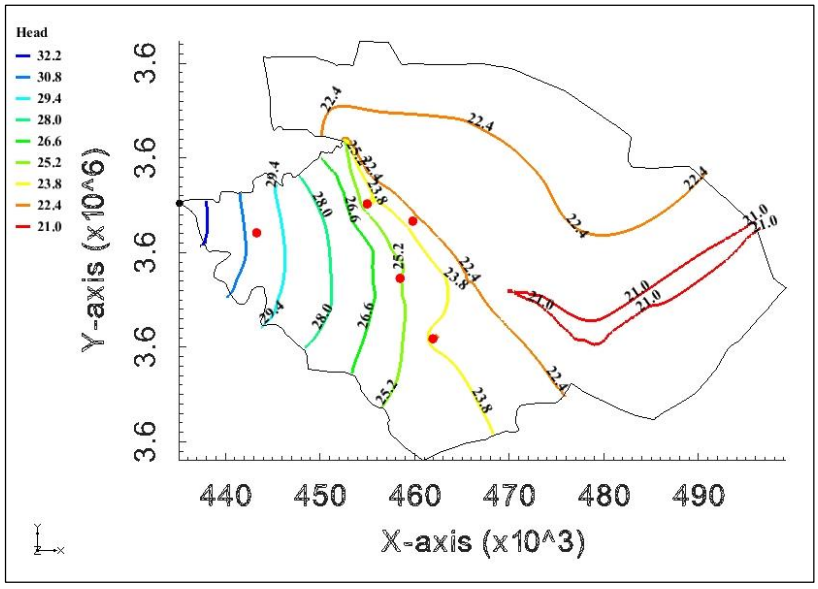

Figure (4.11): Contour map for groundwater levels in study area at dry season.

Figures (4.10) and (4.11) represent the modeled area with groundwater levels (heads) legend fixed on the left side for dry season scinario, it is clear that the maximum groundwater levels was located in Al-Mahaweel administrative center, with a range of 33.5 to 27.5 m above sea level, and it continue to drop toward northeast and south east respectively, until reaching its lowest value in Al-Musayyib Al-Janobi main drain, on the other hand Al-Mashroau district heads can be neglected here due to the lack of wells data within it. Velocity vectors referring to the movement direction of groundwater overall study area is illustrated in Figure (4.12), with a minimum velocity value of 0.00001 m/day and maximum value of 0.04 m/day. It is clear that, the general direction of flow is from west and southwest to the north and northeast (i.e. towards main drains of study area).

4.3 Analysis of Phyisco-Chemical Parameters in Groundwater Samples

The results obtained during this research regarding the physical and chemical parameters involved in the groundwater samples are analyzed and discussed in this section.

Weather conditions in the study area were recorded, that is during January 2021, thirteen water samples were extracted from wells located in the study area (winter season sampling), the temperature ranged from 10 to 18°C, relative humidity ranged from 28% to 67% and the wind speed was ranging from 10 to 21km/hr. Whereas, for the summer season, i.e., May 2021, the re-sampling process again, in which the temperature ranged from 32 to 40°C, relative humidity ranged from 10% to 26% and wind speed was ranging from 0 to 18km/hr.

4.3.1 Characterization of the Physical Parameters

The descriptive statistics for physical parameters of the collected groundwater samples are given in Tables (4.5) and (4.6) for both winter and summer seasons, respectively.

Table (4.5): Summary of descriptive statistics of pH, EC, TH, T, and TDS for winter season.

Parameter / Statistics	pH	EC (µS/cm)	TH (mg/l)	T (C°)	TDS (mg/l)
Mean	7.42	4086.77	1169.23	22.73	2896.31
Maximum	7.7	9150	2340	23.7	6220
Minimum	7.2	1518	520	20.2	968
Median	7.40	2990	840.00	22.90	2060.00
Standard Deviation	0.15	2603.07	645.68	0.84	1960.30
Sample Variance	0.02	6775951.69	416907.69	0.71	3842789.06
Standard Error	0.04	721.96	179.08	0.23	543.69
Kurtosis	-0.63	-0.88	-1.03	7.48	-1.26
Skewness	0.44	0.74	0.66	-2.46	0.68

Table (4.6): Summary of descriptive statistics of pH, EC, TH, T, and TDS for summer season.

Parameter / Statistics	pH	EC (µS/cm)	TH (mg/l)	T (C°)	TDS (mg/l)
Mean	7.05	4517.77	1373.85	23.44	3588.69
Maximum	7.3	9430	2860	24.4	8050
Minimum	6.7	1532	600	22.3	1357
Median	7.1	2940	990	23.3	2734
Standard Deviation	0.19	2889.28	740.91	0.55	2395.56
Sample Variance	0.04	8347914.53	548942.31	0.30	5738715.56
Standard Error	0.05	801.34	205.49	0.15	664.41
Kurtosis	0.12	-1.05	-0.48	0.54	-0.87
Skewness	-0.71	0.76	0.83	-0.30	0.83

As illustrated in Table (4.5), the pH values ranged from maximum value of 7.7 that was recorded in well no. (w5) and a minimum value of 7.2 in well no. (w3) with a mean value of 7.42. In general, the pH value falls with for the alkaline water, which was attributed to solutes that have a buffering effect, indicating that H^+ ions are compensated by OH^- ions as cited by Pradeep et al. (2012). In other words, due to interactions between soil and water, such as limestone dissolution and calcite dissociation equilibrium ($CaCO_3 + H_2O \rightarrow Ca^{+2} + HCO^-_3 + OH^-$) as indicated by Ahmad et al.(2020). Despite the pH has no significant effect on human health, all biochemical reactions are sensitive to variation of pH (Subba Rao and Krishna Rao, 1991).

Results of Table (4.6) reveals that the pH values ranged from maximum value of 7.3 in wells no. (w1 and w13) and minimum value of 6.7 in wells no. (w2 and w7), this could be attributed to the use of fertilizers in the farms near well locations (Ahmad et al., 2020). However, for the two seasons all pH values were within the permissible limits WHO (2011) and IQS (2001) for drinking water.

The high saline water is toxic to the plants and may lead to salinity hazards (Borecka et al., 2016). The total salinity measured by using the electrical conductivity (EC), the maximum EC value in well no. (w3), the minimum value in well no. (w11), and the mean value of 4086.77 µS/cm, were all recorded for the winter season. The cause behind the increase in water salinity may be due to the leaching of salts from surface soil strata by the infiltration and percolation processes accompanying the rainfall to the groundwater in the winter season. In the summer season, well no. (w7) has recorded the maximum value and well no. (w11) has recorded the minimum value; such increase could be explained by the fact of the aridity of Iraq's climate with the interruption of rainfall, the decreasing recharge of the groundwater, and high evaporation rates could be the reason for the concentration of salts in groundwater. According to Abbasnia et al. (2018), the range of EC values from 1518 to 9430 µS/cm represents the high amount of salts in the groundwater.

Ghalib (2017) used this limits to classify EC, when EC value < 1500µS/cm, the groundwater is classified as low saline, when EC value between 1500 to 3000 µS/cm, the groundwater is classified as medium saline, and when EC value >3000µS/cm, the groundwater is classified as highly saline. Accordingly, groundwater in wells no. (w1, w4, w8, w9, w10, w11, w12) at the winter season, and wells no. (w1, w4, w8, w9, w10, w11, w12, w13) at summer season, are classified as moderate saline, whilst the rest wells are classified as high saline. However, wells no. (w1, w4, w11, w12) at the winter, and only wells no. (w1 and w11) at summer season considered within the permissible limits of IQS (2001). Furthermore, throughout the study period, none of the wells were found to be within permissible limits of WHO (2011) regarding the drinking purposes.

The total hardness (TH) measure is determined by detecting the existence of both Ca and Mg ions in groundwater. Todd (1980) indicated that four water categories could be assigned using the (TH) value, for TH less than 75 mg/l the water is said to be soft, from 75 to 150 mg/l moderate, from 150 to 300 mg/l hard and more than 300 mg/l is categorized as very hard. Thus, all groundwater samples are considered ″very hard″ at both seasons. Consequently, the groundwater sample in the study area was found not conforming to the requirements of the standards of IQS (2011) and WHO (2001), respectively.

Temperature is a vital factor, which regulates the biogeochemical activities in the aquatic environment (Pradeep et al., 2012). For the winter season, groundwater temperature ranged from 23.7°C to 20.2°C with an average value of 22.73°C. While for the summer season a maximum value of 24.4C to a minimum value of 22.3C.

The total dissolved salts (TDS) is defined as the sum of all concentrations of dissolved inorganic salts in water, such as carbonate, bicarbonate, chloride, fluoride, sulfate, phosphate, nitrate, calcium, magnesium, sodium, and potassium, (Adimalla and Venkatayogi, 2018). It reflects the suitability of groundwater for drinking, irrigation, and other purposes. The maximum measured values of TDS of 6220 mg/l were recorded

in well no. (w5) and of 8050 mg/l in well no. (w7) at both winter and summer seasons, respectively. On other hand, the minimum measured values for winter and summer seasons of 968 mg/l were recorded in well no. (w11) and of 1537 mg/l in the same well. The averaged TDS values of 2896.31mg/l for the winter season, and 3588.69 mg/l for the summer season, which was expected due to the increased dependence on groundwater resources in the dry season that is concentrated of salts as a result of the reduction of recharge to the groundwater table, other reasons may be, the leaching from the domestic sewage around the wells locations that seeped into the groundwater (Prasanth et al., 2012). Except that the well no. (w11) was recorded a permissible value of TDS during the winter season as per IQS (2011), this attributed to the full year operating time of this well. All groundwater samples investigated in this research did not satisfied the WHO (2001) requirements regarding TDS, for drinking purposes.

4.3.2 Characterization of the Cations K^{+}, Na^{+}, Mg^{+2}, and Ca^{+2}

Figure (4.12) shows the variations of the measured concentrations of cations in the groundwater samples extracted from wells in the study area during the winter and summer, respectively.

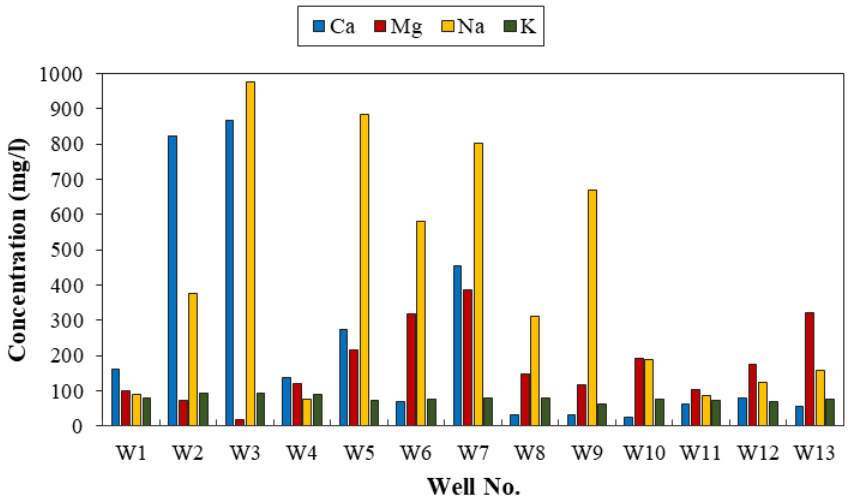

(a) For winter season.

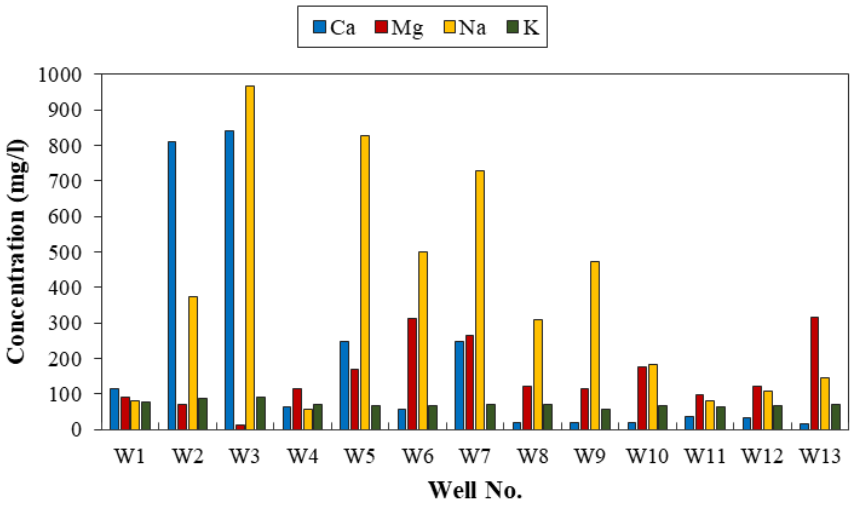

(b) For summer season.

Figure (4.12): Variation of cations in groundwater samples extracted from wells in the study area during the study period.

Figure (4.12) reveals that wells no. (w2, w3, w5, w6, and w7) were recorded higher measured concentrations of chemical elements Na, Ca, and Mg, while the rest are indicated low concentrations for all studied elements. This is probably attributed to the alkali nature of agricultural soil in the study area. In particular, these elements present in silicate rock form minerals and advanced are transported into mineral part of soils. All the investigated groundwater samples did not records cations concentration values to be within the permissible limits of IQS (2001) and WHO (2011) standards for drinking water.

The descriptive statistics for measured concentrations of cations in the groundwater samples are given in Tables (4.7) and (4.8) for both the winter and the summer seasons, respectively.

Table (4.7): Summary of descriptive statistics for measured concentrations of cations at winter season.

Cation / Statistics	Ca (mg/l)	Mg (mg/l)	Na (mg/l)	K (mg/l)
Mean	194.23	153.35	372.40	71.72
Maximum	841.68	318.08	967.97	91.25
Minimum	16.03	13.44	57.10	57.71
Median	56.11	120.96	310.12	72.09
Standard Deviation	291.72	93.07	308.82	9.06
Sample Variance	85098.35	8662.90	95372.04	82.11
Standard Error	80.91	25.81	85.65	2.51
Kurtosis	2.26	-0.24	-0.62	1.00
Skewness	1.86	0.75	0.79	0.92

Table (4.8): Summary of descriptive statistics for measured concentrations of cations at summer season.

Cation / Statistics	Ca (mg/l)	Mg (mg/l)	Na (mg/l)	K (mg/l)
Mean	235.86	176.05	408.99	78.02
Maximum	865.73	387.52	974.60	94.37
Minimum	24.05	17.92	74.4	62.1
Median	80.16	147.84	312.90	76.17
Standard Deviation	295.25	108.87	331.43	9.28
Sample Variance	87169.82	11852.80	109843.97	86.04
Standard Error	81.89	30.20	91.92	2.57
Kurtosis	1.27	-0.31	-1.31	-0.04
Skewness	1.58	0.71	0.59	0.46

From the results of Tables (4.7) and (4.8), the concentration of sodium element (Na) showed a higher average value among the investigated samples, the range of variation for Na element was 910.86 mg/l and 900.20 mg/l at the winter and the summer seasons, respectively. While, the concentration of Potassium element (K) recorded the lower average concentration value among the investigated samples in the study area, the range of variation is 33.54 mg/l and 32.27 mg/l for the winter and the summer

seasons, respectively. Based on the average concentration values, it can be identified the following descending order Na > Ca > Mg > K during the study period.

A standardized way of measured concentrations based on maximum, the minimum, median, and the first and third quartiles by box plot is shown in Figure (4.13) during the study period.

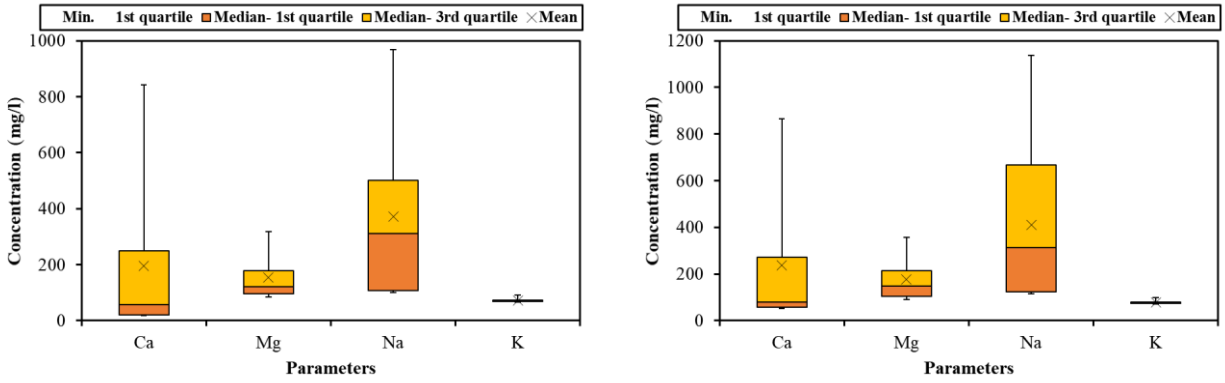

(a) Winter (b) Summer

Figure (4.13): Box plot for the measured concentrations of cations in the groundwater samples during the study period.

4.3.3 Characterization of the Anions Cl^-,SO_4^{-2}, HCO_3^-, NO_3

The variations of measured concentrations of anions in groundwater samples at the winter and the summer seasons are shown in Figure (4.14).

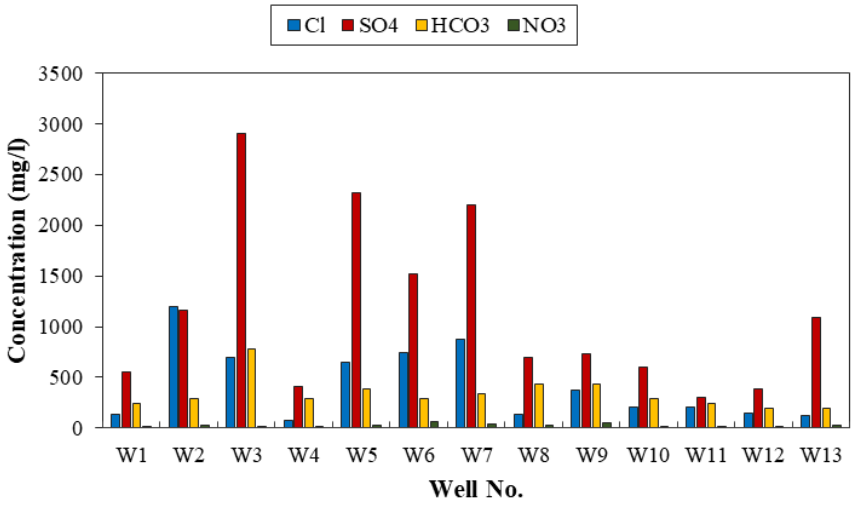

(a) For winter season.

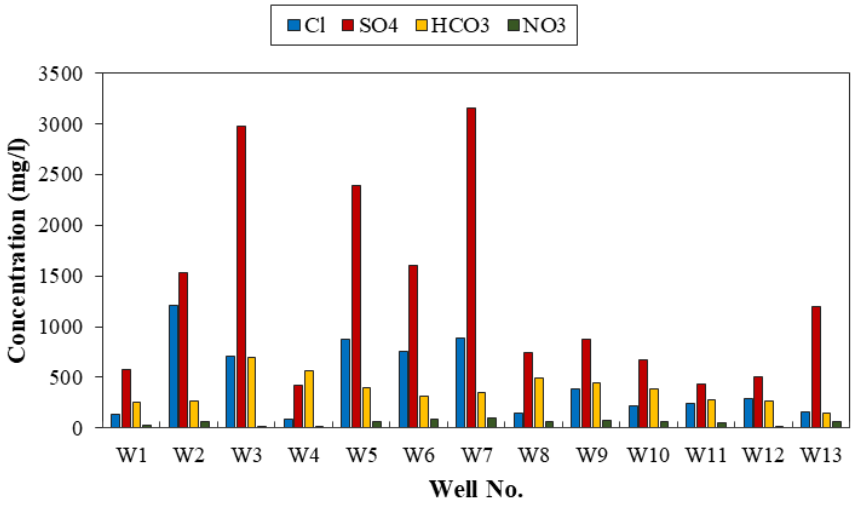

(b) For summer season.

Figure (4.14): Variation of anions in groundwater samples extracted from wells in the study area during the study period.

Figure (4.14) shows that wells no. (w2, w3, w5, w6, and w7) recorded a higher concentration of anions Cl, SO_4, and HCO_3. While the rest are showing low concentrations for all anions. The major source of ions in groundwater is the lithology of rocks in contrast with anthropogenic sources (Abdel-Satar et al., 2017), however, this may result from the agricultural waste that leachate to the groundwater table after intensive activities of agriculture.

The descriptive statistics for measured concentrations of anions in the groundwater samples are given in Tables (4.9) and (4.10) during the study period.

Table (4.9): Summary of descriptive statistics for measured concentrations of anions at winter season.

Anion / Statistics	Cl (mg/l)	SO_4 (mg/l)	HCO_3 (mg/l)	NO_3 (mg/l)
Mean	426.49	1146.22	341.69	25.14
Maximum	1191.63	2903.54	781.02	62.27
Minimum	71.98	300.39	195.25	0.45
Median	211.94	736.59	292.88	23.18
Standard Deviation	362.45	843.64	154.37	18.03
Sample Variance	131373.17	711735.87	23828.65	324.91
Standard Error	100.53	233.98	42.81	5
Kurtosis	-0.32	-0.10	5.44	0.06
Skewness	0.89	1.03	2.09	0.59

Table (4.10): Summary of descriptive Statistics for measured concentrations of anions at summer season.

Anion / Statistics	Cl (mg/l)	SO_4 (mg/l)	HCO_3 (mg/l)	NO_3 (mg/l)
Mean	468.94	1314.77	375.49	51.34
Maximum	1207.62	3153.74	695.59	95.44
Minimum	83.97	419.73	146.44	3.56
Median	290.98	874.85	353.90	59.33
Standard Deviation	368.68	964.90	146.88	29.02
Sample Variance	135926.50	931037.01	21572.80	842.11
Standard Error	102.25	267.62	40.74	8.05
Kurtosis	-0.75	-0.31	0.58	-0.71
Skewness	0.76	1.01	0.74	-0.45

Tables (4.9) and (4.10) show that the average concentration of the sulfate anion (SO_4) was the higher among the investigated samples, the variation in measured concentration of (SO_4) ranged between 2603.15 mg/l to 2734.01mg/l during the study period. Whereas, the Nitrate (NO_3) shows the lower average concentration, with a range of variation between 61.82 mg/l to 91.88 mg/l for both seasons. The measured

concentrations of anions overall investigated wells can be recognized in descending order as following: $SO_4 > Cl > HCO_3 > NO_3$

A box plot of the statistics of the measured concentrations for anions in the groundwater samples is shown in figure (4.15).

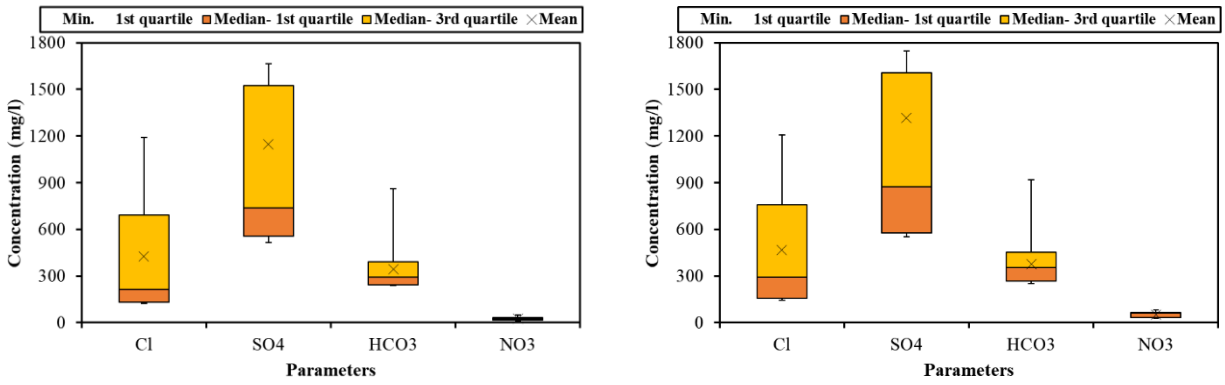

(a) For winter season. (b) For summer season.

Figure (4.15): Box plot for the measured concentrations of anions in the groundwater samples during the study period.

4.3.4 Characterization of the Heavy Metals

Results of the descriptive statistics for concentrations of the heavy metals in investigated groundwater samples during the study period are presented in Table (4.11) and (4.12), respectively.

Table (4.11): Summary of descriptive statistics for measured concentrations of heavy metal at winter season.

Heavy metal / Statistics	Pb (ppm)	Ni (ppm)	Cd (ppm)	Fe (ppm)	Zn (ppm)
Mean	0.1052	0.9252	0.0222	0.3089	0.5189
Maximum	0.2308	1.3576	0.0312	0.5840	2.3942
Minimum	0.0040	0.6220	0.0141	0.1268	0.0146
Median	0.1159	0.886	0.0226	0.3161	0.3998
Standard Deviation	0.0668	0.2031	0.0046	0.1319	0.6115
Sample Variance	0.00447	0.04124	2.09×10^{-05}	0.01741	0.37399
Standard Error	0.0185	0.0563	0.0013	0.0366	0.1696
Kurtosis	-0.5461	0.4866	0.3817	0.0889	8.4369
Skewness	0.0831	0.7806	-0.0006	0.5493	2.7450

Table (4.12): Summary of descriptive statistics for measured concentrations of heavy metal at summer season.

Heavy metal / Statistics	Pb (ppm)	Ni (ppm)	Cd (ppm)	Fe (ppm)	Zn (ppm)
Mean	0.0282	0.0652	0.0512	1.2758	0.3484
Maximum	0.0582	0.1794	0.0920	2.7057	1.7612
Minimum	0.0053	0.0145	0.0025	0.0959	0.0288
Median	0.0291	0.0498	0.0564	1.2658	0.2649
Standard Deviation	0.0166	0.0531	0.0288	0.7484	0.4339
Sample Variance	0.0003	0.0028	0.0008	0.5601	0.1883
Standard Error	0.0048	0.0153	0.0080	0.2076	0.1204
Kurtosis	-0.7558	1.1140	-0.7767	-0.3045	11.6247
Skewness	0.3932	1.3858	-0.1382	0.4072	3.3252

A visualized representation via box plot for the concentration statistics of the heavy metals during the study period is shown in Figure (4.16).

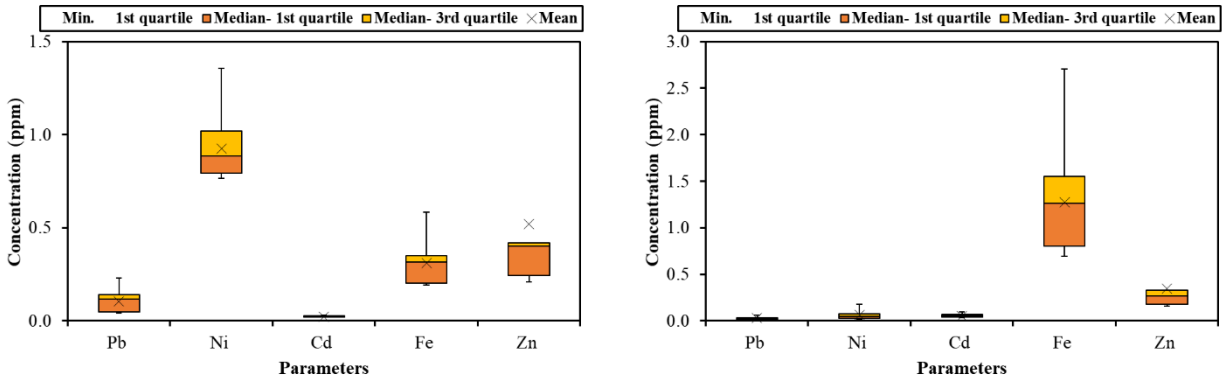

(a) For winter season. (b) For summer season.

Figure (4.16): Box plot for the measured concentrations of heavy metals in the groundwater samples during the study period.

Results of Tables (4.10) and (4.11), in addition to Figure (4.16) revealed that Cadmium metal (Cd) shows a lower measured concentration that varied between 0.0141 to 0.0312 ppm with an average value of 0.0222 ppm at the winter season. While, lead metal (Pb) shows a lower measured concentration that varied between 0.0053 to 0.0582 ppm with an average value of 0.0282 ppm at the summer season. On the other hand, Nickel metal (Ni) shows a higher measured concentration that varied from 0.6220 to 1.3576 ppm with an average concentration of 0.9252 ppm at the winter season, the high presence of (Ni) in the environment is attributed to human activity especially agricultural, for its presence in Iraqi fertilizers (Ismael et al., 2019). According to the chemical analysis, almost all the measured concentrations for heavy metals are higher in the winter season than in the summer season.

The average concentrations for iron metal (Fe) at the wet season are higher than in the dry season. The presence of iron in the water can be attributed to the fact that iron can be found in the organic waste and the remnants of decaying plants in the soil, zinc

and lead could be present due to agricultural activates (Ismael et al., 2019). The results of the investigated samples during the study period are exceeding the permissible limits reported by IQS (2011) and WHO (2001). Based upon the measured concentrations statistics, the concentrations of heavy metals in the groundwater samples within the study area during the study period can be arranged by descending order as following Cd < Pb < Fe < Zn <Ni and Pb < Cd < Ni < Zn <Fe at winter and summer respectively.

4.4 Spatial Distribution of Groundwater Parameters

The comprehensive assessment of groundwater required mapping the investigated parameters by using spatial distribution techniques via ArcGIS software. The investigated parameters measured and/or calculated from extracted samples of available wells in the study area will be covered in detail as follows.

4.4.1 Spatial Analysis of TDS, EC, and TH

Figure (4.17) presents a spatial distribution map for the measured concentrations of TDS in (mg/l) in the groundwater samples extracted from the wells extended around the study area during the study period.

It is evident from Figure (4.17 a), which shows the winter season measurements, that the concentrations of TDS were increased toward the southern part of the study area; these concentrations were concentrated in and around the wells no. (w5 and w7), the variation for higher concentrations ranges from more than 5000 mg/l to less than 6250 mg/l. On other hand, the lower measured concentrations were spread in narrow zones of the northwestern regions of the study area, the range of variation for lower concentrations between more than 950 mg/l to less than 2050 mg/l, It was concentrated in and around the wells no. (w1, w4, w10, w11, w12 and w13). The moderated concentrations were distributed randomly and around the wells no. (w2, w3, w8, and w9) with an average value of more than 3500 mg/l.

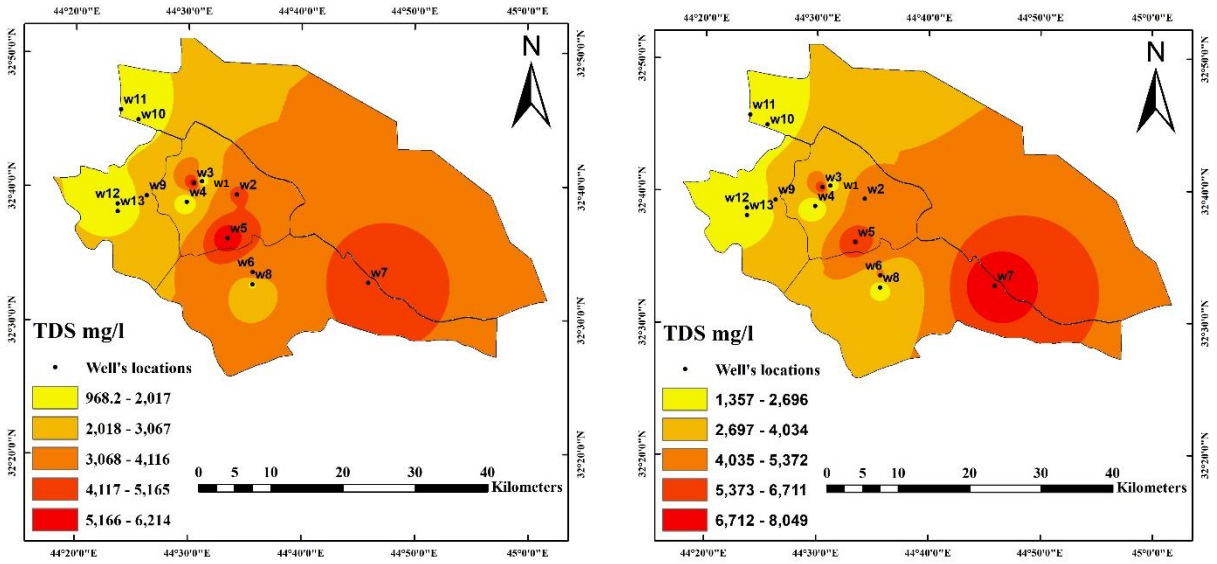

(a) For winter season. (b) For summer season.

Figure (4.17): Spatial distribution map for measured concentrations of TDS throughout the study area during the study period.

For the summer season, from Figure (4.17 b) it is noticed that higher measured concentrations have recorded in zones within the southern and southeastern part of the study area, specifically in and around well no. (w7). The higher concentrations have differed between more than 6500 mg/l to less than 8050 mg/l. As in the winter season, the lower concentrations were located around the wells no (w1, w4, w10, w11, w12 and w13) in addition to well no. (w8). The averaged value of lower concentration was more than 2000 mg/l.

The moderated measured concentrations of TDS were occupy most of the regions of the study area except the wells locations of high and lower concentrations explained above. The value of concentrations ranged from more than 2500 mg/l to less than 6700 mg/l, the average value was about 3400 mg/l.

From the previous discussion, it was obvious that throughout the study area and during the study period, all the measured concentrations of TDS were more than the

limits of (IQS, 2011) with an average value of 500 mg/l and for (WHO, 2001) with an average value of 1000 mg/l.

The map of spatial distribution for the measured electrical conductivity EC in (µS/cm) in the groundwater samples extracted from the wells for the wet and the dry seasons throughout the study area as shown in Figure (4.18).

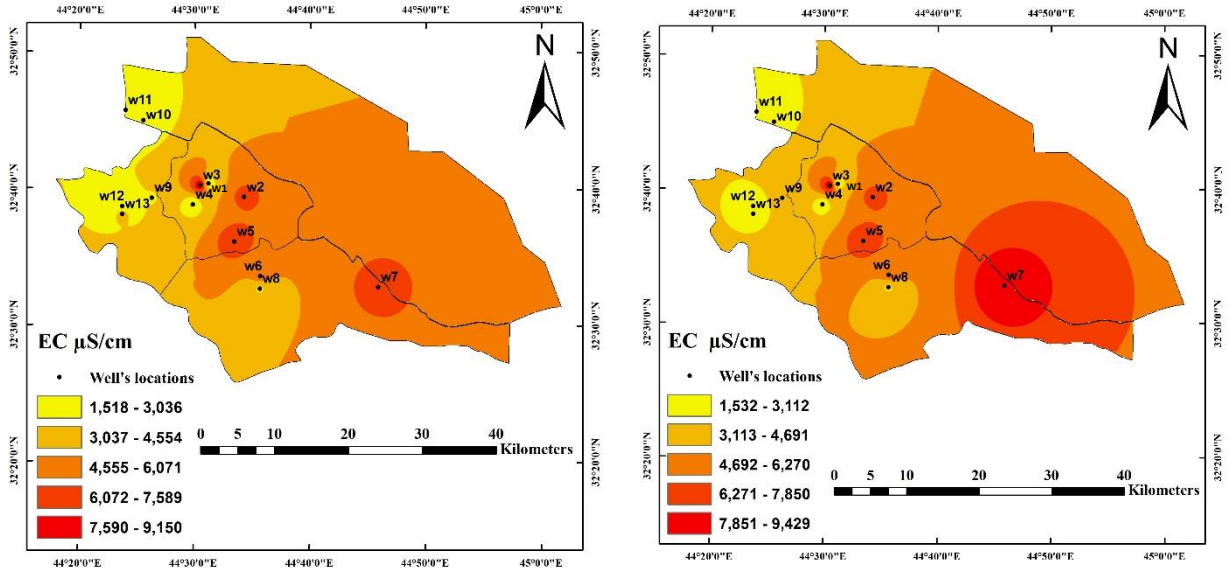

(a) For winter season. (b) For summer season.

Figure (4.18): Spatial distribution map for measured concentrations of EC throughout the study area during the study period.

It is evident from Figure (4.18 a), which shows the winter season measurements, that the concentrations of EC were increased toward the southern part of the study area; these concentrations were concentrated in and around the wells no. (w3), the variation for higher concentrations ranges from more than 7850 µS/cm to 9150 µS/cm. On other hand, the lower measured concentrations were spread in narrow zones of the northwestern regions of the study area, the range of variation for lower concentrations between more than 1500 µS/cm to less than 3000 µS/cm, It was concentrated in and around the wells no. (w10, w11, w12, w13, w1 and w4). The moderated concentrations

were distributed randomly and around the wells no. (w2, w5 and w7) with an average value of more than 5250 µS/cm.

For the summer season, from Figure (4.18 b) it is noticed that higher measured concentrations have recorded in zones within the southern and southwestern part of the study area, specifically in and around wells no. (w3 and w7). The higher concentrations have differed between more than 7850 µS/cm to less than 9530 µS/cm. As in the winter season, the lower concentrations were located around the wells no. (w10, w11, w12, w13, w1 and w4), in addition to well no. (w8). The averaged value of lower concentration was more than 2300 µS/cm.

The moderated measured concentrations of EC were occupy most of the regions of the study area except the wells locations of high and lower concentrations explained above. The value of concentrations ranged from more than 3100 µS/cm to less than 7850 µS/cm, the average value was about 5480 µS/cm.

From the previous discussion, it was obvious that throughout the study area and during the study period, Only w1, w4, w11, w12 for winter, while only w1 and w11 for summer season fall within the permissible limits of IQS (2001) of 2000µS/cm, further more for the two seasons no well found within permissible limits of WHO (2011) which is 1000µS/cm for drinking water.

The map of spatial distribution for the measured total hardness (TH) in (mg/l) in the groundwater samples extracted from the wells for the wet and the dry seasons throughout the study area as shown in Figure (4.19).

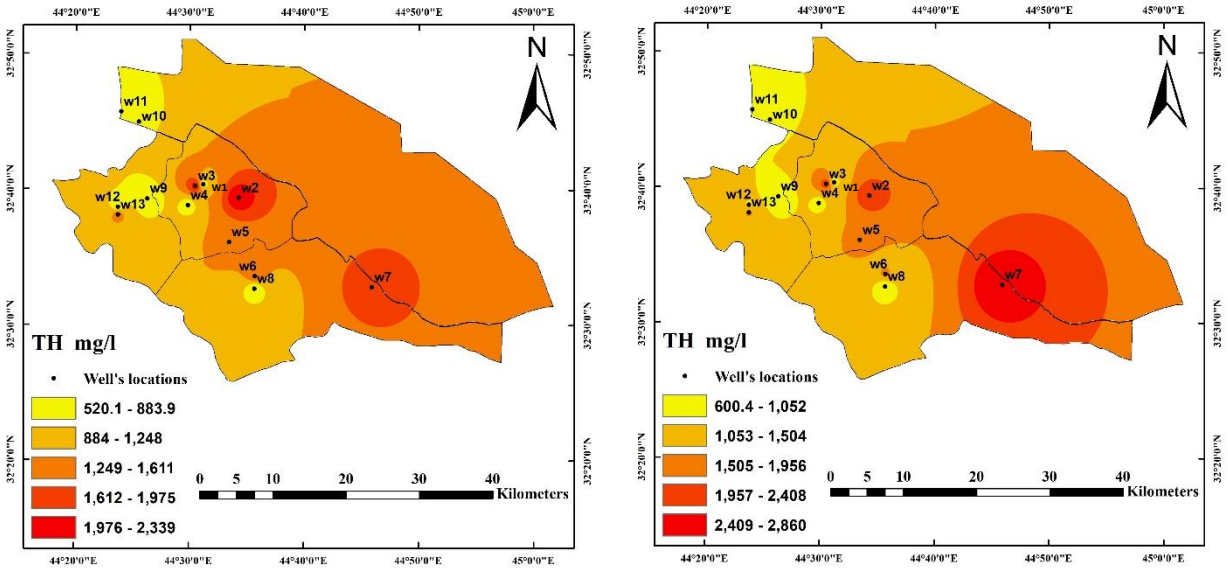

(a) For winter season. (b) For summer season.

Figure (4.19): Spatial distribution map for measured concentrations of TH throughout the study area during the study period.

It is evident from Figure (4.19 a), which shows the winter season measurements, that the concentrations of TH were increased toward the southern, eastern part of the study area; these concentrations were concentrated in and around the wells no. (w2, w3, and w7), the variation for higher concentrations ranges from more than 1976 mg/l to less than 2340 mg/l. On other hand, the lower measured concentrations were spread in narrow zones of the northwestern regions of the study area, the range of variation for lower concentrations between more than 520 mg/l to less than 890 mg/l, It was concentrated in and around the wells no. (w1, w4, w8, w9, w10, w11 and w12). The moderated concentrations were distributed randomly and around the wells no. (w13) with an average value of more than 1430 mg/l.

For the summer season, from Figure (4.19 b) it is noticed that higher measured concentrations have recorded in zones within the southern and southeastern part of the study area, specifically in and around wells no. (w2 and w7). The higher concentrations have differed between more than 2400 mg/l to less than 2900 mg/l. As in the winter

season, the lower concentrations were located around the wells no. (w1, w4, w8, w9, w10 and w11). The averaged value of lower concentration was more than 826 mg/l.

The moderated measured concentrations of TH were occupy most of the regions of the study area except the wells locations of high and lower concentrations explained above. The value of concentrations ranged from more than 1000 mg/l to less than 2450 mg/l, the average value was about 1730 mg/l.

From the previous discussion, it was obvious that throughout the study area and during the study period, all the measured concentrations of TH were more than the limits of (IQS, 2001) with an average value of 500 mg/l and for (WHO, 2011) with an average value of 500 mg/l.

4.4.2 Spatial Analysis of Cations Concentrations

The map of spatial distribution for the measured calcium Ca in (mg/l) in the groundwater samples extracted from the wells for the wet and the dry seasons throughout the study area as shown in Figure (4.20).

It is evident from Figure (4.20 a), which shows winter season measurements, that the concentrations of Ca were increased in the middle part of the study area; these concentrations were concentrated in and around the wells no. (w2, and w3), the variation for higher concentrations ranges from more than 670 mg/l to less than 850 mg/l.

On other hand, the lower measured concentrations were spread in narrow zones of the western regions of the study area, the range of variation for lower concentrations between more than 16 mg/l to less than 185 mg/l, It was concentrated in and around the wells no. (w1, w4, w6, w8, w9, w10, w11, w12 and w13). The moderated concentrations were distributed around the wells no. (w2and w3) with an average value of more than 427 mg/l.

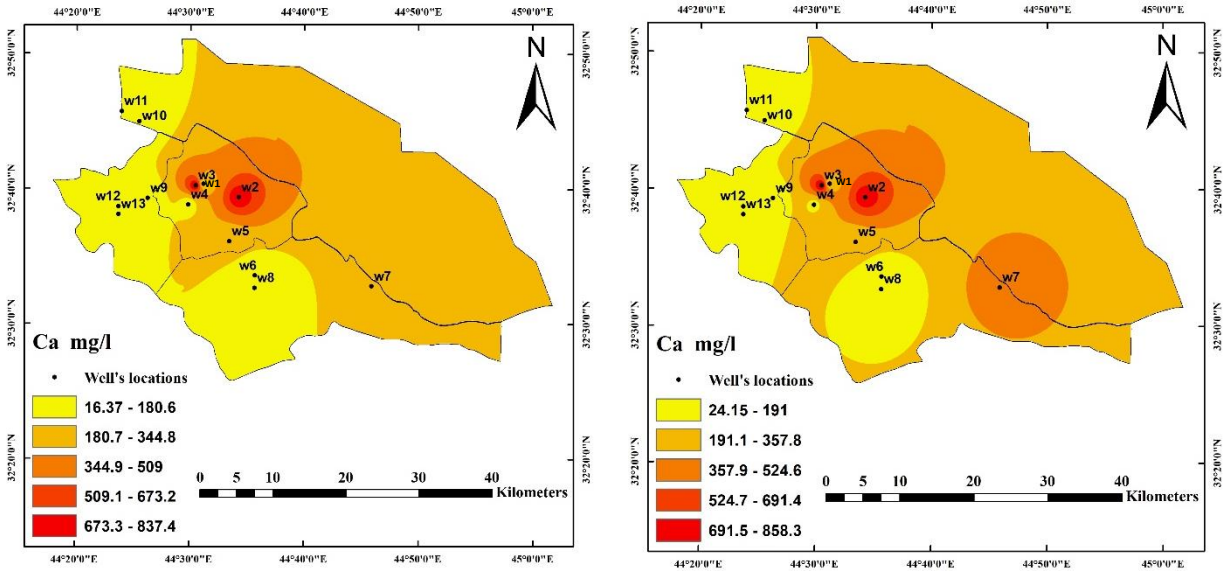

(a) For winter season. (b) For summer season.

Figure (4.20): Spatial distribution map for measured concentrations of Ca throughout the study area during the study period.

For the summer season, from Figure (4.20 b) it is noticed that higher measured concentrations have recorded in zones within the middle part of the study area, specifically in and around wells no. (w2 and w3). The higher concentrations have differed between more than 690 mg/l to less than 860 mg/l. The lower concentrations were located around the wells no. (w4, w6, w8, w9, w10, w11, w12 and w13). The averaged value of lower concentration was more than 108 mg/l.

The moderated measured concentrations of Ca were occupy most of the regions of the study area except the wells locations of high and lower concentrations explained above. The value of concentrations ranged from more than 190 mg/l to less than 690 mg/l, the average value was about 440mg/l.

From the previous discussion, it was obvious that throughout the study area and during the study period, that for (IQS, 2001) only (w8, w9, w10 and w13) for winter season and (w8, w9 and w10) for summer season, were within the limited permissible value which is 50 mg/l, while for (WHO, 2011) only (w1, w2, w3, w5 and w7) for

winter and (w1, w2, w3, w4, w5 and w7) for summer, were found to be out of the limited value of 75 mg/l.

The map of spatial distribution for the measured Magnesium Mg in (mg/l) in the groundwater samples extracted from the wells for the wet and the dry seasons throughout the study area as shown in Figure (4.21).

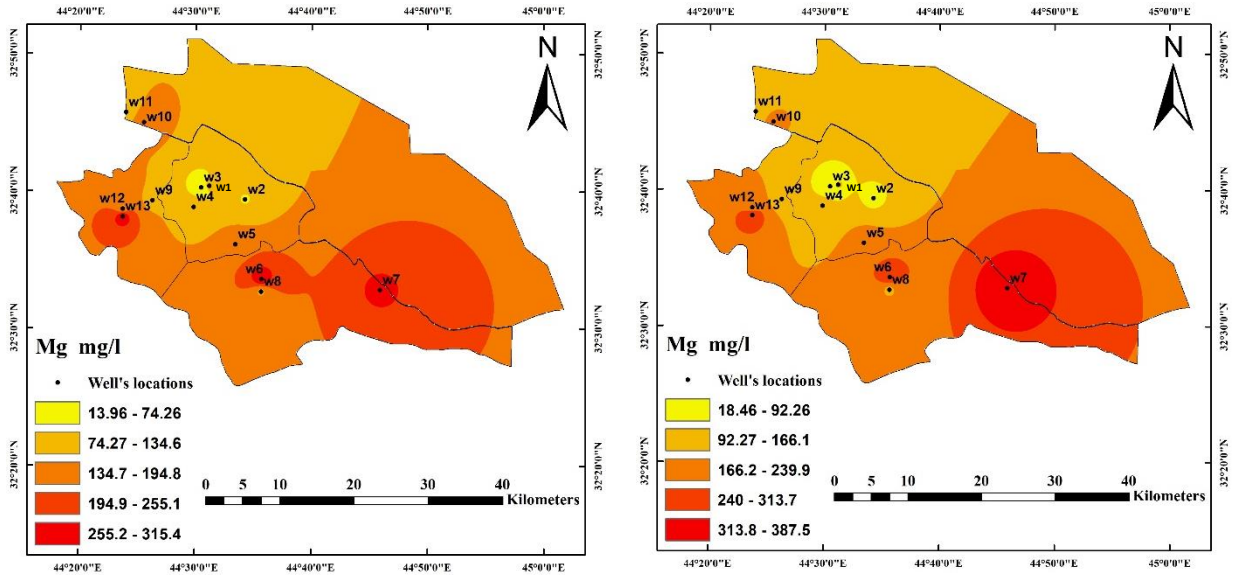

(a) For winter season. (b) For summer season.

Figure (4.21): Spatial distribution map for measured concentrations of Mg throughout the study area during the study period.

It is evident from Figure (4.21 a), which shows winter season measurements, that the concentrations of Mg were increased in all of the study area, except of northwestern which it was occupied with lowest concentrations. The variation of highest concentrations ranges from more than 250 mg/l to less than 320 mg/l, these concentrations were concentrated in and around the wells no. (w7, w6 and w13). On other hand, the range of variation for lower concentrations between more than 13 mg/l to less than 75 mg/l, it was concentrated in and around the wells no. (w2 and w3). The

moderated concentrations were distributed around the rest of wells with an average value of more than 163 mg/l.

For the summer season, from Figure (4.21 b) it is noticed that higher measured concentrations have the same trend as for winter season with higher measured concentrations values The higher concentrations have differed between more than 310 mg/l to less than 390 mg/l. As in the winter season, the lower concentrations were located around the wells no. (w2 and w3) as well as w1. The averaged value of lower concentration was more than 55 mg/l.

The moderated measured concentrations of Mg were occupy most of the regions of the study area except the wells locations of high and lower concentrations explained above. The value of concentrations ranged from more than 165 mg/l to less than 313 mg/l, the average value was about 405 mg/l.

From the previous discussion, it was obvious that throughout the study area and during the study period, that, for both seasons, only (w3) fall under the limited value of (IQS, 2001) and (WHO, 2011) of 50 and 30 mg/l, respectively.

The map of spatial distribution for the measured sodium Na in (mg/l) in the groundwater samples extracted from the wells for the wet and the dry seasons throughout the study area as shown in Figure (4.22).

It is evident from Figure (4.22 a), which shows the winter season measurements, that the concentrations of Na were increased toward the southeastern part of the study area; these concentrations were concentrated in and around the wells no. (w3, w5, and w7) the variation for higher concentrations ranges from more than 780 mg/l to less than 965 mg/l. On other hand, the lower measured concentrations were spread in narrow zones of the northwestern regions of study area, the range of variation for lower concentrations between more than 59 mg/l to less than 240 mg/l, It was concentrated in and around the wells no. (w1,

w4, w10, w11, w12 and w13). The moderated concentrations were distributed randomly and around well no. (w9) with an average value of more than 510 mg/l.

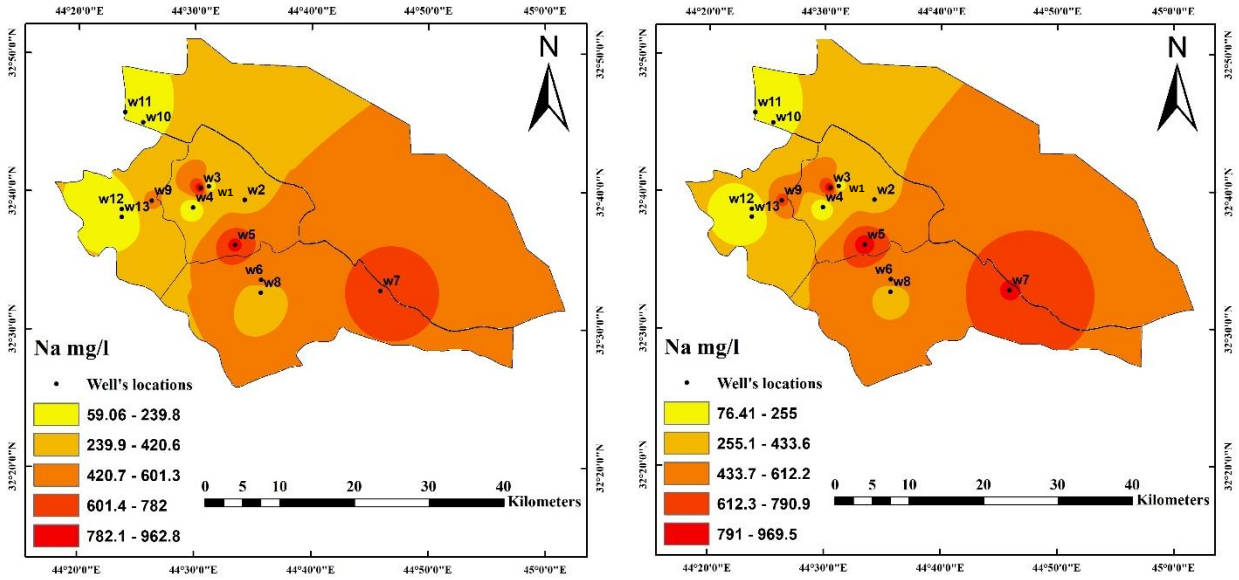

(a) For winter season. (b) For summer season.

Figure (4.22): Spatial distribution map for measured concentrations of Na throughout the study area during the study period.

For the summer season, from Figure (4.22 b) it is noticed that higher measured concentrations have receded the same pattern as winter season with higher values. The higher concentrations have differed between more than 790 mg/l to less than 970 mg/l, specifically in and around wells no. (w3, w5, w7 and w9). As in the winter season, the lower concentrations were located around the wells no. (w1, w4, w10, w11, w12 and w13). The averaged value of lower concentration was more than 165 mg/l.

The moderated measured concentrations of Na were occupy most of the regions of the study area except the wells locations of high and lower concentrations explained above. The value of concentrations ranged from more than 250 mg/l to less than 790 mg/l, the average value was about 523 mg/l.

From the previous discussion, it was obvious that throughout the study area and during the study period, for both winter and summer, only (w1, w4, w10, w11, w12 and w13), fall under the limited values of (IQS, 2001) and (WHO, 2011) of 200 mg/l.

The map of spatial distribution for the measured potassium K in (mg/l) in the groundwater samples extracted from the wells for the wet and the dry seasons throughout the study area as shown in Figure (4.23).

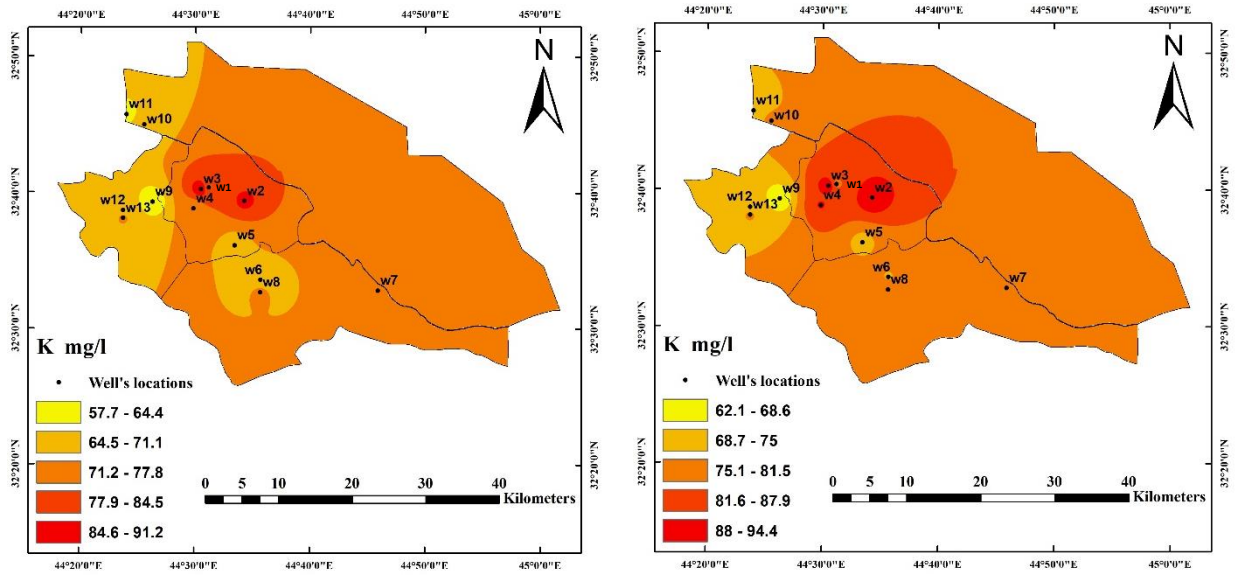

(a) For winter season. (b) For summer season.

Figure (4.23): Spatial distribution map for measured concentrations of K throughout the study area during the study period.

It is evident from Figure (4.23 a), which shows winter season measurements, that the concentrations of K were increased in the middle parts towards the south and southeastern parts of study area; the highest concentrations were recorded in and around the wells no. (w2, and w3), the variation for higher concentrations ranges from more than 84.5 mg/l to less than 92 mg/l. On other hand, the lower measured concentrations were spread in very narrow zones of the western regions of study area, the range of variation for lower concentrations between more than 57 mg/l to less than 65 mg/l, It

was concentrated in and around the wells no. (w11 and w9). The moderated concentrations were distributed randomly around the wells with an average value 75 mg/l.

For the summer season, from Figure (4.23 b) it is noticed that higher measured concentrations have recorded in zones within all parts of the study area, specifically in and around wells no. (w2, w3 and w4). The higher concentrations have differed between more than 88 mg/l to less than 95 mg/l. the lower concentrations were located around the wells no. (w9). The averaged value of lower concentration was more than 65 mg/l.

The moderated measured concentrations of Ca were occupy most of the regions of the study area except the wells locations of high and lower concentrations explained above. The value of concentrations ranged from more than 68 mg/l to less than 88 mg/l, the average value was about 78 mg/l.

From the previous discussion, it was obvious that throughout the study area and during the study period, all the measured concentrations of K were more than the limits of IQS (2001) with an average value of 10mg/l and for WHO (2011) with an average value of 12 mg/l.

4.4.3 Spatial Analysis of Anions Concentrations

The map of spatial distribution for the measured chloride Cl in (mg/l) in the groundwater samples extracted from the wells for the wet and the dry seasons throughout the study area as shown in Figure (4.24).

It is evident from Figure (4.24 a), which shows the winter season measurements, that the concentrations of Cl were increased toward the southeastern parts of study area; these concentrations were concentrated in and around the wells no. (w2), the variation for higher concentrations ranges from more than 965 mg/l to less than 1200 mg/l. On other hand, the lower measured concentrations were spread in narrow zones in the northwestern regions of study area, the range of variation for lower concentrations

between more than 73 mg/l to less than 300 mg/l, It was concentrated in and around the wells no. (w1, w4, w8, w10, w11, w12 and w13). The moderated concentrations were distributed around the wells no. (w3, w7) and remain parts of the study area with an average value of more than 630 mg/l.

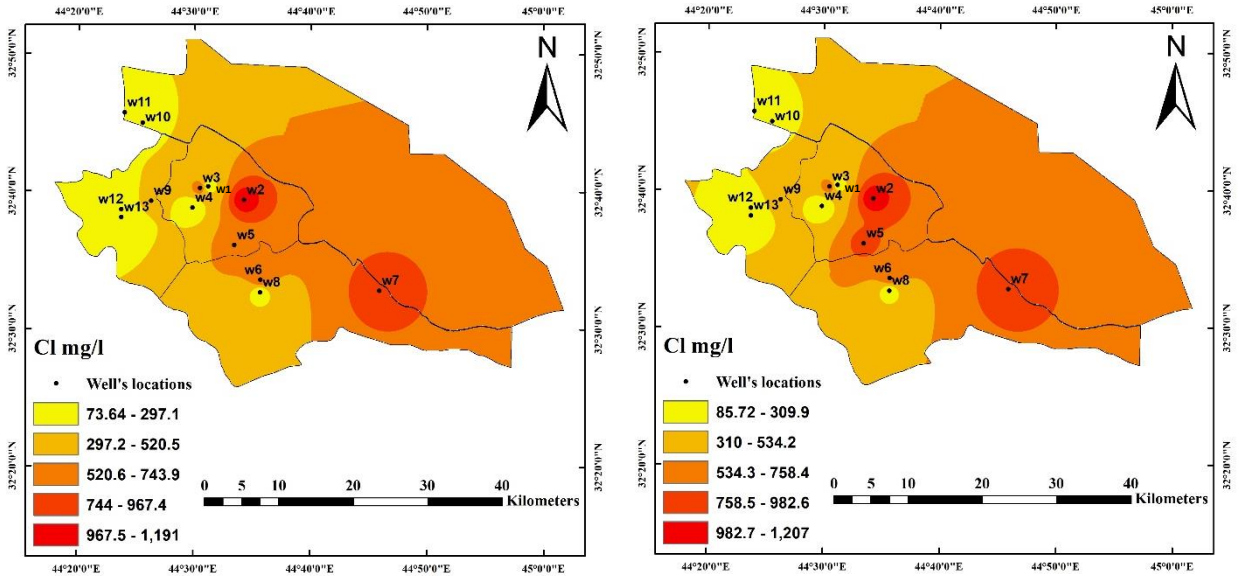

(a) For winter season. (b) For summer season.

Figure (4.24): Spatial distribution map for measured concentrations of Cl throughout the study area during the study period.

For the summer season, from Figure (4.24 b) it is noticed that higher measured concentrations have recorded in almost same pattern as winter season, in and around well no. (w2). The higher concentrations have differed between more than 980 mg/l to less than 1210 mg/l. As in the winter season, the lower concentrations were located around the wells no. (w1, w4, w8, w10, w11, w12 and w13). The averaged value of lower concentration was more than 428 mg/l.

The moderated measured concentrations of Cl were occupy most of the regions of the study area except the wells locations of high and lower concentrations explained

above. The value of concentrations ranged from more than 310 mg/l to less than 983 mg/l, the average value was about 645 mg/l.

From the previous discussion, it was obvious that throughout the study area and during the study period, the measured concentrations of Cl, for winter season only wells no. (w1, w4, w8, w10, w11, w12 and w13), while for summer season only wells no. (w1, w4, w8, w10 and w13) were satisfying the limited value of IQS (2001) and WHO (2011) of 250 mg/l.

The map of spatial distribution for the measured sulfate SO_4 in (mg/l) in the groundwater samples extracted from the wells for the wet and the dry seasons throughout the study area as shown in Figure (4.25).

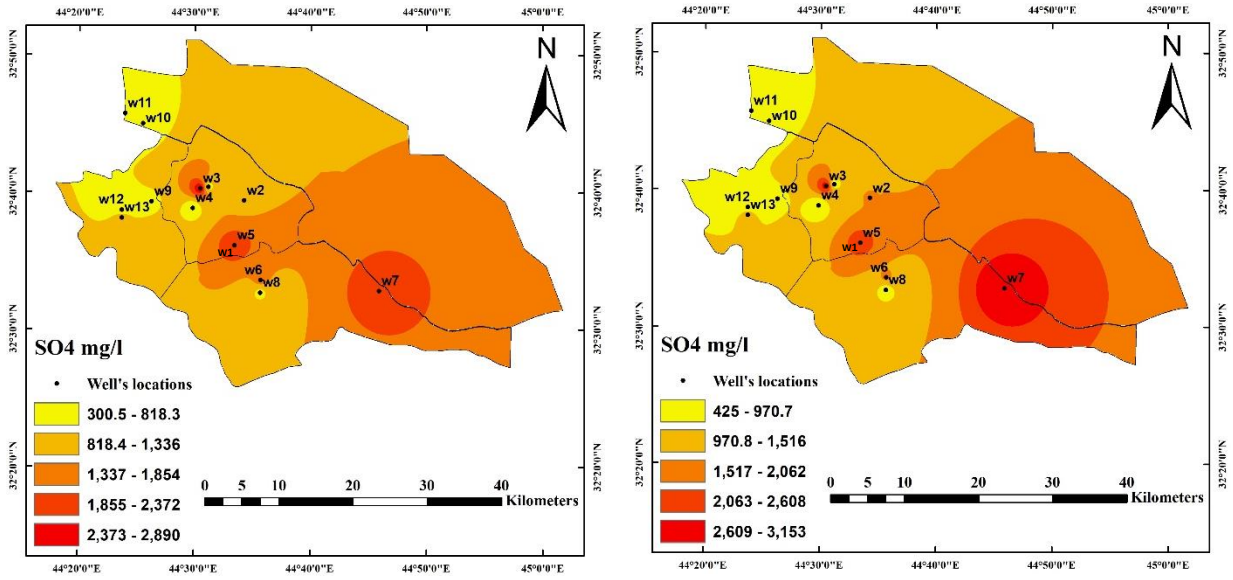

(a) For winter season. (b) For summer season.

Figure (4.25): Spatial distribution map for measured concentrations of SO_4 throughout the study area during the study period.

It is evident from Figure (4.25 a), which shows the winter season measurements, that the concentrations of SO_4 were increased toward the southeastern parts of the study area. The higher concentrations were concentrated in and around the well no. (w3), the

variation for higher concentrations ranges from more than 2370 mg/l to less than 2890 mg/l. On other hand, the lower measured concentrations were spread in narrow zones of the northwestern regions of the study area, the range of variation for lower concentrations between more than 300 mg/l to less than 820 mg/l, It was concentrated in and around the wells no. (w1, w4, w8, w9, w10, w11 and w12). The moderated concentrations were distributed around the wells no. (w5, w6, w7 and w13) and the remain parts of the study area with an average value of more than 1595 mg/l.

For the summer season, from Figure (4.25 b) it is noticed that higher measured concentrations have recorded with same winter season distribution pattern. The higher concentrations have differed between more than 2600 mg/l to less than 3155 mg/l, specifically in and around wells no. (w3, w5 and w7). As in the winter season, the lower concentrations were located around the wells no. (w1, w4, w8, w9, w10, w11 and w12). The averaged value of lower concentration was more than 910 mg/l.

The moderated measured concentrations of SO_4 were occupy most of the regions of the study area except the wells locations of high and lower concentrations explained above. The value of concentrations ranged from more than 970 mg/l to less than 2610 mg/l, the average value was about 1790 mg/l.

From the previous discussion, it was obvious that throughout the study area and during the study period, all the measured concentrations of SO_4 were more than the limited value of (IQS, 2001) and (WHO, 2011) of 250 mg/l.

The map of spatial distribution for the measured bicarbonate HCO_3 in (mg/l) in the groundwater samples extracted from the wells for the wet and the dry seasons throughout the study area as shown in Figure (4.26).

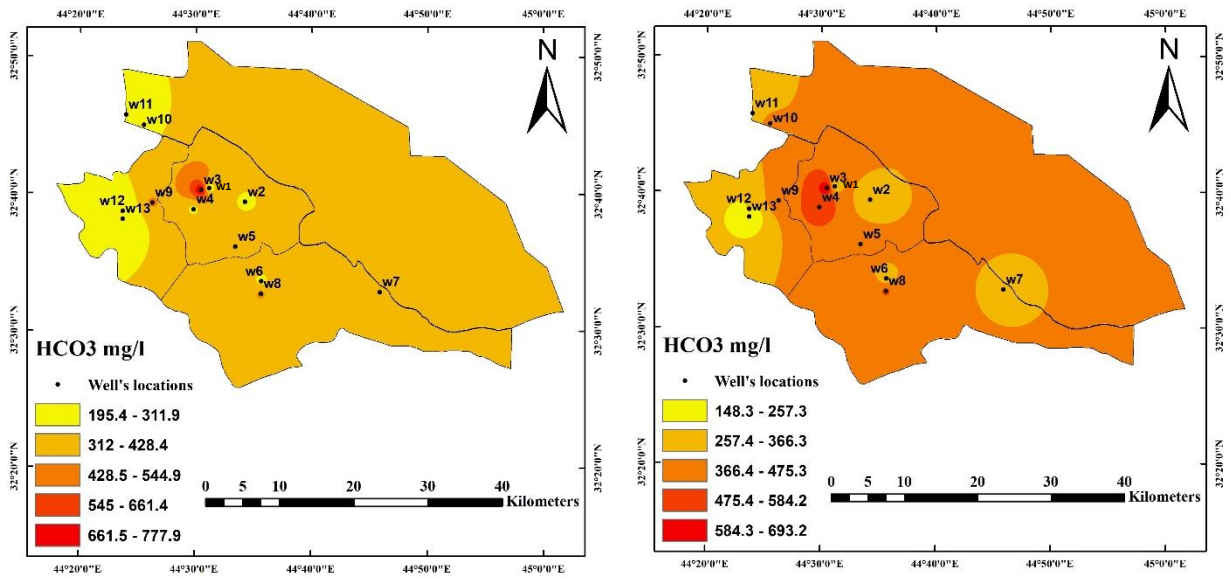

(a) For winter season. (b) For summer season.

Figure (4.26): Spatial distribution map for measured concentrations of HCO_3 throughout the study area during the study period.

It is evident from Figure (4.26 a), which shows the winter season measurements, that except of the high concentrations of HCO_3 in and around the well no. (w3), with variation range from more than 660 mg/l to less than 778 mg/l, all study area was covered with low measured concentration ranging from more than 310 mg/l to less than 430 mg/l. On other hand, the lower measured concentrations were spread in narrow zones, with range of variation for lower concentrations between more than 195 mg/l to less than 312 mg/l, It was concentrated in and around the wells no. (w1, w2, w4, w6, w10, w11, w12 and w13). The moderated concentrations were distributed around the wells no. (w3, w5, w7 and w9) with an average value of more than 485 mg/l.

For the summer season, from Figure (4.26 b) it is noticed that higher measured concentrations have recorded with same winter season pattern, higher concentration found, specifically, in and around well no. (w3). The higher concentrations have differed between more than 584 mg/l to less than 694 mg/l. the lower concentrations were located around the well no. (w12 andw13). The averaged value of lower

concentration was more than 200 mg/l. low measured concentration ranging from more than 257 mg/l to less than 367 mg/l were located in and around the well no. (w1, w2, w6, w7 and w11).

The moderated measured concentrations of HCO_3 were occupy most of the regions of the study area except the wells locations of high, low and lower concentrations explained above. The value of concentrations ranged from more than 367 mg/l to less than 476 mg/l, the average value was about 422 mg/l.

From the previous discussion, it was obvious that throughout the study area and during the study period, that for (IQS, 2001) only (w1, w11, w12 and w13) for winter season and (w13) for summer season, were within the limited permissible value which is 250 mg/l, while for (WHO, 2011) only (w1, w2, w4, w6, w10, w11, w12 and w13) for winter and (w1, w2, w11, w12 and w13) for summer, were found to be out of the limited value of 300 mg/l.

The map of spatial distribution for the measured nitrate NO_3 in (mg/l) in the groundwater samples extracted from the wells for the wet and the dry seasons throughout the study area as shown in Figure (4.27).

It is evident from Figure (4.27a), which shows the winter season measurements, that the concentrations of NO_3 were increased toward the southeastern parts of study area; these concentrations were concentrated in and around the well no. (w6), the variation for higher concentrations ranges from more than 49.5 mg/l to less than 63 mg/l. On other hand, the lower measured concentrations were spread in narrow zones of the northwestern regions of the study area, the range of variation for lower concentrations between more than 0.5 mg/l to less than 13 mg/l, It was concentrated in and around the rest of the wells. (w3, w4 and w12). The moderated concentrations were distributed around the rest of the wells with an average value of more than 31 mg/l.

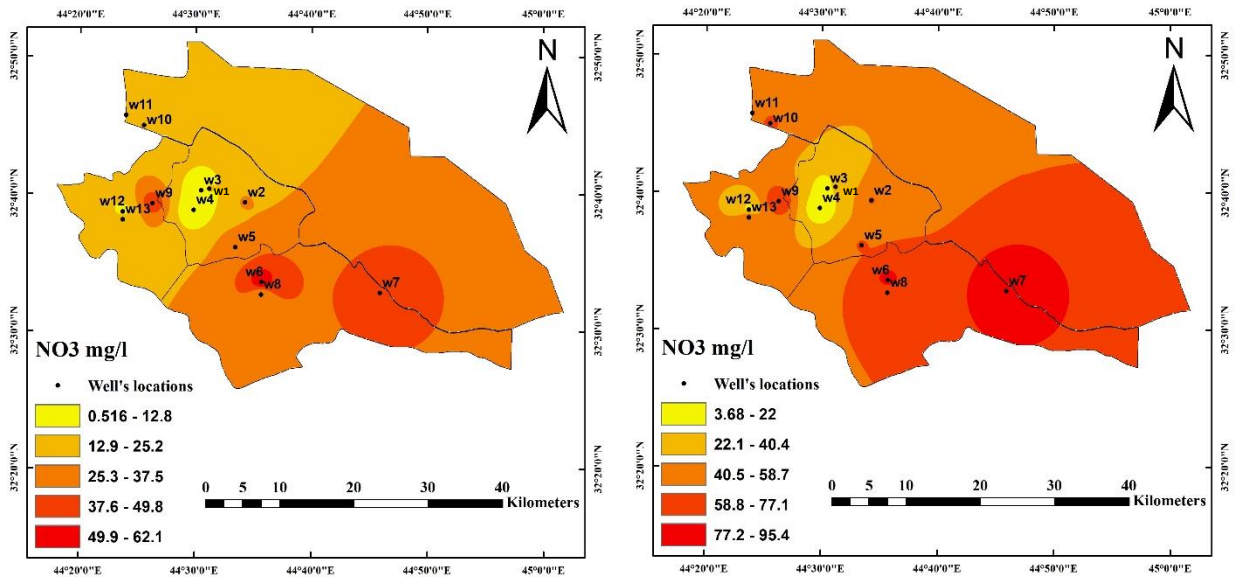

(a) For winter season. (b) For summer season.

Figure (4.27): Spatial distribution map for measured concentrations of NO_3 throughout the study area during the study period.

For the summer season, from Figure (4.27 b) it is noticed that higher measured concentrations have recorded in zones within the southern and southwestern parts of the study area, specifically in and around wells no. (w6 and w7). The higher concentrations have differed between more than 77 mg/l to less than 96 mg/l. As in the winter season, the lower concentrations were located around the wells no. (w3, w4 and w12). The averaged value of lower concentration was more than 12 mg/l.

The moderated measured concentrations of NO_3 were occupy most of the regions of the study area except the wells locations of high and lower concentrations explained above. The value of concentrations ranged from more than 22 mg/l to less than 77 mg/l, the average value was about 50 mg/l.

From the previous discussion, it was obvious that throughout the study area and during the study period, that for (IQS, 2001) only (w6) for winter season and (w2, w5, w6, w7, w8, w9, w10, w11 and w13) for summer season, were out of the limited permissible value which is 50 mg/l, while for (WHO, 2011) only (w6 and w9) for winter

and (w2, w5, w6, w7, w8, w9, w10, w11 and w13) for summer, were found to be out of the limited value of 45 mg/l.

4.4.4 Spatial Analysis of Heavy Metals

The following figures show the spatial distribution of heavy metals in the groundwater samples for winter and summer seasons throughout the study area.

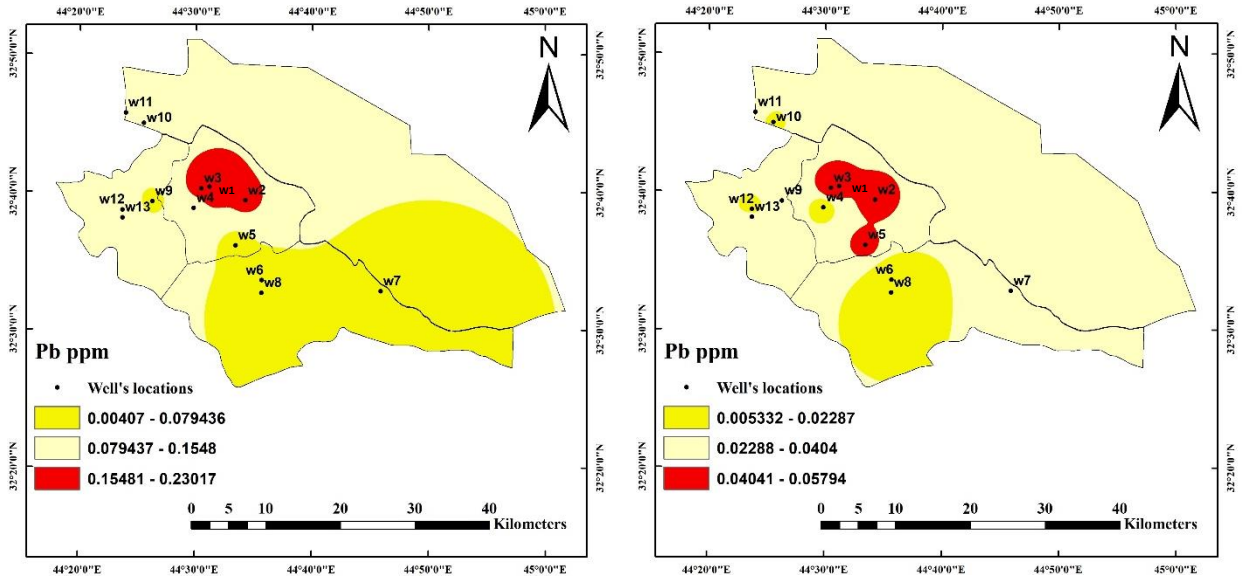

(a) For winter season. (b) For summer season.

Figure (4.28): Spatial distribution map for measured concentrations of Pb throughout the study area during the study period.

For lead metal, as shown in Figure (4.28 a), the higher concentrations were distributed around wells (w1, w2, and w3) with values ranging from 0.156 to 0.23 ppm. The areas with moderated concentration were distributed in the middle toward the north and extend east and west of the study area with averaged concentration value of 0.117 ppm. The lower concentrations in the south part of the study area about 0.004 to 0.008 ppm. While for summer season Figure (4.28 b) the higher concentrations also were distributed around wells (w1, w2, w3 and w5), but in smaller values, the areas with moderated concentration occupied most of study area.

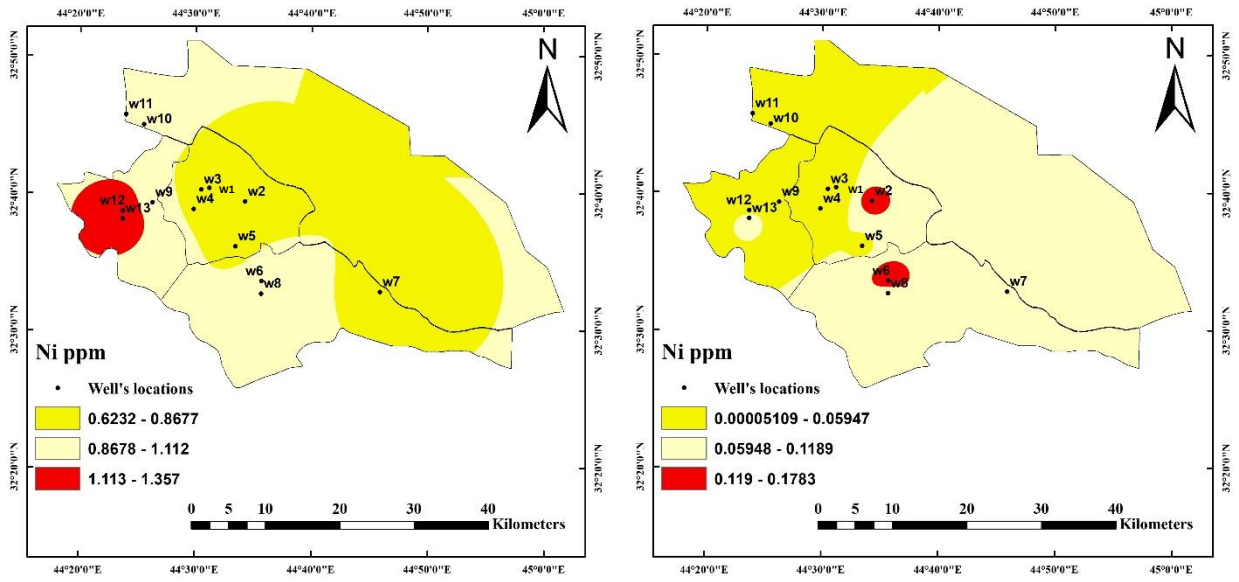

(a) For winter season. (b) For summer season.

Figure (4.29): Spatial distribution map for measured concentrations of Ni throughout the study area during the study period.

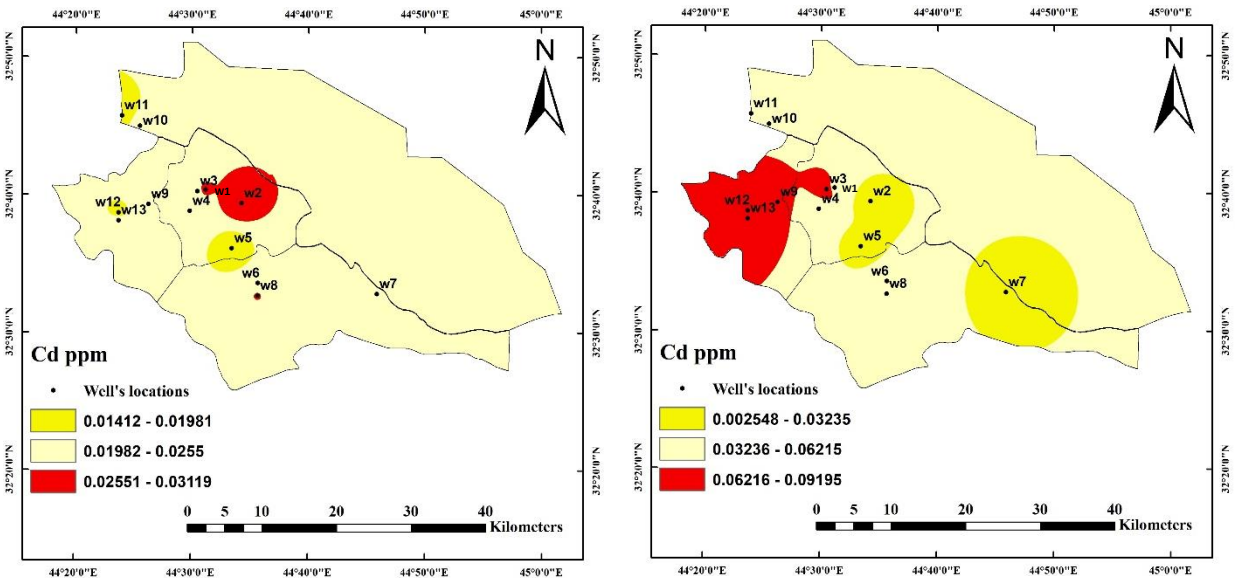

(a) For winter season. (b) For summer season.

Figure (4.30): Spatial distribution map for measured concentrations of Cd throughout the study area during the study period.

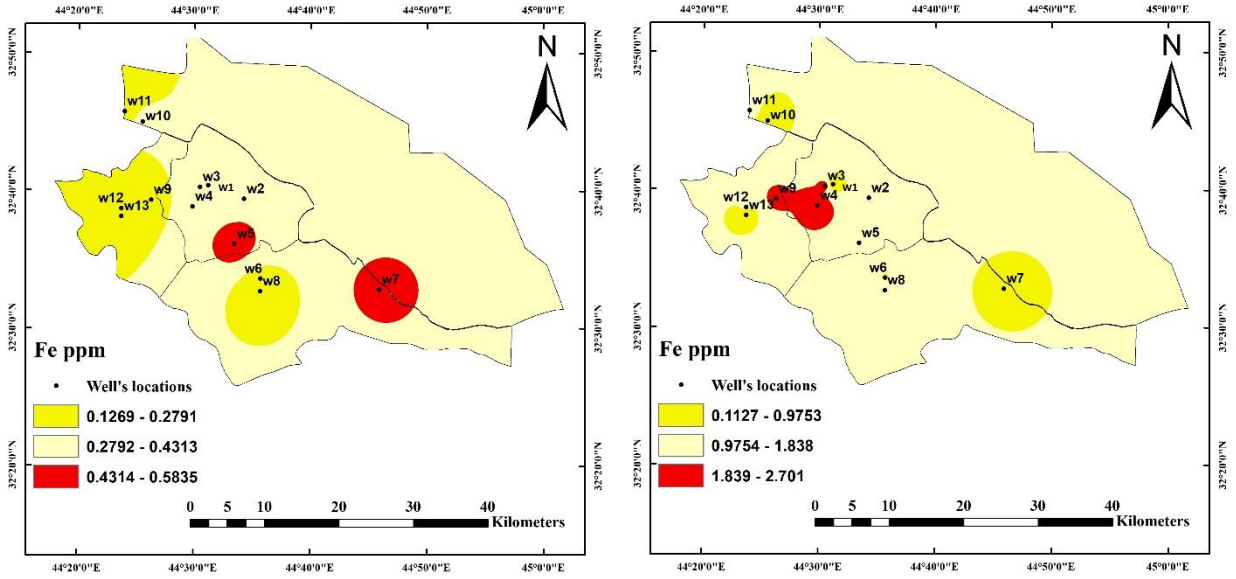

(a) For winter season. (b) For summer season.

Figure (4.31): Spatial distribution map for measured concentrations of Fe throughout the study area during the study period.

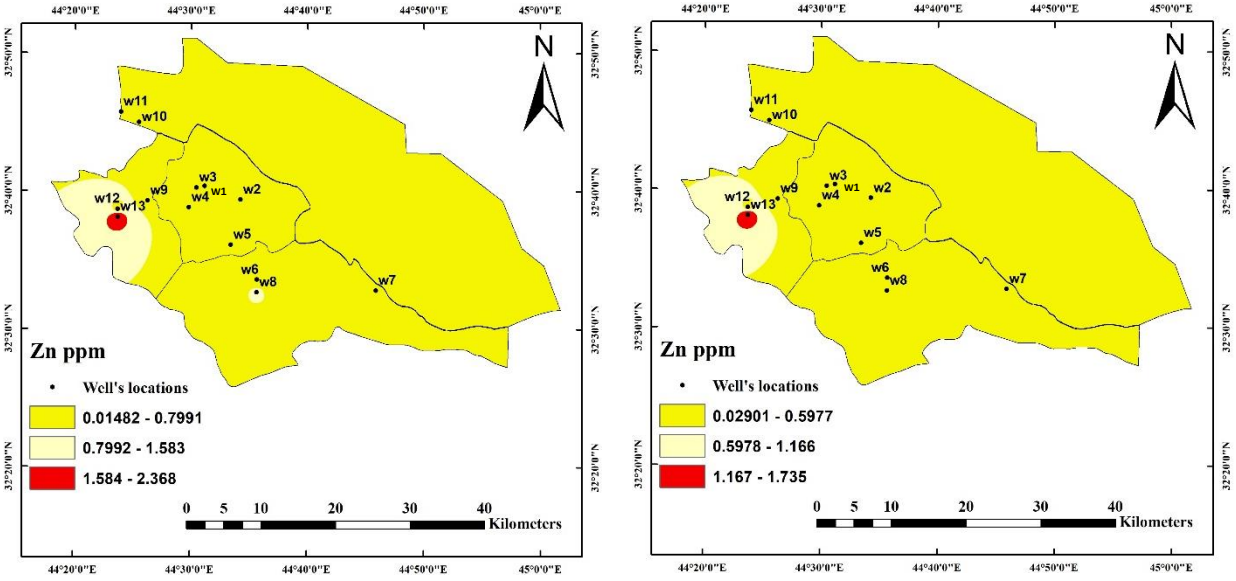

(a) For winter season. (b) For summer season.

Figure (4.32): Spatial distribution map for measured concentrations of Zn throughout the study area during the study period.

The higher concentrations of Nickel-metal surrounding the wells (w12 and w13) as shown in Figure (4.29 a), it is average value was about 1.23 ppm. The most region extending from the middle of the study area towards the east and south, including wells (w1, w2, w3, w5, and w7), was of low concentration between 0.623 to 0.846 ppm. The rest part of the study area was occupied by moderate concentrations between 0.847 to 1.09 ppm. While for summer season Figure (4.29 b) the higher concentrations was found to be around (w2 and w6). The rest of wells except w7 was falling under low concentration area.

Figure (4.30 a) show that, for cadmium metal, a concentrated irregular distribution around the wells (w1 to w2), and around well (w8) with higher concentration values between 0.0231 to 0.0312 ppm. The most of south portion and a few parts from the top of the middle of the study area were occupied by moderated concentration values between 0.024 to 0.023 ppm. The Cd metal concentrations in the west and northwestern parts were lower than 0.0022 ppm. For summer season Figure (4.30 b) the higher concentration bound four wells (w3, w9, w12, and w13). The lowest bound (w2, w5 and w7), the rest fall under moderate areas.

Figure (4.31 a) shows the distribution of Iron metal over the study area, the pattern of distribution was roughly similar to the distribution of Cadmium metal; the higher concentration is around the wells (w5, and w7) with an average value of 0.48 ppm. The regions to the west, up and down the study area are of moderate concentrations between 0.336 to 0.376 ppm. While the remaining portions were the low concentrations between 0.127 to 0.335 ppm. While for dry season the higher concentration had centered with an area that bounding (w3, w4 and w9). The lowest concentration had bounded four wells (w1, w7, w10 and w13), and the rest fall under moderate areas.

Figure (4.32 a) shows that the higher concentration area of Zink metal was fully limited by well (w13) with values between 1.15 to 2.37 ppm, on other hand, most of the study area especially the regions located far from the wells towards the east were

observed as lower concentration values between 0.0148 to 0.431 ppm. The regions located below the study area towards the south and southwest were found to have moderate concentration values between 0.423 to 1.14 ppm. However, for summer season Figure (4.32 b), except of small area that bounding (w8) it could be said it gives the same distribution pattern of winter season with lower concentration values.

Finally, no obvious pattern of distribution for all the investigated heavy metal can be detected, but most of the lower or moderated concentration values were scattered unevenly far away from well locations.

4.5 Criteria for the Quality of the Groundwater

The qualitative evaluation method for groundwater was carried out in this study via WQI for drinking water quality assessment, HPI, and HEI for evaluate the pollution with heavy metals and finally EC, SAR, RSBC, SSP, MH, PI and KR for irrigation water quality assessment indices. At first, calculating of water quality index (WQI) is done using the most commonly measured water quality parameters, the weighted arithmetic water quality index method classified the water quality according to the degree of purity. The ideal values was set to zero for all parameters except pH with ideal value equal to seven (Brown et al., 1972). Figure (4.33), (4.34) and (4.35) show the variations of WQI, HPI and HEI for each well in the study area for winter and summer seasons, respectively.

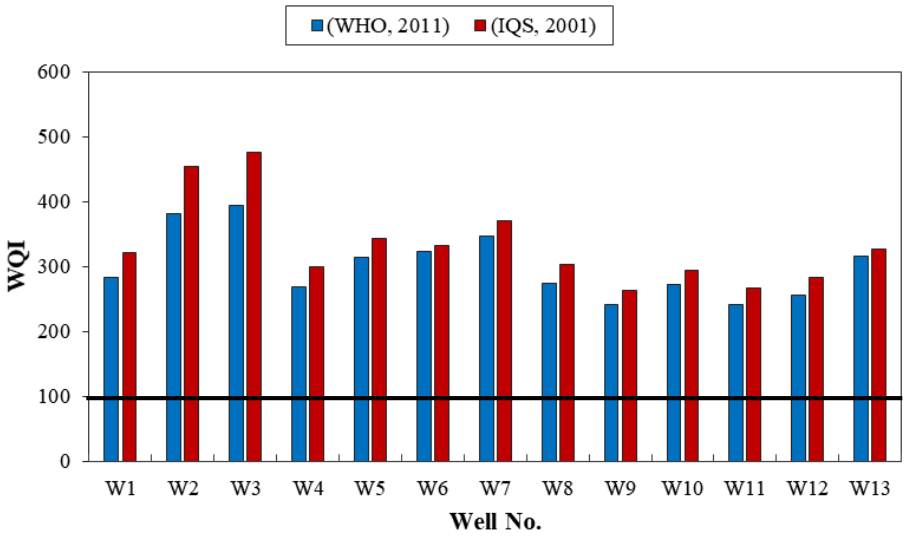

WQI > 100 unsuitable for drinking purpose.

(a) For winter season.

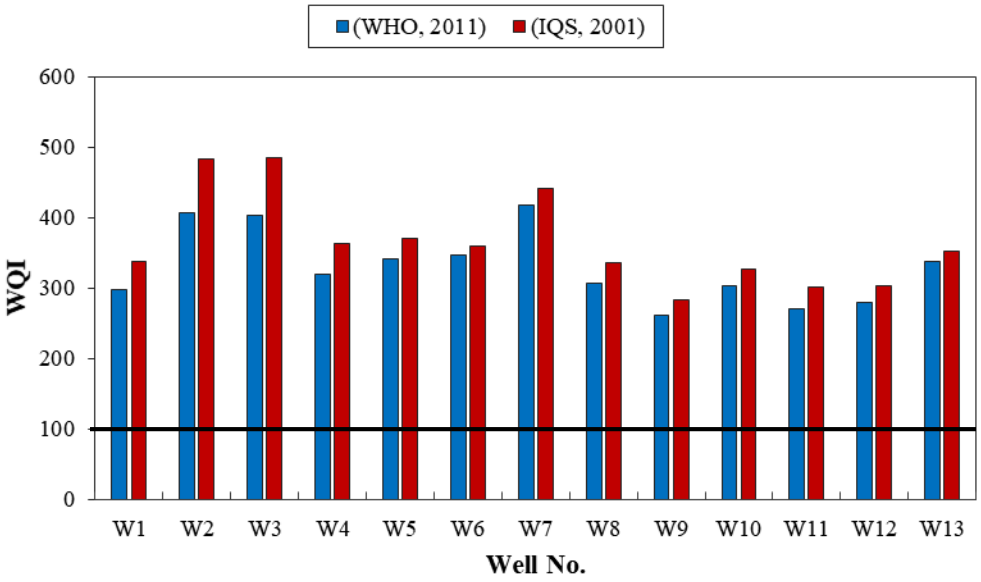

WQI > 100 unsuitable for drinking purpose.

(b) For summer season.

Figure (4.33): Variation of Water Quality Index (WQI) for groundwater in study area.

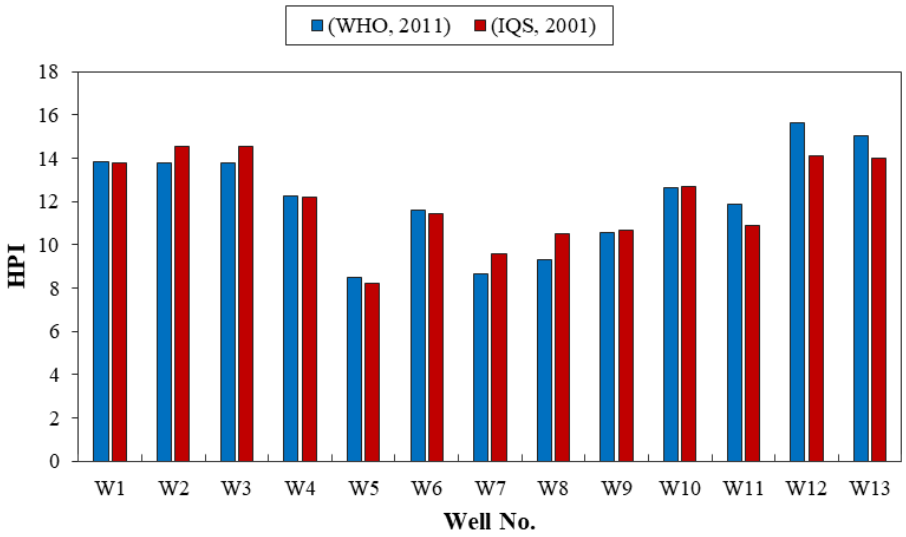

(a) For winter season.

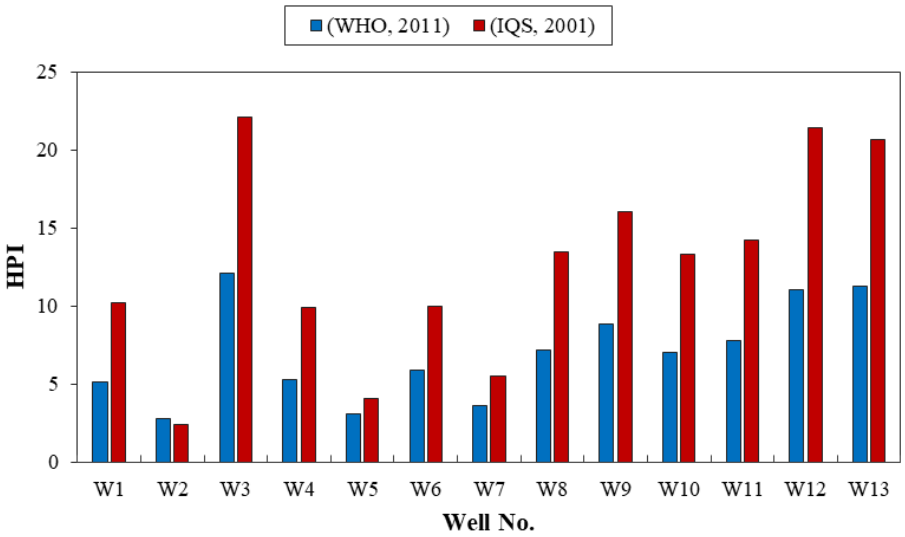

(b) For summer season.

Figure (4.34): Variation of Heavy metal Pollution Index (HPI) for groundwater in study area.

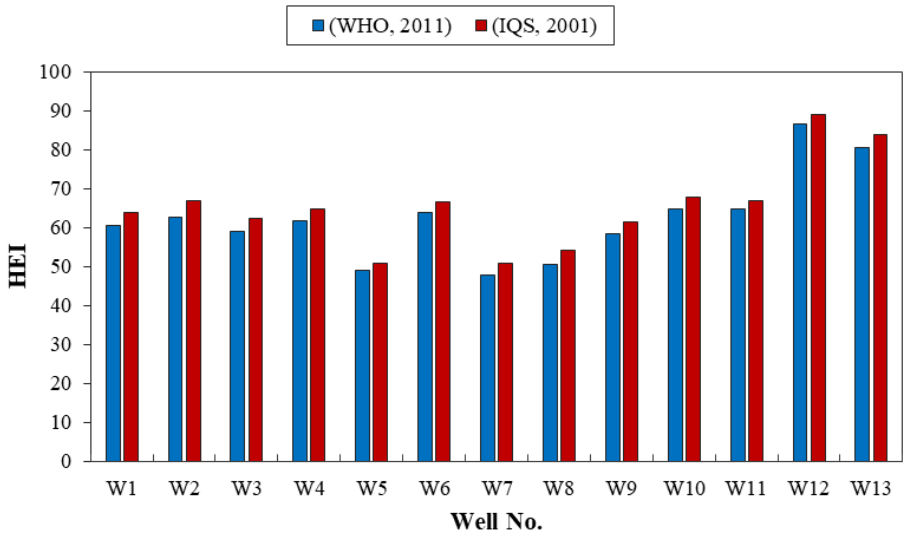

(a) For winter season.

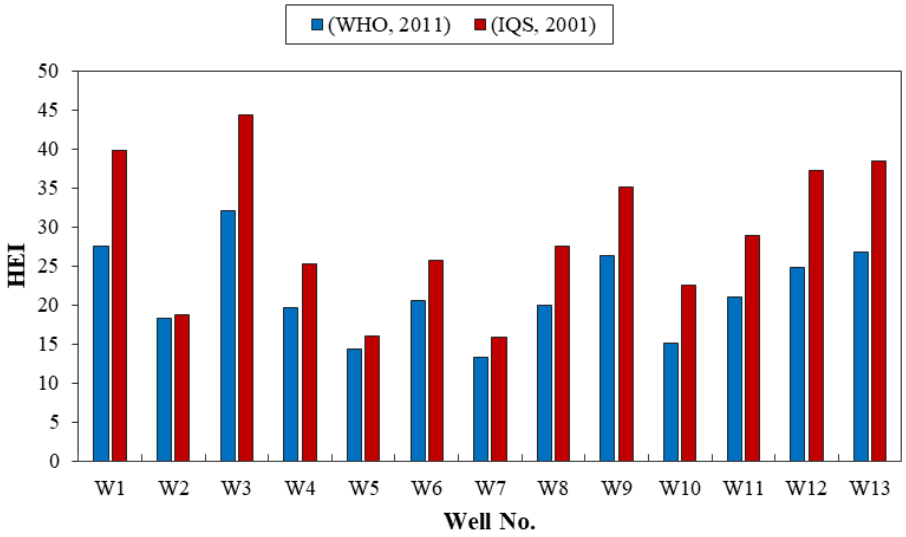

(b) For summer season.

Figure (4.35): Variation of Heavy metal evaluation index (HEI) for groundwater in study area.

From the results shown in Figure (4.33), it has been noticed that WQI in all samples are higher as per (IQS, 2001) than for (WHO, 2011) for both winter and summer. The WQI values for the wells w4, w11 and w12 are has been found less than

other wells. In general, the values of WQI for both seasons has exceeded the desirable values for drinking water according to (IQS, 2001) and (WHO, 2011) standards, respectively.

The HPI measures the ratio of contamination caused by heavy metals presence as well as the combined influence of each heavy metal on overall drinking water quality (Egbueri, 2020). Since these metals or ions should not be found in drinking water, ideal value is set to zero (Elumalai et al., 2017).

The HEI is useful in determining trace metal pollution degree in groundwater due to higher concentrations of the heavy metal in water making it unsuitable for variety of uses, including human use (Egbueri, 2018).

From Figures (4.34 a) and (4.35 a), HPI and HEI values of all samples are much less as per (IQS, 2001) than for (WHO, 2011). For winter and summer samples, the descriptive statistics for such indices are given in Tables (4.13) and (4.14), respectively.

Table (4.13): Summary of descriptive statistics of groundwater indices in study area at winter season.

Index / Statistics	(IQS, 2001)			(WHO, 2011)		
	WQI	**HPI**	**HEI**	**WQI**	**HPI**	**HEI**
Mean	333.5	12.1	62.35	301.29	12.22	62.35
Maximum	476.22	14.6	86.5	394.65	15.7	86.5
Minimum	262.73	8.2	47.9	241.35	8.5	47.9
Median	321.36	12.2	61.8	283.86	12.3	61.8
Standard Deviation	65.86	2.067	11.123	49.96	2.439	11.123
Sample Variance	4338	4.273	123.727	2495.93	5.948	123.727
Standard Error	18.27	0.573	3.085	13.86	0.676	3.085
Kurtosis	1.07	-0.917	0.988	-0.55	-1.118	0.988
Skewness	1.31	-0.364	0.935	0.66	-0.232	0.935

Table (4.14): Summary of descriptive statistics of groundwater indices in study area at summer season.

Index / Statistics	(IQS, 2001)			(WHO, 2011)		
	WQI	**HPI**	**HEI**	**WQI**	**HPI**	**HEI**
Mean	365.09	12.56	28.88	330.27	7	21.52
Maximum	485.52	22.1	44.31	417.12	12.11	32.15
Minimum	283.54	2.4	15.91	260.79	2.8	13.26
Median	351.9	13.31	27.46	320.26	7	20.56
Standard Deviation	65.87	6.44	9.40	52.16	3.11	5.70
Sample Variance	4338.55	41.43	88.29	2721	9.69	32.54
Standard Error	18.27	1.79	2.61	14.47	0.86	1.58
Kurtosis	-0.11	-0.91	-1.20	-0.85	-1.02	-0.71
Skewness	0.94	0.03	0.12	0.53	0.32	0.25

As listed in Table (4.13), the mean overall value of HPI index according to (IQS, 2001) and (WHO, 2011) are almost the same, which is about 12.1, also, for HEI is 62.35, respectively. Subsequently, the groundwater in study area are exceeding desired limits by the standards, and declared as low pollution for winter season.

For summer season as listed in Table (4.14), according to HEI limited to both (IQS, 2001) and (WHO, 2011) it is declared as low pollution. Although mean value of HPI fall under 19 as low pollution limited to (IQS, 2001), but there are three wells fall out of this range, these are (w3= 22.1, w12= 21.5 and w13= 20.7) and this should be categorized as medium heavy metals pollution, this increment should be attributed to Cd higher concentration which is found mainly in domestic wastes, phosphate fertilizer, as well as atmospheric deposition (Ismael et al., 2019). While when HPI is limited to (WHO, 2011), all values fall within low pollution range.

The descriptive statistics for groundwater indices are presenting by box plots as shown in Figures (4.36), (4.37) and (4.38).

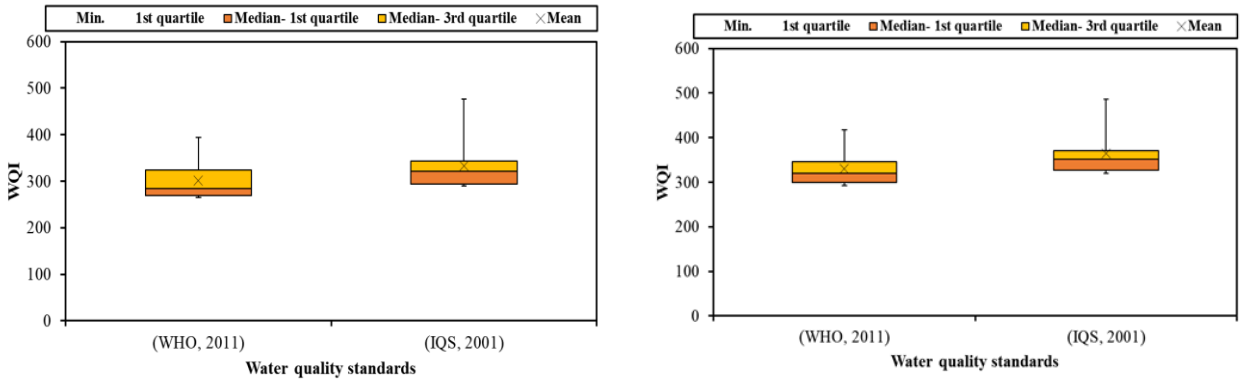

(a) For winter season. (b) For summer season.

Figure (4.36): Box plot representing WQI statistics.

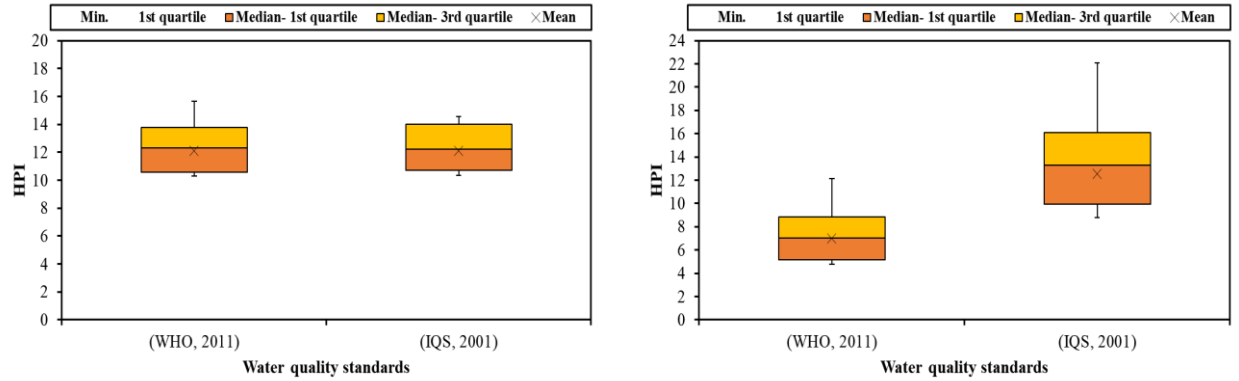

(a) For winter season. (b) For summer season.

Figure (4.37): Box plot representing HPI statistics.

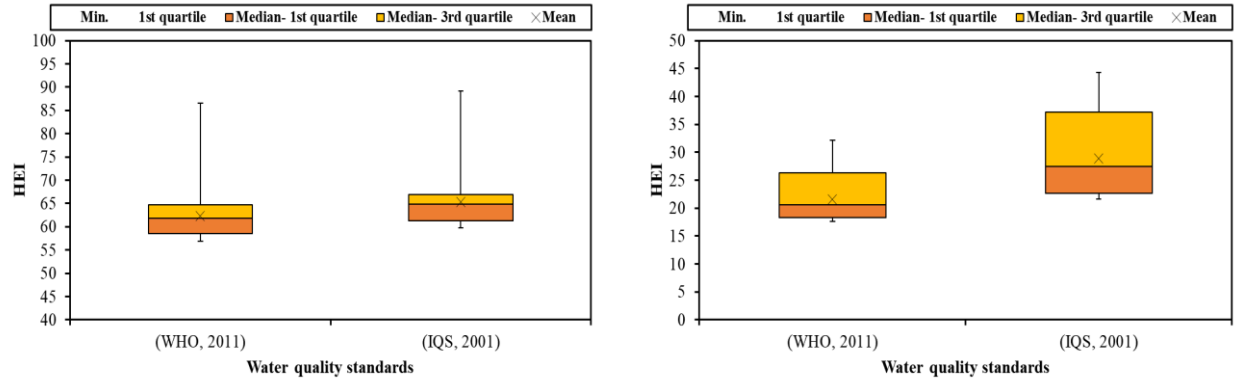

(a) For winter season. (b) For summer season.

Figure (4.38): Box plot representing HEI statistics.

As formerly described, the values of the groundwater indices that are given in Table (4.13) and (4.14) demonstrated with aid of box plots as shown in Figures (4.36), (4.37) and (4.38). That introduce impacts of chosen chemical parameters concentration per each well into the overall indices. It was interpreted by maximum, minimum, median-quartiles statistics. Also, the previous findings have been confirmed.

The descriptive statistics of irrigation water suitability classification controls are given in Tables (4.15), (4.16), (4.17) and (4.18), for summer and winter respectively.

Table (4.15): Summary of descriptive statistics for irrigation water suitability classification controls in the study area for winter season.

Classification controls / Statistics	**EC (µs/cm)**	**SAR**	**RSBC (meq/l)**	**SSP%**	**MH**	**PI**	**KR (meq/l)**
Mean	4086.77	4.70	-4.09	41.96	68.85	47	0.74
Maximum	9150	9.92	6.24	68.03	97.03	78.11	1.99
Minimum	1518	0.98	-35.6	23.27	2.57	23.83	0.19
Median	2990	3.38	1.6	38.43	81.89	44.12	0.51
Standard Deviation	2603.07	3.32	13.23	14.25	30.73	16.34	0.54
Sample Variance	6775951.69	10.99	175.03	202.94	944.31	267.15	0.29
Standard Error	721.96	0.92	3.67	3.95	8.52	4.53	0.15
Kurtosis	-0.882	-1.537	2.45	-0.983	0.89	-0.58	0.83
Skewness	0.737	0.444	-1.84	0.392	-1.35	0.50	1.13

Table (4.16): Summary of quartiles for irrigation water suitability classification controls in study area for winter season.

Classification controls / Statistics	EC (µs/cm)	SAR	RSBC (meq/l)	SSP%	MH	PI	KR (meq/l)
Q1-Min.[1]	369	0.75	29.6	6.09	54.30	9.14	0.16
Med.-Q1[*]	1103	1.65	7.6	9.07	25.03	11.15	0.16
Q3-Med.[2]	3520	4.28	0.8	12.33	8.87	12.80	0.46
Max.-Q3[**]	2640	2.26	3.84	17.27	6.27	21.18	1.01

[1] is the 1st quartile (minimum),
[*] is the median for 1st quartile,
[2] is the median for 3rd quartile, and
[**] is the 3rd quartile (maximum).

Table (4.17): Summary of descriptive statistics for irrigation water suitability classification controls in the study area for summer season.

Classification controls / Statistics	EC (µs/cm)	SAR	RSBC (meq/l)	SSP%	MH	PI	KR (meq/l)
Mean	4517.77	4.86	-5.62	40.14	64.45	45.46	0.72
Maximum	9430	12.3	6.4	73.33	92.88	81.41	2.6
Minimum	1532	1.12	-36.6	23.03	3.3	22.2	0.19
Median	2940	3.37	0.4	37.65	72.6	42.31	0.49
Standard Deviation	2889.28	3.70	14.14	15.14	28.96	16.60	0.66
Sample Variance	8347914.53	13.70	199.98	229.20	838.79	275.41	0.43
Standard Error	801.34	1.03	3.92	4.2	8.03	4.6	0.18
Kurtosis	-1.05	-0.57	1.14	0.10	0.60	0.27	5.40
Skewness	0.76	0.78	-1.50	0.83	-1.17	0.72	2.13

Table (4.18): Summary of quartiles for irrigation water suitability classification controls in study area for summer season.

Classification controls / Statistics	EC (µs/cm)	SAR	RSBC (meq/l)	SSP%	MH	PI	KR (meq/l)
Q1-Min.[1]	1102	0.63	29.6	4.6	53.2	9.3	0.09
Med.-Q1[*]	306	1.62	7.4	9.95	16	10.78	0.20
Q3-Med.[2]	3870	3.32	2	12.4	15.78	12.9	0.46
Max.-Q3[**]	2620	5.60	4	23.2	4.5	26.17	1.65

[1] is the 1st quartile (minimum),
[*] is the median for 1st quartile,
[2] is the median for 3rd quartile, and
[**] is the 3rd quartile (maximum).

From results of Table (4.15) and (4.16). In terms of total salinity measured via the electrical conductivity measure (EC), maximum value of EC was recorded in w3 and minimum value was in w11. The statues of groundwater samples at w2, w3, w5, w6 and w7 show higher values than 5000 µs/cm, which produces the groundwater ″unsuitable″ for irrigation purposes. While the values of EC for groundwater of wells w1, w4, w10, w11 and w12 make these well classified as ″permissible″ category. What remains of the wells can be categorized as ″doubtful″ for irrigation purposes. The overall mean value of EC was found to be 3994 µs/cm, which is classified as ″doubtful″. Highly saline water is toxic to plants and may leads to salinity hazards. (Borecka et al., 2016). Since plants can only transpire "pure" water, the higher the Ec, the less water available to plants, even though the soil appears moist, the soil's solution water being used by the plant gradually decreases as Ec increases (Reddy, 2013).

one of the important parameters is SAR which used to determine the suitability of groundwater for irrigation water and is also used to indicate sodium damage in irrigation water (Yetiş et al., 2019). There is a significant relationship between values of sodium

in irrigation water and the extent to which sodium is absorbed by the soils. While a high salt concentration in water leads to formation of saline soil, high sodium leads to development of an alkaline soil. Alkali hazard of the irrigation water is determined by SAR. If the proportion of Na is high, the alkali hazard is high (Adhikary et al., 2012). The SAR values ranged from minimum value of 0.98 in w4 to maximum value of 9.92 in w5 and that produced all the groundwater to be classified as ″excellent″ for irrigation use i.e. no harmful effect of sodium detected (US, 1954). The overall mean value was 4.7 that it is much lower than the limited category value of 10.

The RCBS values ranged from a maximum value of 6.24meq/l to a minimum value of -35.6 meq/l, except of w8 and w9 which are considering as ″marginal″, all other winter collected samples consider as ″satisfactory″ for irrigation use.

Increase in the sodium percentage in irrigation water is an undesirable condition because it indicates cation exchange with calcium and magnesium in the soil (Richards, 1954). SSP is an estimation of the sodium hazard of irrigation water such as SAR, but represents the percentage of sodium out of the total cations as with SAR, the main problem of high concentration of sodium is its impact on the permeability of the soil, water infiltration and total salinity increase in its therefore harmful to sensitive crop. (Megahed, 2020).

The values of SSP parameter indicated a wide range of water quality for irrigation started from good, permissible to doubtful; also the overall mean value was 41.96, which classified as ″permissible″ for irrigation purposes.

One of the indicators used to determine the suitability of irrigation water is magnesium ratio in cations, High magnesium content in water salts the soil, negatively affecting plant growth and yield (Yetiş et al., 2019). Magnesium ratio is important for assessing suitability of water for irrigation. Magnesium damages soil structure when water contains a lot of sodium and high salinity (Chidambaram et al., 2013). MH which

classify the collected groundwater samples into two groups suitable (<50) and unsuitable (>50). Following this only w2 and w3 is suitable for irrigation use.

Soil permeability can change because of long-term use of irrigation water which includes sodium, calcium, magnesium and bicarbonate (Babithesh Babu et al., 2015). PI values ranged from 78.11 to 23.83, except for w9 that categorized as ″excellent″ and w13, which categorized as ″unsuitable″ for irrigation use, all other collected samples fall under ″good″ class for irrigation uses.

According to Kelley,(1963), the hazardous impacts of sodium on irrigation water quality are defined by Kelly's ratio. In this study, wells recorded a wide KR range, started from (0.19 to 1.99). out of thirteen winter sample set only three wells w5, w8 and w9 has recorded a hazard value (>1) which is count to be unsafe for irrigation.

From results of Table (4.17) and (4.18), for summer set of samples maximum value of EC was recorded in w3 and minimum value was in W11. The statues of groundwater samples at w2, w3, w5, w6 and w7 show higher values than 5000 µs/cm, which produces the groundwater ″unsuitable″ for irrigation purposes. While the values of EC for groundwater of wells w1, w4, w10 and w11 make these well classified as ″permissible″ category. What remains of the wells should be categorized as ″doubtful″ for irrigation purposes. The overall mean value of EC was found to be 4517.77 µs/cm, which is classified as ″doubtful″.

The SAR values for summer season, ranged from minimum value of 1.12 in w4 to maximum value of 12.3 in w9. Except for w9 which classified as ″good″ for irrigation, all the groundwater samples are classified as ″excellent″ for irrigation use. The overall mean value was 4.86 that it is much lower than the limited category value of 10, and slightly higher than the overall mean of SAR for winter samples.

The values of SSP% indicated a wide range of water quality for irrigation started from good, permissible to doubtful; also the overall mean value was 40.14, slightly

lower than the overall mean of SSP% for winter samples which classified as ″permissible″ for irrigation purposes.

The values of RCBS ranged from a maximum value of 6.4meq/l to a minimum value of -36.6 meq/l, except of w8, w9 and w10 that are considering as ″marginal″, all other summer-collected samples consider as ″satisfactory″ for irrigation use.

For MH, which classify the collected samples into two groups suitable (<50) and unsuitable (>50). Following this index only w2 and w3 is suitable for irrigation use.

PI values ranged from 81.41 to 22.2, except for w9 that categorized as ″excellent″ and w13, which categorized as ″unsuitable″ for irrigation use, all other collected samples fall under ″good″ class for irrigation uses.

For the present study, wells recorded a wide KR range, started from (0.19 to 2.6). Out of thirteen sample in summer season, only two wells w5 and w9 has recorded a hazard value (>1) which was declared to be unsafe for irrigation.

CHAPTER FIVE

CONCLUSIONS AND RECOMMONDATIONS

CHAPTER FIVE

CONCLUSIONS AND RECOMMONDATIONS

5.1 Conclusions

The main conclusions of the present study can be drawn down by the following points:

1. The measured values of EC and TDS for collected groundwater samples indicated high values of EC by (53.8%) and (61.5%) at the winter and summer seasons, respectively. Therefore, it was declared as high saline water. All the groundwater samples that were investigated in this research do not satisfy the WHO (2001) requirements regarding (TDS) regarding drinking purposes.
2. The measured concentrations of the main cations and anions in the study area were found to be ranked in the order: Na>Ca> Mg>K and SO_4>Cl>HCO_3> NO_3 during the study period. Their concentrations were much higher than the maximum acceptable limits for drinking water limitations in accordance with IQS (2001) and WHO (2011).
3. The measured concentrations of the heavy metals during study period were found to be ranked in the order: Cd < Pb < Fe < Zn <Ni and Pb < Cd < Ni < Zn <Fe for the winter and the summer seasons, respectively. It was inferred that the probable sources of heavy metals in groundwater were deduced from agricultural activities, because the water samples were taken from wells located in private farms in which many chemical fertilizers and pesticides were frequently and extensively used. In addition, there were another source represented by the human activity, such as the leakage and percolation from landfills and septic tank into the holding layers of groundwater.

4. According to IQS, (2001) and WHO, (2011), the computed water quality index WQI revealed that, for both the winter and the summer seasons, no well was found to be suitable for drinking purposes.
5. Evaluation of groundwater quality for irrigation purposes based on different irrigation quality indices indicated that for the measured values of EC, only 38.46% and 30.77% of wells were "permissible" during the winter and the summer seasons, respectively. Moreover, about 38.5% were classified as "unsuitable" during the study period, while the rest were categorized as "doubtful". Almost, all the calculated indices such as SAR, SSP%, RSBC, MH, PI, and KR were involved that more than 80% of the groundwater samples were considered as excellent to good categories, and less than 20% of samples were considered as unsafe. Therefore, it was concluded, that the groundwater throughout the study area was in general suitable for irrigation.
6. From the spatial distribution of groundwater quality parameters that carried out by GIS, the results show large variations and generally increased toward the southeastern parts of the study area. For heavy metals, it was showed a randomly distributed behavior throughout the study area.
7. The results of the hydraulic modeling by using numerical model for the steady state groundwater were calibrated, for hydraulic conductivity and recharge rates and one scenarios was used to simulate a drought condition with zero recharge and five operating wells with $48 m^3$/day pumping rate, this scenario showed a major decline in water table in the entire area.

5.2 Recommendations

1. Investigation of more heavy metals and other biological contaminations, such as Biochemical Oxygen Demand (BOD), Chemical Oxygen Demand (COD).
2. Performing detailed hydraulic modeling by constructing a conceptual model for the unsteady state of groundwater flow.
3. Conducting a similar study in water lack and/ or water shortage regions.

REFERENCES

References

Abbasnia, A., Yousefi, N., Mahvi, A. H., Nabizadeh, R., Radfard, M., Yousefi, M., and Alimohammadi, M. (2018). Evaluation of groundwater quality using water quality index and its suitability for assessing water for drinking and irrigation purposes: Case study of Sistan and Baluchistan province (Iran). *Human and Ecological Risk Assessment: An International Journal*, 25(4), 988–1005.

Abdel-Satar, Amaal M., Manal H. Al-Khabbas, Waed R. Alahmad, Wafaa M. Yousef, Rani H. Alsomadi, and Tasneem Iqbal. (2017). Quality Assessment of Groundwater and Agricultural Soil in Hail Region, Saudi Arabia. *The Egyptian Journal of Aquatic Research* 43(1):55–64.

Abed, B. S. H., and Hussain, M. R. (2020). Quantitative and qualitative assessment of groundwater: the case of Khanaqin alluvial (Iraq). *Journal of Engineering Science and Technology, 15*(6), 4339–4355.

Adhikary, Partha Pratim, Ch Jyotiprava Dash, H. Chandrasekharan, T. B. S. Rajput, and S. K. Dubey. (2012). Evaluation of Groundwater Quality for Irrigation and Drinking Using GIS and Geostatistics in a Peri-Urban Area of Delhi, India. *Arabian Journal of Geosciences* 5(6):1423–34.

Adimalla, N., and Venkatayogi, S. (2018). Geochemical characterization and evaluation of groundwater suitability for domestic and agricultural utility in semi-arid region of Basara, Telangana State, South India. *Applied Water Science*, *8*(1), 1–14.

Ahmad, A. Y., Al-Ghouti, M. A., Khraisheh, M., & Zouari, N. (2020). Hydrogeochemical characterization and quality evaluation of groundwater suitability for domestic and agricultural uses in the state of Qatar. *Groundwater for Sustainable Development*, *11*, 100467.

Aghazadeh, N., and Mogaddam, A. A. (2010). Assessment of groundwater quality and

its suitability for drinking and agricultural uses in the Oshnavieh area, Northwest of Iran. *Journal of Environmental Protection*, 1(01), 30.

Al-Ansari, N. (2013). Management of water resources in Iraq: perspectives and prognoses. *Engineering*, 5(6), 667–684.

Al-Ansari, N., Ali, A., and Knutsson, S. (2014). Present conditions and future challenges of water resources problems in Iraq. *Journal of Water Resource and Protection*, *6*(12), 1066–1098.

Al-Areedhi, H. H. (2019). Modelling of Groundwater Flow for the Iraqi Aquifers. Ph. D. Thesis, University of Technology, Baghdad, Iraq.

Al-Hessnawi, J. K., Jawad, Z. S., and Fadhil, F. A. (2018). Spatial analysis of natural properties in Mahaweel District. *Journal of University of Babylon*, *26*(8).

Al-Hussaini, S. N. H., Al-Obaidy, A. H. M. J., and Al-Mashhady, A. A. M. (2018). Environmental assessment of heavy metal pollution of Diyala River within Baghdad City. *Applied Water Science*, 8(3), 87.

Al-Mawal, 2019. A company for soil investigations. reports of wells data an soil investigation

Al-Muqdadi, S. W. (2012). Groundwater investigation and modeling-western desert of Iraq. Ph.D. Thesis, Faculty of Geosciences, Geo- Engineering and Mining Technische Universität Bergakademie Freiberg Chair of Hydrogeology institute. Germany.

Al-Mussawy, W. H. (2013). Optimum management models for groundwater use in Karbala desert area. Ph. D Thesis. Al-Mustansiriyah University, Baghdad, Iraq.

Anderson, M. and Woessner, W., (1992), Applied groundwater modeling: Simulation of Flow and advective transport, San Diego, California, Academic Press Inc. Second Edition.

Aquaveo, L. L. C. (2017). *Mesh editing. SMS 12.2 tutorials*.

Babithesh Babu, N., Gajendran, C., Shahul Hameed, A., & James, E. (2015). Appraisal of groundwater quality for drinking and irrigation purposes in Nambiyar river basin, Tamil Nadu, India. *Water Resources, 42*(4).

BCL, 2019. Babylon construction laboratory. Reports of soil investigation.

Borecka, M., Białk-Bielińska, A., Haliński, Ł. P., Pazdro, K., Stepnowski, P., & Stolte, S. (2016). The influence of salinity on the toxicity of selected sulfonamides and trimethoprim towards the green algae Chlorella vulgaris. *Journal of Hazardous Materials*, *308*, 179–186.

Brown, R. M., Mccleiland, N. J., Deiniger, R. A., & O'Connor, M. F. (1972). Water quality index-crossing the physical barrier,(Jenkis, SH, ed.) Proc. *Intl. Conf. on Water Poll. Res. Jerusalem*, *6*, 787–797.

Burrough, P. A., McDonnell, R. A., McDonnell, R., and Lloyd, C. D. (2015). *Principles of geographical information systems*. Oxford university press.

Chidambaram, S., Prasad, M. B. K., Manivannan, R., Karmegam, U., Singaraja, C., Anandhan, P., Prasanna, M. V., and Manikandan, S. (2013). Environmental hydrogeochemistry and genesis of fluoride in groundwaters of Dindigul district, Tamilnadu (India). *Environmental Earth Sciences*, *68*(2), 333–342.

Christensen, S., and Cooley, R. L. (2003). Experience gained in testing a theory for modelling groundwater flow in heterogeneous media. *IAHS PUBLICATION*, 22–27.

DEB, 2019. Ministry of health and environment, directorate of environment in Babylon. Wells data.

Doneen L. D. (1964) Water quality for agriculture. Department of Irrigation, University of California, Davis.

DWRB, 2017. Ministry of water resources, directorate of water resources in Babylon.

DWRB, 2019. Ministry of water resources, directorate of water resources in Babylon. Water levels records of surface water resources within the study area.

Edet, A. E., and Offiong, O. E. (2002). Evaluation of water quality pollution indices for heavy metal contamination monitoring. A study case from Akpabuyo-Odukpani area, Lower Cross River Basin (southeastern Nigeria). *GeoJournal*, *57*(4), 295–304.

Edokpayi, J. N., Enitan, A. M., Mutileni, N., and Odiyo, J. O. (2018). Evaluation of water quality and human risk assessment due to heavy metals in groundwater around Muledane area of Vhembe District, Limpopo Province, South Africa. *Chemistry Central Journal*, 12(1), 1–16.

Egbueri, J. C. (2018). Assessment of the quality of groundwaters proximal to dumpsites in Awka and Nnewi metropolises: a comparative approach. *International Journal of Energy and Water Resources*, *2*(1–4), 33–48.

Egbueri, J. C. (2020). Heavy metals pollution source identification and probabilistic health risk assessment of shallow groundwater in Onitsha, Nigeria. *Analytical Letters*, *53*(10), 1620–1638.

El-Rawy, M., Ismail, E., and Abdalla, O. (2019). Assessment of groundwater quality using GIS, hydrogeochemistry, and factor statistical analysis in Qena Governorate, Egypt. *Desalination and Water Treatment*, 162, 14–29.

Elumalai, V., Brindha, K., and Lakshmanan, E. (2017). Human exposure risk assessment due to heavy metals in groundwater by pollution index and multivariate statistical methods: a case study from South Africa. *Water*, 9(4), 234.

GCGW, 2019. General commission of groundwater in Baghdad. Wells data.

Ghalib, H. B. (2017). Groundwater chemistry evaluation for drinking and irrigation utilities in east Wasit province, Central Iraq. Applied Water Science, 7 (7), 3447–3467.

GMS User Manual, (2018). v10.4, Groundwater Modeling System software tutorial.

Hadi, S. H., and Alwan, H. H. (2020). The effect of effect of Shatt Al- Diwaniya on the groundwater levels of Shatt Al- Diwaniya. M. SC. Thesis, University of Kerbala ,

Kerbala, Iraq.

Hosseinifard, S. J., & Aminiyan, M. M. (2015). Hydrochemical characterization of groundwater quality for drinking and agricultural purposes: a case study in Rafsanjan plain, Iran. *Water Quality, Exposure and Health, 7*(4), 531–544.

Hussain, M. R., and Abed, B. S. (2019). Simulation and assessment of groundwater for domestic and irrigation uses. Civil Engineering Journal, 5(9), 1877–1892.

Hussain, T. A., Ismail, M. M., and Al-Ansari, N. (2021). Simulation of the ground water flow in Karbala Governorate, Iraq. *Environmental Earth Sciences*, 80(5), 1–6.

IMOS, 2019. Iraqi meteorological organization and seismology, 2019. Temperature and rainfall records.

Iqbal, A. B., Rahman, M. M., Mondal, D. R., Khandaker, N. R., Khan, H. M., Ahsan, G. U., Jakariya, M., and Hossain, M. M. (2020). Assessment of Bangladesh groundwater for drinking and irrigation using weighted overlay analysis. *Groundwater for Sustainable Development*, 10, 100312.

Ismael, M. H., Al-Tawash, B. S., and Al-Saady, Y. I. (2019). Hydrochemical characteristics and environmental evaluation of surface and groundwater quality at Al-Tarmiyah Area, Baghdad, Iraq. *Iraqi Journal of Science*, *60*(5), 1069–1084.

Issa, H. M., and Alshatteri, A. (2018). Assessment of Heavy Metals Contamination in Drinking Water of Garmian Region, Iraq. *UHD Journal of Science and Technology*, 2(2), 40–53.

Jalut, Q. H. (2021). Groundwater Modeling of Ahmed Taher and Bakhtiari areas southwest of Khanaqin Basin in Diyala Governorate–Iraq. *IOP Conference Series: Materials Science and Engineering*, 1076(1), 12093.

Kaur, T., Bhardwaj, R., and Arora, S. (2017). Assessment of groundwater quality for drinking and irrigation purposes using hydrochemical studies in Malwa region, southwestern part of Punjab, India. Applied Water Science, 7(6), 3301–3316.

Kelley, W. P. (1963). Use of saline irrigation water. *Soil science, 95*(6), 385-391.

Kumar, P. J. S., Delson, P. D., and Babu, P. T. (2012). Appraisal of heavy metals in groundwater in Chennai city using a HPI model. *Bulletin of Environmental Contamination and Toxicology, 89*(4), 793–798.

Makki, Z. F., Zuhaira, A. A., Al-Jubouri, S. M., Al-Hamd, R. K. S., and Cunningham, L. S. (2021). GIS-based assessment of groundwater quality for drinking and irrigation purposes in central Iraq. *Environmental Monitoring and Assessment*, 193(2), 1–27.

Mallick, J., Singh, C. K., AlMesfer, M. K., Kumar, A., Khan, R. A., Islam, S., and Rahman, A. (2018). Hydro-geochemical assessment of groundwater quality in Aseer Region, Saudi Arabia. *Water*, 10(12), 1847.

Megahed, H. A. (2020). GIS-based assessment of groundwater quality and suitability for drinking and irrigation purposes in the outlet and central parts of Wadi El-Assiuti, Assiut Governorate, Egypt. *Bulletin of the National Research Centre*, 44(1), 1–31.

Mirzabeygi, M., Abbasnia, A., Yunesian, M., Nodehi, R. N., Yousefi, N., Hadi, M., and Mahvi, A. H. (2017). Heavy metal contamination and health risk assessment in drinking water of Sistan and Baluchistan, Southeastern Iran. *Human and Ecological Risk Assessment: An International Journal*, 23(8), 1893–1905.

Mohan, S. V., Nithila, P., and Reddy, S. J. (1996). Estimation of heavy metals in drinking water and development of heavy metal pollution index. *Journal of Environmental Science & Health Part A, 31*(2), 283–289.

Pradeep, V., Deepika, C., Urvi, G., and Hitesh, S. (2012). Water quality analysis of an organically polluted lake by investigating different physical and chemical parameters. *Int. J. Res. Chem. Environ*, *2*(1), 105–111.

Prasad, B., and Bose, J. (2001). Evaluation of the heavy metal pollution index for surface and spring water near a limestone mining area of the lower Himalayas.

Environmental Geology, *41*(1), 183–188.

Rahman, M. A. T. M. T., Saadat, A. H. M., Islam, M. S., Al-Mansur, M. A., and Ahmed, S. (2017). Groundwater characterization and selection of suitable water type for irrigation in the western region of Bangladesh. *Applied Water Science*, *7*(1), 233–243.

Raghunath, H. M. (1987). Groundwater Wiley Eastern Ltd. New Delhi, India.

Reddy, K. S. (2013). Assessment of groundwater quality for irrigation of Bhaskar Rao Kunta watershed, Nalgonda District, India. *International Journal of Water Resources and Environmental Engineering*, *5*(7), 418–425.

Richards, L. A. (1954). Diagnosis and improvement of saline and alkali soils (Vol. 78, Issue 2). LWW.

Seyedmohammadi, J., Esmaeelnejad, L., and Shabanpour, M. (2016). Spatial variation modelling of groundwater electrical conductivity using geostatistics and GIS. *Modeling Earth Systems and Environment*, 2(4), 1–10.

Shankar, B. S. (2019). A critical assay of heavy metal pollution index for the groundwaters of Peenya Industrial Area, Bangalore, India. *Environmental Monitoring and Assessment*, 191(5), 289.

Subba Rao, N., and Krishna Rao, G. (1991). Groundwater quality in Visakhapatnam urban area, Andhra Pradesh. *Indian Journal of Environmental Health*, *33*(1), 25–30.

Todd, D. (1980) Groundwater hydrology, 2nd edn. Wiley, New York. (US), R. S. L. (1954). *Diagnosis and improvement of saline and alkali soils* (Issue 60). US Department of Agriculture.

Wilcox, Lv. (1955). *Classification and use of irrigation waters* (Issue 969). US Department of Agriculture.

Yetiş, R., Atasoy, A. D., Yetiş, A. D., and Yeşilnacar, M. İ. (2019). Hydrogeochemical characteristics and quality assessment of groundwater in Balikligol Basin,

Sanliurfa, Turkey. *Environmental Earth Sciences*, *78*(11), 1–17.

Appendix (A)

Iraqi and World Health Organization limitation for water quality parameters used in the present study

Parameter	WHO, 2011	IQS, 2001
pH	6.5 -8.5	6.5- 8.5
Ec ɯs/cm	1500	2000
TDS mg/l	500	1000
T.H mg/l	500	500
Ca mg/l	75	50
Mg mg/l	30	50
Na mg/l	200	200
k mg/l	12	10
CL mg/l	250	250
so4 mg\l	250	250
Hco3 mg/l	300	250
NO3 mg/l	45	50
Pb	0.01	0.01
Ni	0.02	0.02
Cd	0.005	0.003
Fe	0.3	0.3
Zn	5	3

الخلاصة

خلال موسم الجفاف الذي يمتد من شهر أيار إلى شهر أيلول، تصبح المياه الجوفية مصدرًا مائيًا حيويًا لأغراض الري بصورة رئيسية والشرب في في بعض مناطق قضاء المحاويل. الهدف الرئيسي من هذه الدراسة هو تقديم تقرير عن كمية المياه الجوفية الحالية باستخدام برنامج نظم نمذجة المياه الجوفية (GMS) ، والجودة لأغراض الشرب والري ، وأخيراً إنتاج خرائط التوزيع المكاني للعناصر المستخدمة في عملية التقييم باستخدام برنامج نظم المعلومات الجغرافية (GIS). لتحقيق هذا الهدف ، تم أخذ 13 عينة من المياه الجوفية من مواقع مختلفة خلال منطقة الدراسة وتحليلها لعدة عناصرهي: تركيز أيون الهيدروجين (pH) ، والتوصيل الكهربائي (EC) ، ودرجة الحرارة (T) ، والصلابة الكلية (TH) ، وإجمالي المواد الصلبة الذائبة (TDS) ، الكاتيونات (K^+، Na^+، Mg^{+2}، Ca^{+2}) ، الأنيونات (Cl^-، SO_4^{-2}، HCO_3^-، NO_3^-) وخمسة معادن ثقيلة (Fe، Zn، Cd، Pb ، Ni). تم استخدام ثلاثة مؤشرات لتقييم جودة المياه الجوفية لأغراض الشرب، وهي: مؤشر جودة المياه (WQI) ، مؤشر تلوث المعادن الثقيلة (HPI) ومؤشر تقييم المعادن الثقيلة (HEI). بالإضافة إلى ذلك ، تم تقييم جودة المياه لاستخدامات الري من خلال مقاييس تصنيف ملائمةمياه الري ، وهي الموصلية الكهربائية (EC) ، ونسبة امتصاص الصوديوم (SAR) ، وبيكربونات الصوديوم المتبقية (RSCB) ، ونسبة الصوديوم القابلة للذوبان (SSP) ، ونسبة مخاطر المغنيسيوم. (MH) ، مؤشر النفاذية (PI) ، ونسبة كيلي (KR).

تمت معايرة النمذجة الهيدروليكية للمياه الجوفية والحالة المستقرة ، للتوصيل الهيدروليكي ومعدلات التغذية ، واستخدم سيناريو واحد لمحاكاة حالة الجفاف مع مساواة التغذية المطرية للصفر وخمسة آبار تشغيلية بمعدل ضخ 48 $م^3$ / يوم ، وأظهر هذا السيناريو وجود انخفاض كبير في منسوب المياه الجوفية في المنطقة بأكملها. كما أظهر مؤشر جودة المياه المحسوب أنه خلال فترة الدراسة ، وفقًا لمنظمة الصحة العالمية والمعايير العراقية لم يتم العثور على بئر صالحة لأغراض الشرب. كما أظهر التقييم النوعي للمياه الجوفية من خلال مؤشرين تلوث جودة المياه أنه باستثناء ثلاثة آبار تقع خارج نطاق التلوث المنخفض وتم تصنيفها على أنها ذات تلوث معادن ثقيلة متوسط عندما تم اعتماد HPI وللمعايير القياسية العراقية خلال موسم الصيف ، وتشير بقية النتائج إلى وجود معدل منخفض للتلوث بالمعادن الثقيلة في جميع عينات المياه الجوفية الشتوية والصيفية الأخرى ، لذلك تم الإعلان عن احتمالية مخاطر مياه الشرب في المياه الجوفية على أنها ذات تلوث منخفض المستوى. أشار تقييم

جودة المياه الجوفية لأغراض الري بناءً على مؤشرات جودة الري المختلفة إلى أنه بالنسبة للقيم المقاسة للتوصيل الكهربائي ، فإن 38.46٪ و 30.77٪ فقط من الآبار "مسموح بها" خلال فصلي الشتاء والصيف على التوالي. علاوة على ذلك ، صُنف حوالي 38.5٪ على أنها "غير مناسبة" خلال فترة الدراسة ، بينما صُنفت البقية على أنها "مشكوك فيها". واخيراً ، تضمنت جميع المؤشرات المحسوبة أن أكثر من 80٪ من عينات المياه الجوفية اعتُبرت فئات ممتازة إلى جيدة ، وأقل من 20٪ من العينات اعتبرت غير آمنة. لذلك تم الاستنتاج أن المياه الجوفية في جميع أنحاء منطقة الدراسة كانت مناسبة بشكل عام للري. أظهر التوزيع المكاني لنتائج عناصر جودة المياه الجوفية تباينات كبيرة وزادت بشكل عام نحو الأجزاء الجنوبية الشرقية من منطقة الدراسة. اما بالنسبة للمعادن الثقيلة ، فقد أظهرت توزيع عشوائي في جميع أنحاء منطقة الدراسة.

أخيرًا ، تشير للنتائج التي تم الحصول عليها إلى أن جميع التركيزات التي تم قياسها للكاتيونات والأنيونات قد زادت في موسم الجفاف بدلاً من موسم الأمطار ، مما يُعزى إلى التبخر والسحب المكثف للمياه الجوفية من الآبار في الصيف. من ناحية أخرى ، تشير التركيزات التي تم قياسها للمعادن الثقيلة إلى قيم أقل في موسم الجفاف منها في موسم الأمطار ؛ تكشف هذه النتائج عن عدم وجود مصدر معين لهذه المعادن داخل الطبقات تحت السطحية ، وعلى سطح الأرض في جميع أنحاء منطقة الدراسة. ومع ذلك ، فإن وجود تركيزات من المعادن الثقيلة يُعزى إلى النشاط الزراعي مثل الاستخدام المكثف للأسمدة والمبيدات الزراعية ، حيث تتسرب المادة المرتشحة للملوثات وتتسرب بعمق في طبقات التربة رأسياً إلى أسفل نحو منسوب المياه الجوفية عن طريق مياه الري وهطول الأمطار في موسم الأمطار.

جمهورية العراق
وزارة التعليم العالي والبحث العلمي
جامعة بابل/ كلية الهندسة
قسم الهندسة المدنية

التقييم النوعي والهيدروليكي للمياه الجوفية لأغراض الشرب والري في منطقة المحاويل -العراق

رسالة مقدمة إلى قسم الهندسة المدنية، كلية الهندسة، جامعةِ بابل وهي جزء مِنْ متطلبات الحصول على درجة الماجستير علوم في الهندسة/ الهندسة المدنية / الموارد المائية

من قبل:

طيبة محمد يحيى إبراهيم

بكالوريوس علوم في الهندسة المدنية 2017

بأشراف:

أ. م. د: عماد حبيب عبيد ***أ. م. د: يحيى كاظم حسين***

February, 2022 **شباط ,1443**